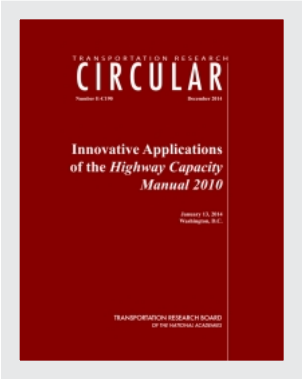

Innovative Applications of the Highway Capacity Manual 2010

DETAILS

0 pages | 8.5 x 11 | PAPERBACK
ISBN 978-0-309-43289-4 | DOI 10.17226/22236

AUTHORS

TRANSPORTATION RESEARCH
CIRCULAR

Number E-C190 December 2014

Innovative Applications of the *Highway Capacity Manual 2010*

January 13, 2014
Washington, D.C.

TRANSPORTATION RESEARCH BOARD
OF THE NATIONAL ACADEMIES

TRANSPORTATION RESEARCH CIRCULAR E-C190

Innovative Applications of the *Highway Capacity Manual 2010*

January 13, 2014
Marriott Wardman Park Hotel
Washington, D.C.

Editors
Tian Zong, University of Nevada, Reno
Manual G. Romana, Technical University of Madrid, Spain
Rod J. Troutbeck, Queensland University of Technology, Australia
Lily Elefteriadou, University of Florida

Sponsored by
Highway Capacity and Quality of Service Committee
Transportation Research Board

December 2014

Transportation Research Board
500 Fifth Street, NW
Washington, D.C.
www.TRB.org

TRANSPORTATION RESEARCH CIRCULAR E-C190
ISSN 0097-8515

The **Transportation Research Board** is one of six major divisions of the National Research Council, which serves as an independent advisor to the federal government and others on scientific and technical questions of national importance. The National Research Council is jointly administered by the National Academy of Sciences, the National Academy of Engineering, and the Institute of Medicine. The mission of the Transportation Research Board is to provide leadership in transportation innovation and progress through research and information exchange, conducted within a setting that is objective, interdisciplinary, and multimodal.

The **Transportation Research Board** is distributing this Circular to make the information contained herein available for use by individual practitioners in state and local transportation agencies, researchers in academic institutions, and other members of the transportation research community. The information in this circular was taken directly from the submission of the authors. This document is not a report of the National Research Council or the National Academy of Sciences.

Transportation Research Board
500 Fifth Street, NW
Washington, DC 20001
www.TRB.org

Lea Camarda, Production Editor; Jennifer Correro, Proofreading and Layout

Preface

This Transportation Research Circular includes seven full technical papers and three extended abstracts focusing on innovative applications of the *Highway Capacity Manual 2010* (HCM 2010). All of these papers were submitted to the Highway Capacity and Quality of Service Committee in response to a special call for papers for the 93rd Annual Meeting of the Transportation Research Board in January 2014. The peer review and selection followed the same TRB paper review guidelines and selection criteria as all other papers submitted for the TRB Annual Meeting. All of these papers were presented in a special session at the Annual Meeting, which was well-received by the conference participants.

HCM 2010 involves many significant updates and additions to previous editions of the HCM. The papers in this Circular include case studies, performance measures, data collection, model enhancement, and many other aspects of HCM methodologies. The publication of this Circular is timely and will serve as an important reference for transportation researchers and professionals throughout the world.

Thanks go to the authors for participating in the Annual Meeting session. Special thanks also go to the members and friends of the Highway Capacity and Quality of Service Committee, who provided valuable reviews, and to the TRB staff who facilitated the publication of this Circular.

The views expressed in the technical papers are those of the individual authors and do not necessarily represent the views of TRB or the National Research Council. The papers have not been subjected to the formal TRB peer-review process.

—Lily Elefteriadou, *Chair*
Highway Capacity and Quality of Service Committee

Contents

Empirical Analysis of Critical Headway for Drivers Turning Right on Red at Signalized Intersections

BRENDAN J. RUSSO
PETER T. SAVOLAINEN
Wayne State University

Right turn on red (RTOR) movements can significantly affect the capacity of right-turn lanes at signalized intersections. Vehicles turning right on red must wait for an adequate opening in conflicting vehicle traffic (or pedestrian traffic, if present) in order to complete the turn and, consequently, there exists an RTOR critical headway. The *Highway Capacity Manual* (HCM) recommends field measurements of RTOR vehicles in calculating capacity at signalized intersections, but this is not always possible. In these cases, the RTOR must either be assumed to be zero, which may lead to significantly inflated right-turn delay calculations, or estimated based on intersection geometry and traffic patterns. Previous research on the effects of RTOR on capacity and delay has assumed an RTOR critical headway equal to that of the HCM base critical headway values for two-way stop-controlled (TWSC) intersection minor street right-turns. To assess this assumption, an empirical analysis of the critical headway for RTOR maneuvers was conducted using observational data obtained from five signalized intersection approaches in different regions of the United States. Headway acceptance and rejection data were extracted manually from high-definition videos taken at the intersection approaches and the RTOR critical headway was determined. It was found the RTOR critical headway is generally less than the HCM base critical headway values for TWSC intersection minor street right-turns, indicating drivers are more aggressive at traffic signals. Implications of RTOR critical headway on capacity and delay calculations for signalized intersections are discussed.

Right turn on red (RTOR) occurs when a vehicle completes a right turn at a signalized intersection when their approach is faced with a red traffic signal. RTOR is allowed at most signalized intersections in the United States after a vehicle has come to a complete stop at the stop bar, unless prohibited for reasons such as limited sight distance. Vehicles turning right on red must wait for an adequate opening in conflicting vehicle traffic (or pedestrian traffic, if present) in order to complete the turn. Accordingly, there exists a critical headway for every RTOR driver in which that driver would reject any headway less than their critical headway, and would accept any headway larger.

RTOR can significantly increase the capacity of right-turn movements at signalized intersections, particularly at approaches with exclusive right turn lanes. Consequently, the overall capacity and delay of an intersection can be significantly affected by the behavior of RTOR vehicles. The *Highway Capacity Manual* (HCM) (*1*) states that RTOR flow rates should be collected in the field when possible because RTOR is difficult to predict as it depends on many different factors. However, field measurement is not possible for new intersections or intersections undergoing significant reconstruction or alignment changes. In situations where field measurement is not possible, the HCM recommends assuming zero RTOR vehicles, which can result in significantly inflated delay predictions for right-turn movements. If estimated right-turn delays are inflated, unneeded capacity may be added or unnecessary green time may be provided to

approaches with the RTOR movements. It may be more beneficial for the analyst to assume a reasonable prediction for RTOR movements based on expected (or existing) conditions at the intersection.

RTOR can occur when cross street through traffic has a green signal indication, or during protected left-turn phases. In the case of cross street protected left-turn phases, RTOR vehicles in an exclusive right-turn lane do not encounter any conflicting vehicle traffic. The HCM recommends reducing the number of right turns by the number of "shadowed" left-turning vehicles. This paper, however, focuses solely on the regime where cross-street through traffic has a green indication and RTOR vehicles must select headway in cross street traffic to complete the RTOR. In this situation, the RTOR volume is much more difficult to predict. This scenario has been likened to the case of a minor street vehicle turning right at a two-way stop-controlled (TWSC) intersection. This comparison is known as the "stop sign analogy". The HCM (*1*) provides default critical headway values for right-turning vehicles at TWSC intersections as 6.2, 6.9, and 7.1 s for two-lane, four-lane, and six-lane major roadways, respectively. These critical headway values have been applied in calculating predicted RTOR flow rates in traffic simulation software such as Synchro/SimTraffic (*2*) (although in the case of Synchro/SimTraffic, the critical headway is set at 6.2 s regardless of the number of lanes on the cross street). However, the critical headway for drivers at a signalized intersection turning right on red may in fact differ from that of drivers at TWSC intersections. For example, signalized intersections would generally be located in more urbanized areas and would tend to experience higher traffic volumes than TWSC intersections which could affect driver behavior.

This paper presents an empirical analysis of the critical headways for drivers turning right on red using observational data obtained from five signalized intersection approaches in different regions of the United States. All study intersection approaches have flat grades and intersect at 90-degree angles. The headway acceptance and rejection data for vehicles turning right on red are extracted from field videos when the conflicting through traffic has a green signal indication. The RTOR critical headway is then calculated and compared to the default values in the HCM under the stop sign analogy, as well as default values used in some traffic simulation software. The implications on capacity and delay calculations are discussed.

LITERATURE REVIEW

The HCM (*1*) suggests simply reducing the number of right turns by the field observed number of RTOR vehicles in calculating capacity at signalized intersections (in the absence of a shadowed left-turn phase). There are two problems with this: the first is that field observations are not always possible, and the second is that by subtracting vehicles from the approach volume, their effect on signal delay is ignored (*3*). Ignoring these vehicles can ultimately affect the level of service of the intersection. Despite this shortcoming, there is only a limited body of research analyzing the effects of RTOR on capacity and delay at signalized intersections. Most studies have focused on developing predictive models based on a number of traffic and driver related factors, while only a few have investigated the critical headway characteristics of RTOR drivers.

Tarko (*4*) developed a model to predict RTOR volumes at isolated and coordinated signals based on several parameters such as intersection geometry, patterns of arriving vehicles (both right-turning vehicles and conflicting vehicles), and signal timing parameters. However, in the development of the model, a critical headway time for RTOR vehicles was assumed to be 6.9 s. This

assumption follows the HCM suggestion for TWSC intersections with four-lane major roads (*1*). Qureshi and Han (*5*) developed a delay model for right turn lanes with RTOR traffic based on queuing theory. They also assumed the HCM default critical headway value for right turns at TWSC intersections, which was 5.5 s at that time. Creasey et al. (*6*) developed RTOR volume estimation models and incremental capacity models for shared right turn lanes, which also utilized the HCM default critical headway values for right turns at TWSC intersections.

Virkler and Maddela (*7*) tested both the left-turn shadowing method and the stop sign analogy of accounting for RTOR vehicles to determine the effects on intersection capacity with data from 40 intersections. It was found that both methods improve intersection capacity, indicating that if RTOR vehicles are ignored, the HCM method for signalized intersections may over-estimate delay. Again, the critical headway for RTOR vehicles was assumed to follow HCM default values for right-turning vehicles at TWSC intersections. Virkler and Krishna (*3*) provide another analysis of the stop sign analogy and assess SIDRA software. The SIDRA software uses a default RTOR critical headway of 6.0 s which is slightly lower than the current HCM default values for TWSC intersections in the United States. An observational RTOR headway acceptance study was conducted at three intersections and the critical headway for RTOR was found to be 4.05, 4.47, and 5.54 s for each of the three intersections. This is one of the first field-observed RTOR critical headway analyses on record; however, the conditions at the three intersections are not applicable to all scenarios. One of the intersections had a yield-controlled right-turn lane which allowed for "free right-turns" (and is really not necessarily applicable to an RTOR scenario). As for the other two intersections, one included a one-way street with two conflicting through traffic lanes and the other had only one conflicting through lane.

Chen et al. (*8*) estimated RTOR capacity for dual right-turn lanes at signalized intersections considering both left turn shadowing situations and the stop sign analogy. Of greater relevance to the current study, Chen et al. (*9*) performed an empirical assessment of headway-acceptance behavior of RTOR drivers at dual right-turn lanes. Using data from six intersections (all either interchange ramps or frontage roads), the critical headway for RTOR drivers was found to be 5.6 s for drivers in the curb lane and 6.7 s for drivers in the inside right-turn lane. These findings are useful for analyses of dual right-turn situations, but may not be applicable to single right-turn lanes. Overall, it is clear that research on the critical headway for RTOR drivers is limited, as almost all analyses of RTOR impacts on capacity and delay assume the critical headway is equal to that of right-turning vehicles at TWSC intersections. This study provides important empirical data to address this gap in the research literature.

DATA DESCRIPTION

The data for this study were extracted from an existing database of video taken at numerous intersection approaches across the United States. This database contains 4 to 6 h of video at 87 different intersection approaches from California, Maryland, Michigan, and Virginia. The video at each site generally started after the a.m. peak hour (around 11 a.m.) and continued for 4 to 6 h into the p.m. peak hour. The sites were originally chosen at random from intersections with at least two through lanes and where municipalities granted permission for video recording. It is important to note that many of these sites were not viable candidates for an RTOR headway acceptance analysis. To identify appropriate sites, 1 h of video was reviewed for each site to record the number of usable RTOR headway acceptances observed. Several sites were eliminated immediately due to their

geometry (e.g., T-intersections, yield-controlled free right-turns) as well as in cases of low right-turn or conflicting through traffic volumes (i.e., no useable RTOR headway acceptances). Ultimately, five intersection approaches were chosen as good candidates for an RTOR headway acceptance study based on their geometry and traffic patterns. Summary statistics for the five study sites are shown in Table 1.

The videos are shot from high-definition video cameras, which are mounted on telescoping poles approximately 20 ft above the pavement surface. The cameras are attached to street signs, allowing for covert monitoring of driver behavior. The elevated view provides an excellent vantage point for conducting a headway study. Figure 1 shows a screen shot of the video taken at Westminster Avenue and Harbor Boulevard in Santa Ana, California, in which a vehicle in the right-turn lane is waiting to accept a headway in the cross street through traffic.

To analyze the critical headway of RTOR drivers, both headway acceptances and rejections were recorded for all RTOR vehicles. This was done manually with a stopwatch while watching the videos in real time (although videos were frequently rewound to confirm accuracy of a measured headway or to capture a headway that the observer had initially missed). For the purpose of this study, only headways (and not lags) were recorded because a driver's reaction to a lag may not be the same as to headway and the inclusion of lags may bias the results of the study (*10*). It should be noted that not all the observed RTOR vehicles had a usable observed accepted headway. In cases where an RTOR driver rejected several headways but did not find an adequate one to accept during the red phase, their rejected headways were recorded as usable data but there was no observed accepted headways for those drivers. Similarly, in cases where an RTOR driver turned right after all cross street traffic had already passed, those drivers' rejected headways were recorded as usable data, but there was no observed accepted headway (because the accepted headway size in these cases is not measurable). It should be noted that no RTOR headway data were collected during protected left-turn phases; as this study focused solely on the traffic regime in which cross street through traffic had a green signal indication. The headway sizes were recorded to the tenth of a second and the data were later compiled into bins.

RTOR CRITICAL HEADWAY ANALYSIS RESULTS

After headway data collection was complete, the Ramsey and Routledge (*11*) method of determining critical headway was utilized to determine the RTOR critical headway. The Ramsey and Routledge method is recommended in the *Manual of Transportation Engineering Studies* (*12*) and has advantages over other methods of critical headway calculation. The main advantage of this method is that it does not require any assumption of the distribution of critical headways in the driver population. The method efficiently estimates the entire distribution of critical headways using all headway data (accepted and rejected headways) (*12*). Additionally, this method is relatively simple to use and has been shown to provide good precision and accuracy when compared with other methods (*10*). One requirement when using this technique, however, is that the proportions of accepted headways must increase with headway size. This is usually not an issue (and was not in the case of this study) because drivers would tend to reject smaller headways and accept larger headways. Table 2 presents the results of the RTOR critical headway analysis including a summary of the RTOR headway acceptance and rejection data and the calculated critical headway for all five locations, as well as for the aggregated dataset.

TABLE 1 Summary of Study Sites Selected for RTOR Headway Acceptance Analysis

Study Approach	Location	Cross Street Speed Limit	No. of Through Lanes on Cross Street	Hours of Video Reviewed
1. WB Westminster Ave. at Harbor Blvd.	Santa Ana, Calif.	40 mph	3	6
2. NWB Waters Rd. at Ann Arbor Saline Rd.	Ann Arbor, Mich.	40 mph	2	6
3. WB Lee Jackson Memorial Hwy. at Walney Rd.	Chantilly, Va.	45 mph	3	5
4. WB Six Mile Rd. at Newburgh Rd.	Livonia, Mich.	45 mph	2	4
5. NB Newburgh Rd. at Six Mile Rd.	Livonia, Mich.	45 mph	3	6

NOTE: no. = number; WB = westbound; ave. = avenue; blvd. = boulevard; NWB = northwest bound; rd. = road; NB = northbound.

FIGURE 1 Screen shot of video at Westminster Ave. and Harbor Blvd. in Santa Ana, California.

The final sample size of RTOR headway acceptances was 259. To obtain accurate critical headway calculations, Ramsey and Routledge suggest a minimum of 200 acceptances for 2-s bins and a minimum of 500 acceptances for 1-s bins (*11*). Therefore, a bin size of 2 s was selected for this study, which is considered adequate for most headway acceptance studies (*12*). The proportions of accepted headways increased with headway size for all five study locations, as well as for the overall analysis. It should be noted that data for headways less than 2 s are not included in Table 2 because no RTOR drivers were observed to accept a headway of less than 2 s and such data do not influence the determination of critical headway in the Ramsey and Routledge method.

The RTOR critical headways were found to be 5.01, 5.21, 5.00, 4.92, and 4.56 s for the five study locations. These RTOR critical headway results for the individual study sites, however, are based on a relatively low sample size of RTOR headway acceptances at each individual site. Of most importance is the overall (aggregate) RTOR critical headway analysis, which showed a mean critical headway of 4.88 s. This is significantly less than the HCM assumed values for TWSC intersections (6.2, 6.9, and 7.1 s for two-lane, four-lane, and six-lane major roadways, respectively). This indicates RTOR drivers tend to be more aggressive than drivers turning right at TWSC intersections, possibly due to differences in drivers and traffic conditions between rural TWSC and urban–suburban signalized intersections. The distributions of the RTOR critical headways estimated by the Ramsey and Routledge method were approximately normal for each site individually, as well as for the aggregate data for the five

TABLE 2 Summary of RTOR Critical Headway Analysis

Study Approach		Headway Sizes (mean of bins)					RTOR Mean Critical Headway
		3 s	5 s	7 s	9 s	Total	
1. WB Westminster Ave. at Harbor Blvd.	No. acceptances	1	5	14	9	29	5.01 s
	No. rejections	125	10	3	0	138	
	% accepting	0.8	33.3	82.4	100.0		
2. NWB Waters Rd. at Ann Arbor Saline Rd.	No. acceptances	5	7	20	24	56	5.21 s
	No. rejections	190	33	9	1	233	
	% accepting	2.6	17.5	69.0	96.0		
3. WB Lee Jackson Memorial Highway at Walney Rd.	No. acceptances	2	3	10	12	27	5.00 s
	No. rejections	87	8	2	1	98	
	% accepting	2.2	27.3	83.3	92.3		
4. WB Six Mile Rd. at Newburgh Rd.	No. acceptances	1	12	18	14	45	4.92 s
	No. rejections	123	32	8	3	166	
	% accepting	0.8	27.3	69.2	82.4		
5. NB Newburgh Rd. at Six Mile Rd.	No. acceptances	12	29	24	37	102	4.56 s
	No. rejections	349	122	61	28	560	
	% accepting	3.3	19.2	28.2	56.9		
Total for all study approaches	**No. acceptances**	**21**	**56**	**86**	**96**	**259**	**4.88 s**
	No. rejections	**874**	**205**	**83**	**33**	**1,195**	
	% accepting	**2.3**	**21.5**	**50.9**	**74.4**		

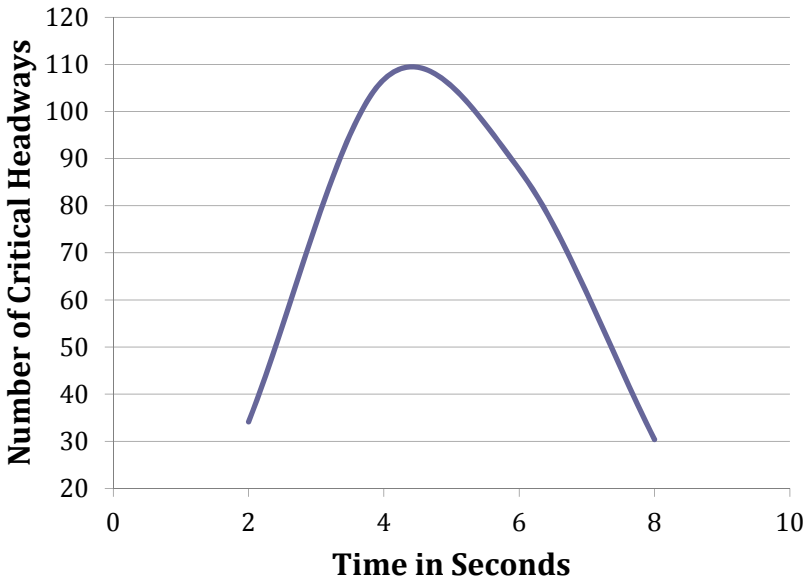

FIGURE 2 RTOR critical headway distribution for the overall analysis.

locations. The distribution of RTOR critical headways is shown graphically in Figure 2. The potential impacts of the RTOR critical headway on the calculation of capacity and delay for right turns at signalized intersections are discussed in the next section.

IMPACT OF RTOR CRITICAL HEADWAY ON CAPACITY AND DELAY ESTIMATES

The RTOR mean critical headway for this empirical study was found to be 4.88 s. This critical headway time is significantly less than the default value for the right-turn critical headway at TWSC intersections found in the HCM. As discussed previously, nearly all prior research on the impact of RTOR on capacity and delay at signalized intersections has assumed that the RTOR critical headway is equal to that of right-turning minor street traffic at TWSC intersections (i.e., the stop sign analogy). Similarly, the Synchro/Simtraffic traffic simulation software assumes an RTOR critical headway of 6.2 s for all intersection geometries (*2*).

Since the critical headway for RTOR drivers in this study is found to be less than the commonly used default values, it seems delay calculations for right turns may be frequently overestimated.

Synchro/Simtraffic fully models RTOR movements by calculating a saturation flow rate for RTOR and applying that flow rate to right-turn movements when they are red (*2*). The formula used to calculate RTOR saturation flow, which is very similar to Equation 19-32 in the HCM used to calculate capacity at TWSC intersections, is as follows:

$$sRTORi = \frac{vxi * e^{\left(-vx * \frac{6.2}{3600}\right)}}{1 - e^{\left(-vxi * \frac{3.3}{3600}\right)}} \quad (1)$$

where

sRTORi = RTOR saturation flow rate in vehicles per hour (vph) (1,091 vph if zero conflicting traffic);
vxi = merging volume during time interval *i*;
6.2 = assumed RTOR critical headway time in seconds; and
3.3 = assumed follow up time in seconds.

In assuming the RTOR critical headway time is 6.2 s, this formula may be under-predicting the actual RTOR saturation flow rate. For example, for conflicting traffic of 900 vph, the sRTOR is calculated to be 340 vph (intermediate calculations involving cycle and phase lengths are left out here for simplicity). However, if the assumed 6.2-s RTOR critical headway is replaced with the 4.88-s RTOR critical headway found empirically in this study, the resulting sRTOR is 473 vph. Using the 4.88-s RTOR critical headway found in this study, the resulting sRTOR was 133 vph higher representing a 39.1% increase. This potential increase could significantly affect the capacity and delay estimates for right turns, as well as for the overall intersection.

Most of the existing literature that attempts to estimate RTOR effects on capacity or delay uses the default critical headway values for TWSC intersections from the HCM (*4*–*7*). The results from this study, however, suggest using an RTOR critical headway of 4.88 s may provide greater accuracy, and would yield higher RTOR capacities. It should be noted that this RTOR critical headway can be applied to exclusive or shared right-turn lanes, but the method for determining capacities would differ as shared lanes have the added restriction of possible blockages by through vehicles.

CONCLUSIONS

RTOR movements can significantly affect the capacity of right-turn lanes at signalized intersections. Vehicles turning right on red must wait for an adequate opening in conflicting traffic in order to complete the turn. Therefore, there exists an RTOR critical headway. This paper presented an empirical analysis of the critical headway for drivers turning right on red using data from five signalized intersection approaches in the United States. Headway acceptance and rejection data were extracted manually from high-definition videos collected at these approaches. Using the Ramsey and Routledge method, it was found that the RTOR critical headway is 4.88 s.

The results of this study indicate that RTOR drivers are more aggressive than right turning drivers at TWSC intersections. This shows that previous research on RTOR using the "stop sign analogy" may have underestimated RTOR effects on capacity and delay. An example of RTOR saturation flow showed that using RTOR critical headway of 4.88 s resulted in a 39.1% increase in RTOR saturation flow as compared to the default value of 6.2 s. This example demonstrates the importance of accurately accounting for RTOR, as failure to do so could result in adding unneeded capacity to intersections or providing unneeded green time.

RTOR is a topic which could benefit from further detailed research as traffic congestion in urban areas continues to be a major concern and transportation engineers are always seeking to improve efficiency, even incrementally. Future research could examine RTOR critical

headway at intersections with differing geometry and traffic patterns to determine if the value found in this study is consistent with different scenarios. The effect of differing cross street speed limits could also be investigated, as this study was limited to sites with 40 mph or 45 mph cross street speed limits. Additionally, RTOR follow-up headways could be analyzed with observational data and compared to values found in the HCM for base follow-up headways at TWSC intersections. Left-turn-on-red critical headway at one-way streets could also be examined with observational data, as this movement is allowed at intersections with one-way streets in most states in the United States.

REFERENCES

1. *Highway Capacity Manual 2010.* Transportation Research Board of the National Academies, Washington, D.C., 2010.
2. Husch, D., and J. Albeck. Synchro Studio 7 User Guide. Trafficware, Ltd., Sugar Land, Tex., 2006.
3. Virkler, M. R., and M. A. Krishna. Gap Acceptance Capacity for Right Turns at Signalized Intersections. In *Transportation Research Record 1646,* TRB, National Research Council, Washington, D.C., 1998, pp. 47–53.
4. Tarko, P. A. Predicting Right Turns on Red. In *Transportation Research Record: Journal of the Transportation Research Board, No. 1776,* TRB, National Research Council, Washington, D.C., 2001, pp. 136–142.
5. Qureshi, M. A., and L. D. Han. Delay Model for Right-Turn Lanes at Signalized Intersections with Uniform Arrivals and Right Turns on Red. In *Transportation Research Record: Journal of the Transportation Research Board, No. 1776,* TRB, National Research Council, Washington, D.C., 2001, pp. 143-150.
6. Creasy, F. T., N. Stamatiadis, and K. Viele. Right-Turn-on-Red Volume Estimation and Incremental Capacity Models for Shared Lanes at Signalized Intersections. In *Transportation Research Record: Journal of the Transportation Research Board, No. 2257,* Transportation Research Board of the Academies, Washington, D.C., 2011, pp. 31–39.
7. Virkler, M. R., and R. R. Maddela. Capacity for Right Turn on Red. In *Transportation Research Record 1484,* TRB, National Research Council, Washington, D.C., 1995, pp. 66–72.
8. Chen, X., Y. Qi, and D. Li. Estimating Right-Turn-on-Red Capacity for Dual Right-Turn Lanes at Signalized Intersections. In *Transportation Research Record: Journal of the Transportation Research Board, No. 2286,* Transportation Research Board of the National Academies, Washington, D.C., 2012, pp. 29–38.
9. Chen, X., Y. Qi, and G. Liu. Empirical Study of Gap-Acceptance Behavior of Right-Turn-on-Red Drivers on Duel Right-Turn Lanes. *Journal of Transportation Engineering*, Vol. 139, American Society of Civil Engineers, 2013, pp. 173–180.
10. Hewitt, R. H. A Comparison Between Some Methods of Measuring Critical Gap. *Traffic Engineering and Control,* Vol. 26, 1985, pp. 13–22.
11. Ramsey, J. B. H., and I. W. Routledge. A New Approach to the Analysis of Gap Acceptance Times. *Traffic Engineering and Control,* Vol. 15, 1973, pp. 353–357.
12. *Manual of Transportation Engineering Studies 2nd Edition.* Institute of Transportation Engineers, Washington, D.C., 2010.

Speed–Flow Relationship and Capacity for Expressways in Brazil

GUSTAVO RIENTE DE ANDRADE
JOSÉ REYNALDO SETTI
Universidade de São Paulo, Brazil

This paper presents the development of a speed–flow model for expressways in Brazil, similar to the one used in the *Highway Capacity Manual 2010* (HCM 2010). The model was developed using a sample of 788,122 observations collected at 24 stations on four expressways in the state of São Paulo. The data analysis showed that, as proposed by the HCM 2010, there is a range of flows in which the average speed of the passenger cars remains constant and equal to the free-flow speed. It was also found that the classification scheme used by the HCM 2010, based on controlling access (freeways versus multilane highways), is not adequate for expressways in the state of São Paulo. A new scheme, based on abutting land use (urban versus rural) is proposed. For these highway classes, representative values for the capacity were found, and speed–flow relationships were calibrated.

The *Highway Capacity Manual 2010* (HCM 2010) has been widely adopted outside the United States as the standard to estimate levels of service. In Brazil, it has been adopted to assess both existing operational conditions and the benefits of proposed highway improvements (*1*). However, many Brazilian highway administrators, practitioners, and researchers have advocated the adaptation of HCM 2010 procedures to local road and traffic characteristics (*1–6*). The main aspects to be adapted are speed–flow relationships, including base conditions and the capacity, and passenger car equivalents for trucks (*5*). While the latter have already been studied to some extent (*2, 7*), the calibration of speed–flow relationships has been slower due to a lack of suitable traffic data.

The calibration of speed–flow curves requires empirical data (average speed and flow rate disaggregated for passenger cars and heavy vehicles) for a representative sample of road segments. One of the byproducts of the Brazilian highway privatization program was to implement systematic traffic data collection by means of a large number of permanent traffic-counting stations. The research reported in this paper was possible due to the availability of a large data set, collected at 24 traffic-counting stations on four major expressways in the state of São Paulo.

The main objectives of the research were to calibrate a family of speed–flow relationships for expressways in Brazil and to estimate the capacity for these roads. This paper is organized such that initially, the mathematical modeling of the speed–flow relationship is discussed; next, the traffic data used is presented. Then the procedure used for the estimation of key parameters (density-at-capacity and the transition point) is presented, followed by the calibration of the speed–flow relationships and a comparison of the new curves with the HCM 2010 relationships.

MATHEMATICAL MODELING OF THE HCM SPEED–FLOW RELATIONSHIP

The mathematical model adopted to describe the speed–flow relationship in the HCM 2010 is the same one used in the HCM 2000 (*8*). Furthermore, the same basic structure is used both for freeways and multilane highways. Assuming a traffic stream containing only passenger cars, this model comprises two regions (Figure 1*a*): (*a*) a flat segment where traffic stream speed S is constant and equal to free-flow speed (FFS) and (*b*) a convex segment, in which traffic stream speed varies between FFS and speed at capacity (*CS*). The flow rate limits for the flat segment are 0 and *BP*, which is the transition point where the traffic stream speed starts to decrease due to an increase in the flow rate. The convex segment limits are *BP* and capacity *C*.

Empirical evidence from several studies supports this model (*9–14*). The speed–flow function is anchored by two points: (*BP*, FFS) and (*C*, *CS*). The mathematical function $S = f(\text{FFS}, q)$ that represents the speed–flow model for freeways can be written as (*15*) Equation 1.

$$S = \begin{cases} FFS, & 0 \le q \le BP \\ FFS - \left[\dfrac{1}{28}(23FFS - 1800)\left(\dfrac{q + 15FFS - 3100}{20FFS - 1300}\right)^{2.6}\right], & BP < q \le C; \end{cases} \quad (1)$$

where S is traffic stream speed (km/h); q, traffic flow rate in passenger cars per hour per lane (pcph/lane); and FFS, *BP*, and *C* are as previously defined. The HCM 2000 assumes density at the capacity as 28 passenger cars per kilometer per lane (pcpkm/lane), a value that is hard-coded into Equation 1, but could be called *CD*.

Equation 1 can be used to create a family of speed–flow relationships for a set of FFSs $\{\text{FFS}_1, \text{FFS}_2\}$ (Figure 1*b*) using appropriate values of *BP* and *C*, which can be calculated using Equations 2 and 3:

$$BP = -15\ \text{FFS} + 3{,}100 \quad (2)$$

$$C = 5\ \text{FFS} + 1{,}800 \quad (3)$$

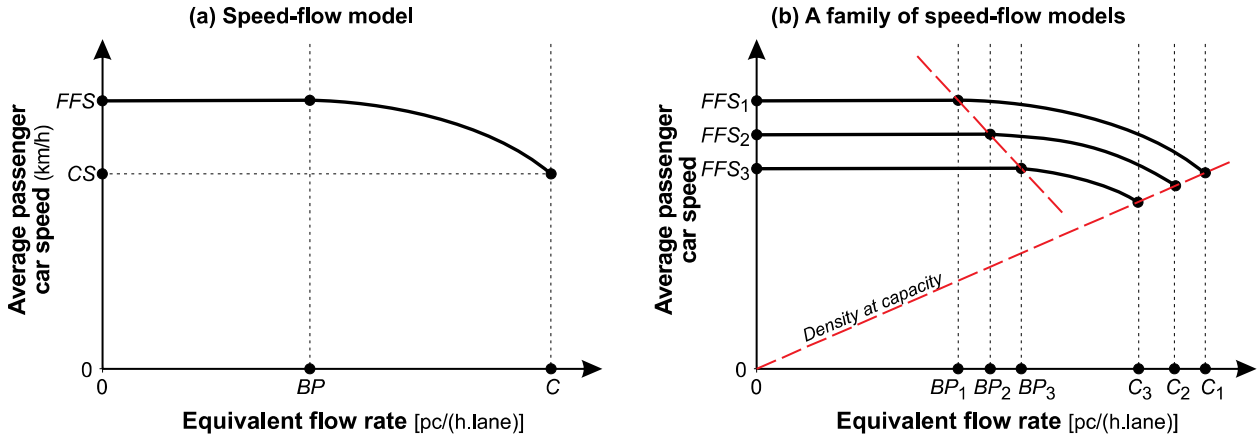

FIGURE 1 General characteristics of the HCM 2010 speed–flow model.

Equation 2 shows that *BP* decreases linearly with increases in FFS. Equation 3 assumes that density at the capacity remains constant and is equal to 28 pcpkm/lane for any FFS.

By substituting Equations 2 and 3 into Equation 1 and making *CD* = 28 pcpkm/lane and $\gamma = 2.6$, the relationship between *S* and *C*, *CD*, *BP*, and FFS becomes

$$S = FFS - \left(FFS - \frac{C}{CD} \right) \cdot \left(\frac{q - BP}{C - BP} \right)^{\gamma}. \quad (4)$$

Assuming that $C = CS \times CD$ and thus, $CD = C/CS$, Equation 4 can be simplified into

$$S = FFS - \left[(FFS - CS) \frac{(q - BP)^{\gamma}}{(C - BP)^{\gamma}} \right]. \quad (5)$$

Equations 2 and 3 can also be generalized, as they indicate that *BP* and *C* vary linearly with FFS. Therefore, these functions are

$$BP = a_{BP} FFS + b_{BP}; \text{ and} \quad (6)$$

$$C = a_C FFS + b_C, \quad (7)$$

in which a_{BP}, b_{BP}, a_c, and b_c and are calibration constants.

Equations 5, 6, and 7 specify a generalized speed–flow model for freeways and divided multilane highways, from which the HCM 2010 relationships can be obtained. The next sections in this paper show how a set of speed–flow relationships was obtained for Brazilian expressways, by finding appropriate values for the parameters in these three equations.

SPEED–FLOW DATA FROM TRAFFIC SENSORS

Data for the calibration of the speed–flow relationship should ideally originate from streams containing only passenger cars and should also reflect normal operating conditions for uncongested flows (*16*).

Data used in this study were collected at 24 traffic-counting stations in the metropolitan region of São Paulo, using inductive loops installed in each traffic lane. The data were collected between 1/1/2010 and 8/31/2011 and consisted of the number of vehicles (passenger cars and heavy vehicles) and average speed (for passenger cars and for heavy vehicles). For 11 of the 24 sites, data were available for 6-min intervals; for the others, for 5-min intervals. The HCM 2010 used 15-min data points (*8*); several other studies, however, recommend the use of a 5-min interval (*17–19*), which is deemed suitably short to represent the traffic behavior in greater detail and sufficiently long to avoid the introduction of bias in the estimation of speed and flow due to the inherent variability of driver behavior.

The process used for choosing sites for the sample is described in detail elsewhere (*20*). All segments in the sample meet conditions necessary to warrant uninterrupted flow, such as the existence of a physical median, no traffic signals, and no ramps at least 3 km away from the site.

According to the HCM, all sites in the sample could be classified either as freeways (expressways with controlled access) or as divided multilane highways (expressways without controlled access). Lane width (3.5 m) and left and right shoulder widths (respectively 0.6 m and 2.5 m) were constant across all segments, which contained at least three lanes in each direction (except two sites with two lanes in each direction).

Sites in the sample were also classified as rural or urban, according to abutting land use. Rural expressways comprised highways isolated from the local road network, bearing mostly longer trips; urban expressways are those with greater integration with the local network, with greater density of ramps or points of access, within an urbanized environment and carrying a significant portion of local trips. For each site in the sample, FFS was estimated to the nearest km/h, varying between 78 and 130 km/h. Speed–flow data indicate that the capacity is often reached in eight of the 24 sites.

There are two major differences between traffic streams in Brazil and in the United States. In Brazil, the truck percentage is higher (usually over 25%); and Brazilian trucks have higher mass-to-power ratios when compared to American trucks. Furthermore, the practice in Brazil is to have two speed limits: a greater one (up to 120 km/h) for light vehicles (passenger cars) and a lower one (90 km/h) for heavy vehicles (trucks and buses). On expressways with three or more lanes, trucks and buses are not allowed to travel in the leftmost lane (closest to the median). The combined effect of this rule and poor performance characteristics is that trucks tend to stay in the right lanes (closest to the shoulder), while cars mostly travel in the left lanes, creating something similar to two fluids flowing with different speeds within the same stream. Speed–flow data show that the percentage of heavy vehicle in the flow is typically very low (usually less than 5%) in the leftmost lane, in which peak flow rates are greater than 2,100 vehicle per hour per lane (vphpl). In the rightmost lane, trucks comprise about 45% of the flow and the greatest flow rates observed barely reach 1,500 vphpl. In the center lane, where truck percentages are between these two extremes (usually around 20%), intermediate behavior was observed: the greatest flow rates observed were between 1,500 and 1,800 vphpl.

In order to use speed–flow data closest to base conditions, only data collected by the sensors in the leftmost lane of each site were used. Speed–flow data collected under bad weather conditions (rain) were also discarded from the sample. Additionally, observations with $P_T > 5\%$ were discarded; data points with $0 < P_T \leq 5\%$ were used, to avoid excessive thinning of the data set, especially in the region closer to the capacity. For these cases, however, heavy vehicles were converted into passenger car equivalents using equivalence factors derived for these expressways in another study (*7*). After this selection, 788,122 observations for the 24 sites were available for use.

Initially, the data were divided into four groups: freeways (rural and urban) and divided multilane highways (rural and urban). The major factors used to classify each site were access control and surrounding land use. A visual inspection of these data sets, however, suggested that the differences between rural and urban sites were much stronger than the differences due to road type (freeway vs. multilane highways), as the graphs in Figure 2 illustrate. Data point colors in Figure 2 indicate the number of observations for given speed–flow combinations, as shown in the legend.

The graphs in Figure 2*a* and 2*b* show data collected on a rural freeway segment and an urban freeway segment with similar characteristics. Average traffic speeds are nearly constant over a greater range of flow rates in the rural segment, when compared to the urban segment.

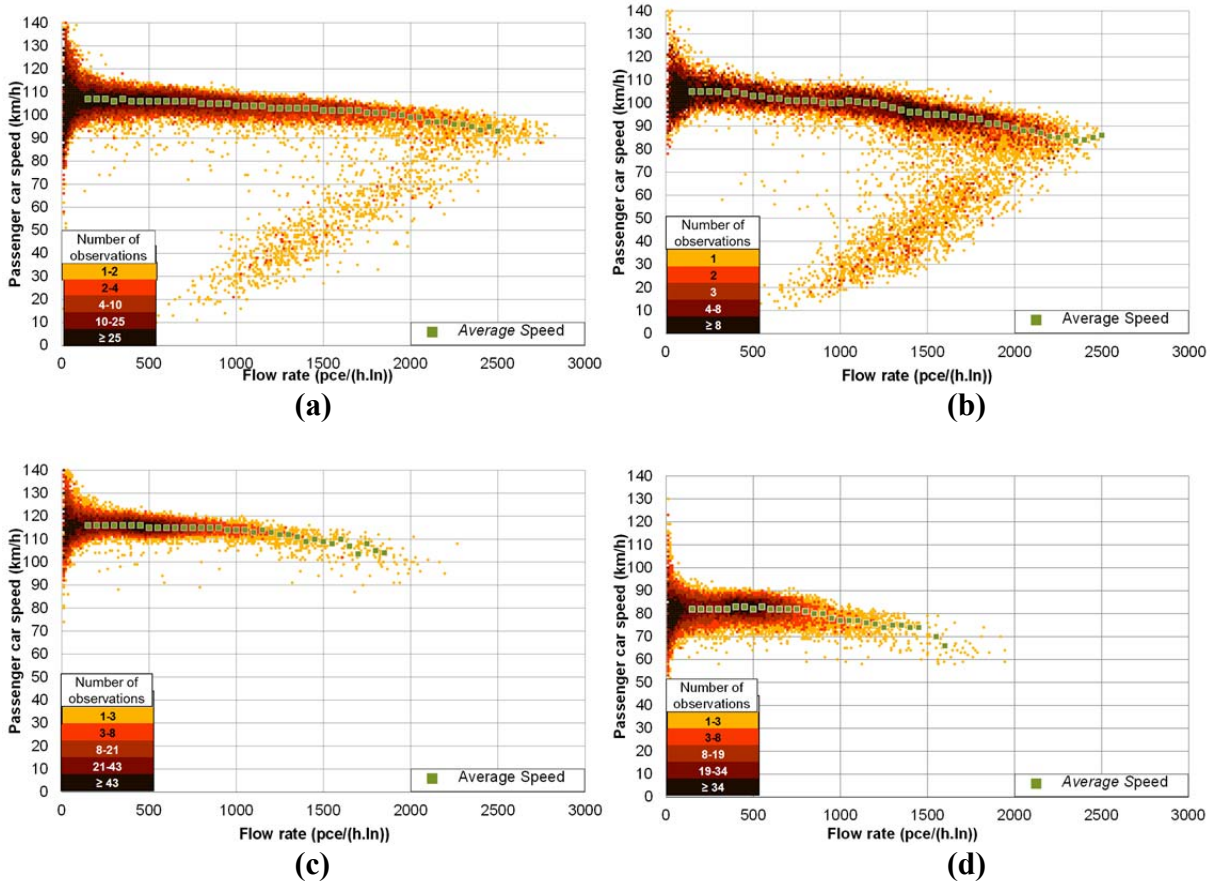

FIGURE 2 Speed–flow data for rural and urban expressway segments: (*a*) rural freeway, FFS = 107 km/h; (*b*) urban freeway, FFS = 107 km/h; (*c*) rural divided multilane highway, FFS = 116 km/h; and (*d*) urban divided multilane highway, FFS = 82 km/h.

Moreover, average speed appears to decrease at a greater rate in the urban segment when compared to the rural freeway section. Speed–flow data collected at rural divided multilane highways show characteristics closer to those of rural freeways than those collected at urban divided multilane highway segments, as Figures 2*c* and 2*d* illustrate. The capacity for urban segments seems to be smaller than for rural segments and the speed-at-capacity is also smaller for urban expressways. Therefore, it was decided that the speed–flow models should be calibrated for rural and urban expressways, instead of the freeway versus multilane highway approach used in the HCM.

ESTIMATION OF DENSITY AT CAPACITY FOR BRAZILIAN EXPRESSWAYS

While the capacity is stochastic by nature (*21*), the speed–flow model shown in Figure 1 and in Equations 5, 6, and 7 requires the estimation of deterministic values for capacity (*C*), free-flow speed (*FFS*), density at capacity (*CD*), and the traffic stream breakdown flow (*BP*). This section describes the procedure used to estimate a value for density at capacity. The adopted approach was adapted from the literature (*19*, *22*).

Traffic Stream Breakdown and the Definition of Capacity

Breakdown in an uninterrupted traffic stream may be defined as the transition between proper operation and unacceptable flow conditions (*22*) and corresponds to a sudden reduction in average travel speed, reflecting the change from uncongested to congested flow. Recent studies (*19, 21*, *22*) have suggested using breakdown flows to define the capacity of an expressway lane. This definition of capacity ("the volume below which the facility conditions are acceptable and above which the facility condition becomes unacceptable") is stochastic by nature (*21*).

The approach used to estimate the capacity via traffic breakdown events is based on the product limit method (PLM) and an analogy with lifetime data analysis (*23*). The method assumes that the capacity distribution function is

$$F_c(q) = p(c \le q), \tag{8}$$

in which $F_c(q)$ is the capacity distribution function, c is the capacity, and q is the traffic flow rate (*19*). Using an analogy to lifetime data analysis, capacity c is analogous to lifetime T of a technical component. The lifetime distribution function is

$$F(t) = p(T \le t) = 1 - S(t), \tag{9}$$

where $F(t)$ is the distribution function of lifetime, that is, the probability that lifetime $T \le t$; and $S(t)$ is the survival function, that is, the probability that lifetime $T > t$.

The PLM can be used to estimate the survival function using the expression (*19*):

$$\hat{S}(t) = 1 - \prod_{j:t_j<t} \frac{n_j - d_j}{n_j}, \tag{10}$$

where $\hat{S}(t) =$ the estimated survival function; n_j = number of individuals with a lifetime $T \ge t_j$; and d_j is number of deaths at time t_j. Each observed lifetime is used as one t_j value and, thus, $d_j = 1$ in Equation 10.

Assuming that $\hat{S}(t) = S(t)$, the distribution function for the capacity analysis can be rewritten as

$$F_c(q) = 1 - \prod_{i:q_i \le q} \frac{k_i - d_i}{k_i}; \quad i \in \{B\}, \tag{11}$$

where

$F_c(q)$ = distribution function of capacity c;
q = traffic flow rate (pcph);
q_i = traffic flow rate during interval i (pcph);
k_i = number of intervals in which $q \ge q_i$;

d_i = number of breakdowns at a flow rate of q_i; and
$\{B\}$ = set of breakdown intervals.

To use Equation 11, observations of average speed and traffic flow rates during short intervals are required, usually 5-min intervals (*19*, *21*, *22*). The available speed–flow observations are arranged chronologically and classified into one of the following sets:

$\{F\}$ = traffic is uncongested in time interval i and also in time interval $i + 1$, suggesting that flow rate q_i is not greater than the capacity;

$\{B\}$ = traffic is uncongested in time interval i, but the observed flow rate in time interval $i + 1$, q_i, causes the average speed to drop below a threshold, indicating that a breakdown occurs in time interval $i + 1$; and

$\{C\}$ = traffic is congested in time interval i, either in the segment under consideration or spilling back from a downstream location, i.e., the average speed is below the threshold value. This time interval does not provide information about the capacity value and these flow rates are not used in the analysis.

Once the traffic flow observations are classified into these sets, the distribution function $F_c(q)$ can be plotted for flow rate values in $\{B\}$ set. A more detailed description of this procedure can be found in (*19*).

Definition of Speed Threshold Values to Identify Breakdowns

The key to identifying a breakdown event is, therefore, a sudden drop (below a predefined threshold) in average speed during the next time interval. Previous researchers have adopted deterministic values for this threshold. In a study using data from freeways in Canada, a threshold of 90 km/h was adopted (*24*). Another study, using data from German freeways, used a threshold of 70 km/h, but stressed that other locations would likely produce different values (*22*).

Given the stochastic character of the breakdown event pointed out in the literature (*19*, *22*, *24*), in this study a statistical approach was used to find the threshold, assuming that the speed that marks the transition from uncongested to congested conditions could be different for each site in the sample.

Speed threshold values were estimated using cluster analysis. The *k*-means method was used with the distance metric being the Euclidian distance (*25*). For each of the eight sites where the capacity was reached, speed–flow observations for flow rates greater than 1,750 pcph/lane were classified into two clusters (uncongested and congested flow). The threshold is the speed that is simultaneously the lowest speed value for observations belonging to the uncongested flow regime and the highest speed for observations in the congested regime. Threshold values varied between 75 and 90 km/h, with an average of 83.3 km/h and a median of 83.5 km/h. FFS for these sites ranged from 105 to 116 km/h, with an average of 109 km/h and a median of 107 km/h; speed limits for passenger cars were 100, 110, or 120 km/h, depending on the site.

Estimation of Capacity

Once all observations were classified into the appropriate sets, the survival function could be estimated, using the PLM. The maximum value of the distribution function of capacity only reaches 1 if the highest flow rate in the sample belongs to the $\{B\}$ set. In this case, the product in Equation 11 is 0 and $F_c(q) = 1$; otherwise $F_c(q) < 1$. When the highest observed flow rate does not cause a breakdown in the next time interval, it is impossible to estimate the complete capacity distribution function and some assumption about the mathematical type of $F_c(q)$ must be made (*19*). Based on previous studies (*19*, *21*, *22*), the Weibull distribution was used in this research.

Capacity, under this approach, is not a deterministic value, but a random variable, following a statistical distribution. Should a capacity value be required, it can be estimated assuming a breakdown probability value under $F_c(q)$. The estimate for the capacity is obtained from the flow rate associated with this breakdown probability through the speed–flow curve, as shown in Figure 3. The horizontal axis shows flow rates; the left vertical axis represents the average speed; the right *y*-axis shows the breakdown probability associated with the PLM model (red dots) and the fitted Weibull distribution (black line). Once a suitable value for the breakdown probability is chosen, the corresponding flow rate, which represents the capacity, is found from the Weibull distribution function (dotted line).

The value for the acceptable breakdown probability is key to the estimation of the capacity. Geistefeldt (*26*) suggested $p = 3\%$ (i.e., the third percentile of the fitted Weibull distribution); Washburn et al. (*19*) suggested using the fourth percentile. In this study, the value adopted was $p = 4\%$.

Once capacity C is known, density at capacity CD can be calculated using $CD = C/CS$. Speed at capacity CS, for this study, was assumed to be the average of all observations for flow rate C in the uncongested flow regime.

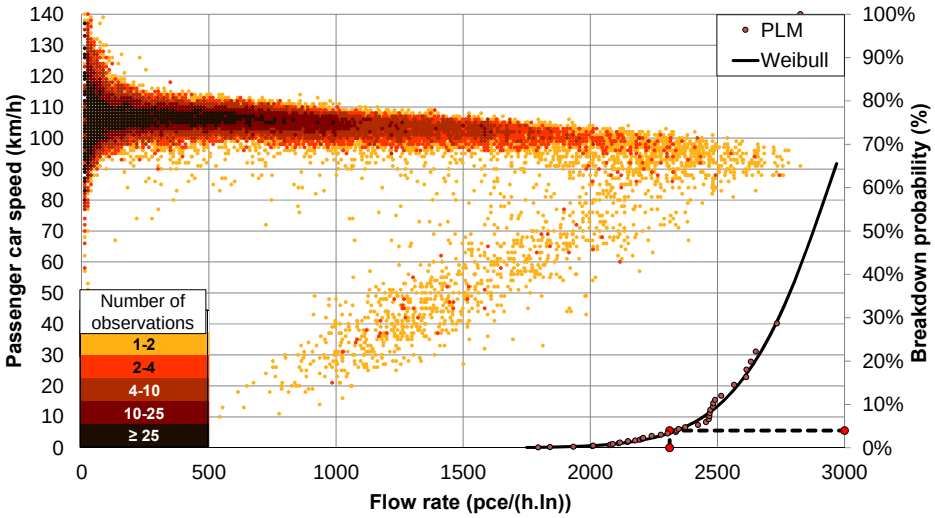

FIGURE 3 Speed–flow data, PLM model, and fitted Weibull distribution for site SP021, km 22 N.

Results for Estimation of Density at Capacity

The procedure was applied to the eight sites where the capacity was reached. Figure 3 shows data collected at km 22 N on SP021. The capacity is 2250 pcph/lane and the average traffic speed at capacity is 88 km/h; thus density at capacity is 2,250/88 – 25.6 pcpkm/lane. Table 1 summarizes the results.

The estimates for *CD* in Table 1 are very similar, except for two of the sites. These sites are the steepest climbing grades. Thus, an explanation for lower capacity could be the combined effects of grade magnitude and length. Therefore, these two sites were excluded from the sample, to avoid any bias in the estimation of *CD*. The average *CD* for urban sites is 25 pcpkm/lane and the average *CD* for rural sites is 26 pcpkm/lane. The HCM 2010 adopts 28 pcpkm/lane for freeways and 25 pcpkm/lane for multilane highways.

TRANSITION POINT *BP*

The other key point that defines the speed–flow function is *BP*, the transition point between the flat and the curved portions of the functions (Figure 1). The estimation of values for *BP* was based on the method used in the HCM 2010 (*8*). In the development of the HCM 2010, the data set used for the calibration of the functions was built by clustering all speed-flow observations for sites with similar FFS. However, Roess (*8*) argues that the results were unsatisfactory, from a regression statistics viewpoint, and required judgmental adjustments. A slightly different approach was used in this research: *BP* was estimated for each site and this set of *BP* values was used to fit a *BP* function.

Method

Assuming that in the first portion of the speed-flow relationship, the average speed is equal to FFS, the standard deviation σ of the observed speeds x_i with a relation to FFS can be calculated:

$$\sigma = \sqrt{\frac{\sum (x_i - FFS)^2}{N}} \tag{12}$$

TABLE 1 Capacity, Speed at Capacity, and Density at Capacity Estimates for the Sample

Location	Land Use	FFS (km/h)	*C* (pcph/lane)	*CS* (km/h)	*CD* (pcpkm/lane)	Grade (%)
SP348 km 32 N	Rural	116	2,400	93	25.8	3.5
SP021 km 18 N	Rural	108	2,390	90	26.5	–1.0
SP021 km 18 S	Rural	105	2,375	87	27.3	1.0
SP021 km 22 N	Rural	107	2,312	95	24.3	–2.0
SP280 km 27 E	Urban	107	2,145	88	24.4	3.5
SP280 km 29 E	Urban	105	2,165	86	25.2	2.0
SP280 km 37 E	Rural	116	1,950	96	20.3	5.0
SP280 km 51 E	Rural	110	1,975	88	22.4	4.5

where x_i is the observed speeds for a given range of traffic flows (e.g., 200 to 250 pcph/lane); N is the number of speed observations for that flow range; and FFS is the free-flow speed for the site.

To find *BP*, Roess (*8*) plotted σ versus flow rate; *BP* corresponds to the minimum value of σ. In this study, a third-degree polynomial was fitted to the function $\sigma = f(q)$ and *BP* was defined as the flow rate for which the derivative of the fitted polynomial becomes positive, corresponding to the minimum value of σ. The third-degree polynomial was chosen because it provided the best fit to the data. Furthermore, this procedure can be automated in an Excel spreadsheet and provides a criterion for selecting *BP* that does not depend on personal judgment.

Results for Estimation of Break Points

The method was applied to all sites in the sample because the transition point can be found even for sites that do not reach the capacity. For each site, σ was calculated for each 50-pcphpl range for flows rates greater than 200 pcph/lane (i.e., 200 to 250, 250 to 300, and so on). The graphs in Figure 4 illustrate the procedure.

The left vertical axis in Figure 4 shows the speed and the right *y*-axis, the standard deviation for speeds around FFS. Speed–flow observations are orange-to-black points; green data points are σ versus flow data; and the green curve is the fitted polynomial. The bigger green dot represents *BP* for the site (i.e., the minimum of the fitted polynomial). For the site shown in the graph of Figure 4*a*, a rural location, *BP* is 530 pcph/lane; for the other site, an urban location, *BP* is estimated as 420 pcph/lane.

The results suggest that the vertical profile has little influence on *BP*, thus data from all sites could be used in the analysis. Note that *BP* decreases as FFS increases, and that the rate of decrease is greater for urban sites. The values for *BP* found for urban expressways were smaller than those found for rural expressways. The relationship between *BP* and FFS, for rural expressways, was

$$BP = -7.6\ \text{FFS} + 1{,}422 \quad (R^2 = 0.53) \tag{13}$$

and the model fitted for urban expressways was

$$BP = -3.75\ \text{FFS} + 835 \quad (R^2 = 0.62) \tag{14}$$

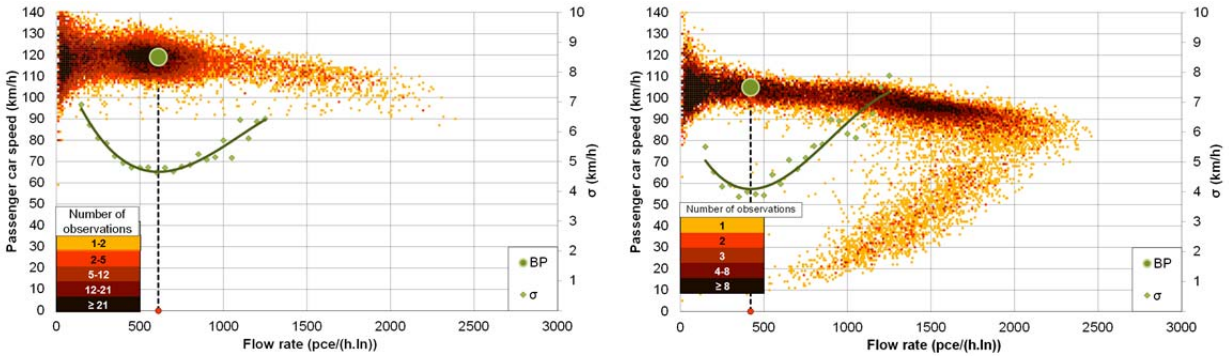

(a) **(b)**

FIGURE 4 *BP* and σ, the speed standard deviation around FFS, for two sites in the sample: (*a*) rural freeway (SP280, km 59 E) and (*b*) urban freeway (SP280, km 29 E).

In both cases, the values found for *BP* (in km/h) are significantly lower than those presented in the HCM 2010, showing evidence of the differences between American and Brazilian drivers. Whereas these differences undoubtedly exist, they might be smaller, since Roess has also found lower values for *BP*, which were later increased by the freeways committee to make the curves achieve a more uniform appearance (*8*).

SPEED–FLOW RELATIONSHIPS FOR EXPRESSWAYS IN BRAZIL

Once the anchor points for the convex segment of the speed–flow relationships were estimated, the next step was the calibration of the speed–flow functions. This calibration involves finding the best values for parameters used in Equations 5, 6, and 7; i.e., those values that minimize the differences between observed speed-flow data and speed-flow estimates obtained using the model. The adopted approach consisted of finding the calibration parameter set that minimized the error for all data collection locations simultaneously.

Data Set for Calibration and Calibration Procedure

To create the data set for calibration of the speed–flow functions, speed–flow observations for the 24 stations were divided into sets covering 50-pcph ranges (i.e., 0 to 50, 51 to 100 pcph and so on). The median for speeds was then calculated for each set, for sets with at least 10 observations. Thus, a total of 957 points (average and median) were obtained, including 237 points for urban sites and 720 for rural sites. Figure 5*a* illustrates the data, showing the median of observed speeds for three of the 24 sites in the sample.

Using the median for each flow rate range, instead of the actual speed–flow observations was chosen to avoid bias due to greater density of information for lower flow rates, when compared to the number of observations closer to capacity (*18*). The adopted approach ensures two conditions: (*a*) each flow range has the same weight when calibrating the speed-flow function and (*b*) the data from sites where the capacity is reached have a greater influence on the calibrated function than data from sites where the capacity is not reached.

The calibration procedure used involves an optimization problem whose objective is to minimize the squared error between the speed estimated using the model and the median of observed speeds for each of the 957 points in the sample, as used in other studies (*27*, *28*).

Given that the "anchor points" *BP* and *CD* are fixed, there are three unknowns: the constants a_c and b_c in Equation 7, which defines the capacity, and the exponent γ in Equation 5, which determines the concavity of the function. Furthermore, in order to produce a consistent set of curves (i.e., curves with similar shapes), the following restrictions were imposed: (*a*) $\gamma \geq 1$ and has the same value for any FFS, to ensure the same concavity and shape for all speed–flow curves; (*b*) *BP* must be constant or a function of FFS (as in Equations 13 and 14); and (*c*) *C* and *CS* must also be a function of FFS.

A nonlinear optimization algorithm, the generalized reduced gradient algorithm, implemented in MS-Excel was used to solve the problem. To avoid local optima, the procedure was replicated 10 times, with different seeds, and the best solution was chosen.

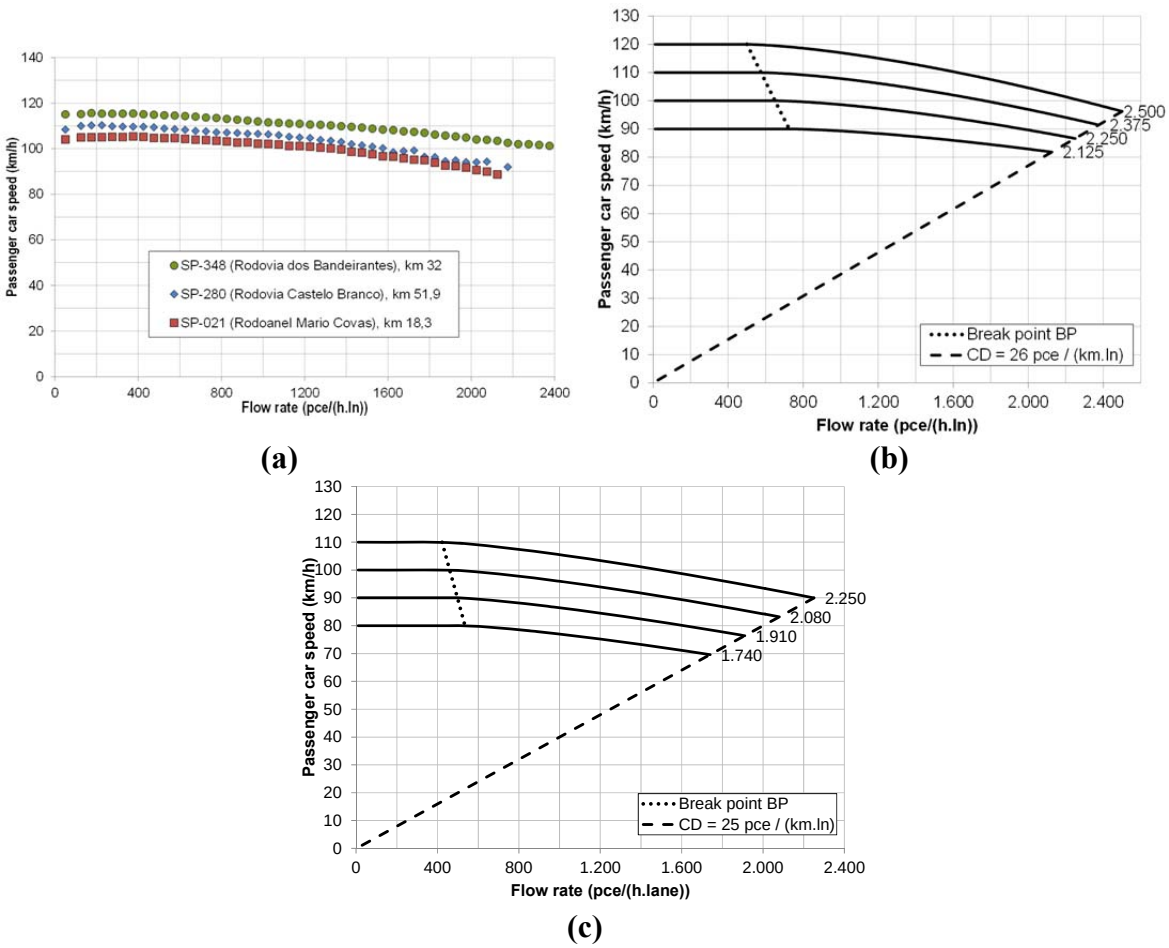

FIGURE 5 Proposed speed–flow relationships for expressways in Brazil: (*a*) data set for calibration of the models; (*b*) calibrated models for rural expressways; (*c*) calibrated models for urban expressways.

Figure 5*b* illustrates the proposed speed–flow relationships for rural expressways. The calibrated model is

$$S = \begin{cases} FFS, & \text{if } v \le -7.5FFS + 1400 \\ FFS - \left(FFS - \dfrac{C}{26}\right)\left[\dfrac{v - (-7.5FFS + 1400)}{C - (-7.5FFS + 1400)}\right]^{1,5} \end{cases} \quad (15)$$

with $C = 12.5FFS + 1000,$

where S is the traffic stream average speed (km/h); v is the traffic flow rate (pcph/lane); FFS is the FFS (km/h); and C is capacity (pcph/lane). The dotted line in Figure 5*b* shows *BP*, the limit for the flat portion of the speed–flow relationship; and the broken line in Figure 5*b* represents density at the capacity (26 pcpkm/lane).

The graph in Figure 5*c* shows the proposed speed–flow relationships for urban expressways, which can be written as

$$S = \begin{cases} FFS, & \text{if } v \le -3.75FFS + 835 \\ FFS - \left(FFS - \dfrac{C}{25}\right)\left[\dfrac{v - (-3.75FFS + 835)}{C - (-3.75FFS + 835)}\right]^{1,3} \end{cases} \quad (16)$$

with $C = 17FFS + 380$.

The transition point *BP* is represented by a dotted line in Figure 5*c* and capacity at density, by a broken line. Note that, for urban expressways, the transition point *BP* appears at lower flow rates, compared to rural expressways. Furthermore, estimates of capacity *C* and speed at the capacity *CS* are greater for rural expressways than for urban expressways.

The graphs in Figure 6 compare the HCM 2010 model for freeways (green line) to the proposed model (blue line) and the empirical speed–flow data, for a rural expressway and for an urban expressway. In both cases, the proposed models are clearly a better fit. The HCM 2010 models, which were calibrated using data from American freeways, overestimate the speed for flow rates between 1,000 and 1,800 pcph/lane and underestimate the speed for flow rates greater than 2000 pcph/lane. Table 2 summarizes the comparison between the proposed models and the HCM 2010 models.

CONCLUSIONS

This paper presents a set of speed–flow relationships for expressways in Brazil developed to replace the original curves presented in the HCM 2010. The models are based on formulations adopted in the development of the HCM 2010 speed–flow curves and were calibrated using speed–flow data collected in 24 permanent traffic-counting stations in highways in the state of São Paulo. The empirical data showed that access control does not influence traffic behavior as much as abutting land use. Therefore, the proposed models are divided into urban versus rural instead of using the HCM 2010 freeways versus multilane highways scheme. Compared to the HCM 2010 models, the proposed speed–flow relationships present: (*a*) lower density at capacity: 26 pcpkm/lane for rural sites and 25 pcpkm/lane for urban segments; (*b*) significantly lower break points *BP*, beyond which congestion starts to reduce the speed of the traffic stream; (*c*) higher speed at capacity; and (*d*) greater capacity for segments with higher FFS (120 and 110 km/h) and lower capacity for segments with lower FFS (100 and 90 km/h).

As expected, the proposed models were better fitted to the traffic data than the HCM 2010 models. However, it would be very desirable to increase the sample size, to include not just more sites, but especially sites with FFS around 90 km/h and segments in mountainous terrain, which were missing in the available sample. An extension of this research is currently under way to analyze traffic flows on a lane-by-lane basis, given the observed differences in truck percentages.

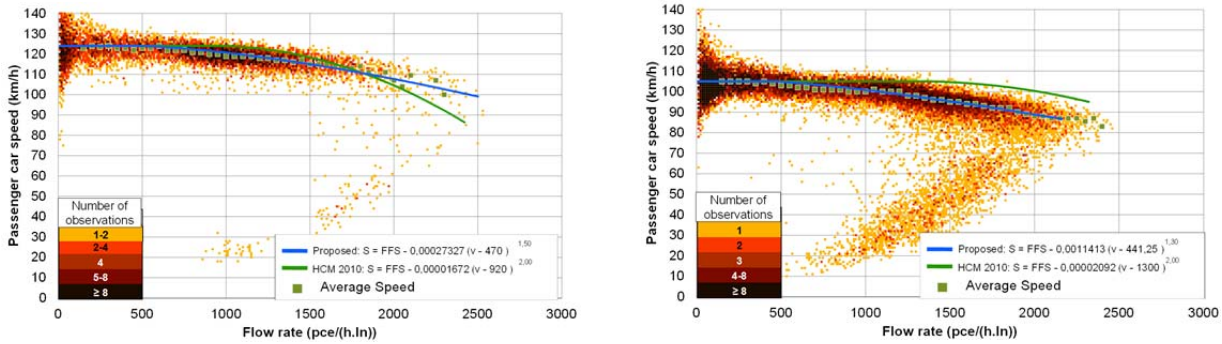

FIGURE 6 Comparison of speed–flow relationships (proposed model and HCM 2010 model) to empirical data for two sites in Brazil: (*a*) rural expressway (SP348 km 50 N) and (*b*) urban expressway (SP280 km 29 E).

TABLE 2 Estimated Values for Main Parameters of Speed–Flow Relationships for Rural and Urban Expressways in Brazil

FFS (km/h)	Transition Point *BP* (pcph/lane)		Capacity *C* (pcph/lane)		Speed at Capacity *CS* (km/h)	
	Proposed Model	HCM 2010	Proposed Model	HCM 2010	Proposed Model	HCM 2010
Rural						
120	500	1,000	2,500	2,400	96	86
110	575	1,200	2,375	2,350	91	84
100	650	1,400	2,250	2,300	87	82
90	725	1,600	2,125	2,250	82	80
Urban						
110	420	na	2,250	na	90	na
100	460	na	2,080	na	83	na
90	500	na	1,910	na	76	na
80	535	na	1,740	na	70	na

NOTE: na = not applicable.

ACKNOWLEDGMENTS

The authors recognize the support from ARTESP, CCR RodoAnel, CCR ViaOeste, and CCR AutoBan, which kindly provided traffic data. The authors also acknowledge the financial support provided by CNPq for this research (Grant 303341/2008-4).

REFERENCES

1. DNIT. *Manual de Estudos de Tráfego*. Publication IPR-723. Departamento Nacional de Infraestrutura de Transportes, Instituto de Pesquisas Rodoviárias, Rio de Janeiro, Brazil, 2006.
2. Demarchi, S. H., and J. R. Setti. Limitations of Passenger-Car Equivalent Derivation for Traffic Streams with More Than One Truck Type. In *Transportation Research Record: Journal of the*

Transportation Research Board, No. 1852, Transportation Research Board of the National Academies, Washington, D.C., 2003, pp. 96–104.
3. Egami, C. Y., and J. R. Setti. Adaptação do HCM2000 para Determinação do Nível de Serviço em Rodovias de Pista Simples no Brasil. *Transportes*, Vol. 14, No. 2, 2006, pp. 27–34. Available at http://revistatransportes.org.br/anpet/article/view/66. Accessed July 29, 2013.
4. Andrade, G. R., K. C. Rodrigues-Silva, and R. G. Gouvêa. Aplicabilidade das Metodologias Rodoviárias do Highway Capacity Manual 2000 no Brasil. In *Anais do XXII Congresso de Pesquisa e Ensino em Transportes—Fortaleza*. CD-ROM. Associação Nacional de Pesquisa e Ensino em Transportes, Rio de Janeiro, Brazil, 2008.
5. Setti, J. R. Highway Capacity Manual ou Manual de Capacidade Viária? In *Anais do 6° Congresso Brasileiro de Rodovias e Concessões—CBR&C 2009*. CD-ROM. Associação Brasileira de Concessionárias de Rodovias, Florianópolis, Brazil, 2009.
6. Andrade, G. R., K. C. Rodrigues-Silva, and S. A. Puty-Filho. Panorama Normativo e Tecnológico da Avaliação Operacional das Concessões Rodoviárias. In *Anais do 7° Congresso Brasileiro de Rodovias e Concessões—CBR&C 2011*. CD-ROM. Associação Brasileira de Concessionárias de Rodovias, Foz do Iguaçu, Brazil, 2011.
7. Cunha, A. L., and J. R. Setti. Truck Equivalence Factors for Divided, Multilane Highways in Brazil. Proc., 6th International Symposium on Highway Capacity and Quality of Service, 2011, Stockholm. Procedia–Social and Behavioral Sciences. Elsevier, Amsterdam, Vol. 16, 2011, pp. 248–258.
8. Roess, R. P. Speed–Flow Curves for Freeways in the 2010 HCM. In *Transportation Research Record: Journal of the Transportation Research Board, No. 2257*, Transportation Research Board of the National Academies, Washington, D.C., 2011, pp. 10–21.
9. Hall, F. L., and K. Agyemang-Duah. Freeway Capacity Drop and the Definition of Capacity. In *Transportation Research Record 1320*, TRB, National Research Council, Washington, D.C., 1991, pp. 91–98.
10. Urbanik II, T., W. Hinshaw, and K. Barnes. Evaluation of High-Volume Urban Texas Freeways. In *Transportation Research Record 1320*, TRB, National Research Council, Washington, D.C., 1991, pp. 110–118.
11. Banks, J. H. Flow Processes at Freeway Bottleneck. In *Transportation Research Record 1287*, TRB, National Research Council, Washington, D.C., 1990, pp. 20–28.
12. Persaud, B. N. and V. F. Hurdle. Some New Data that Challenge Some Old Ideas About Speed-Flow Relationships. In *Transportation Research Record 1194*, TRB, National Research Council, Washington, D.C., 1988, pp. 191–198.
13. Hall, F. L., and L. M. Hall. Capacity and Speed-Flow Analysis of Queen Elizabeth Way in Ontario. In *Transportation Research Record 1287*, TRB, National Research Council, Washington, D.C., 1990, pp. 20–28.
14. Chin, H. C., and A. D. May. Examination of the Speed-Flow Relationships at the Caldecott Tunnel. In *Transportation Research Record 1320*, TRB, National Research Council, Washington, D.C., 1991, pp. 75–82.
15. *Highway Capacity Manual*. TRB, National Research Council, Washington, D.C., 2000.
16. *Highway Capacity Manual 2010*. Transportation Research Board of the National Academies, Washington, D.C., 2010.
17. Demarchi, S. H., and J. R. Setti. Calibração da curva fluxo-velocidade-densidade para rodovias de pista dupla brasileiras. In *Anais do XI Congresso Panamericano de Engenharia de Trânsito e Transportes—Gramado, Rio Grande do Sul*. Associação Nacional de Pesquisa e Ensino em Transportes, Rio de Janeiro, Brazil, 2000, pp. 131–144.
18. Bassan, S. and A. Polus. Meaning of Actual Capacity of Freeways and its Estimation. *Canadian Journal of Civil Engineering*, Vol. 37, 2010, pp. 77–87.
19. Washburn, S. S., Y. Yin, V. Modi, and A. Kulshrestha. *Investigation of Freeway Capacity, Part B: Freeway Capacity Estimation for Florida Freeways, Final Report*. Transportation Research Center, University of Florida, Tallahassee, FL, 2010.

20. Andrade, G. R., and J. R. Setti. Método para Caracterização e Classificação de Trechos Homogêneos Rodoviários. *Anais do 7° Congresso Brasileiro de Rodovias e Concessões—CBR&C 2011*. CD-ROM. Associação Brasileira de Concessionárias de Rodovias, Foz do Iguaçu, Brazil, 2011.
21. Brilon, W., J. Geistefeldt, and H. Zurlinden. Implementing the Concept of Reliability for Highway Capacity Analysis. In *Transportation Research Record: Journal of the Transportation Research Board, No. 2027*, Transportation Research Board of the National Academies, Washington, D.C., 2007, pp. 1–8.
22. Brilon, W., J. Geistefeldt, and M. Regler. Reliability of Freeway Traffic Flow: A Stochastic Concept of Capacity. *Proc., 16th International Symposium on Transportation and Traffic Theory*, College Park, Md., 2005, pp. 125–144.
23. Kaplan, E. L., and P. Meier. Nonparametric Estimation from Incomplete Observations. *Journal of the American Statistical Association*, Vol. 53, 1958, pp. 457–481.
24. Lorenz, M., and L. Elefteriadou. A Probabilistic Approach to Defining Freeway Capacity and Breakdown. In *Transportation Research Circular E-C108: Proceedings of the 4th International Symposium on Highway Capacity,* TRB, National Research Council, Washington, D.C., 2001.
25. Bessa Jr., J. E., and J. R. Setti. Derivation of ATS and PTSF Functions for Two-lane, Rural Highways in Brazil. *Proc., 6th International Symposium on Highway Capacity and Quality of Service, 2011, Stockholm. Procedia—Social and Behavioral Sciences*. Elsevier, Amsterdam, Vol. 16, 2011, pp. 282–292.
26. Geistefeldt, J. Empirical Relation Between Stochastic Capacities and Capacities Obtained from the Speed–Flow Diagram. In *Transportation Research Circular E-C149: 75 Years of the Fundamental Diagram for Traffic Flow Theory*, Transportation Research Board of the National Academies, Washington, D.C., 2011, pp. 147–156.
27. Rakha, H. and M. Arafeh. Calibrating Steady-State Traffic Stream and Car-Following Models Using Loop Detector Data. *Transportation Science*, Vol. 44, No. 2, 2010, pp. 151–168.
28. Sun, L., J. Yang, H. Mahmassani, W. Gu, and B. J. Kim. Data Mining-Based Adaptive Regression for Developing Equilibrium Speed-Density Relationships. *Canadian Journal of Civil Engineering*, Vol. 37, 2010, pp. 389–400.

Room for Improvement
A Critique of the HCM Freeway Analysis Procedure

DAVID STANEK
Fehr & Peers

With an update of the *Highway Capacity Manual* (HCM) scheduled for 2015, now is the time to revisit the freeway analysis procedures. In this paper, three areas for improvement are identified, some of which will require further research. Clarifications and corrections that have recently been released have provided additional guidance on selecting the appropriate analysis procedure for a given freeway segment. While the manual discusses the overlap of a merge segment followed by a diverge segment, the overlap of influence areas for other combinations are not covered. An approach for handling adjacent segments separated by less than 1,500 ft is suggested based on the configuration and analysis results. Capacity checkpoints are used in the merge and diverge segment procedures to determine if the ramp roadway, upstream freeway, or downstream freeway volumes exceed certain capacity thresholds. These checkpoints should be added to the weaving procedure since the same capacity constraints may occur. In fact, the capacity checkpoints use general threshold values, so a better approach would be to substitute the basic segment procedure for the capacity checkpoints. Despite the 2010 HCM update, the weaving segment procedure remains insensitive to the split in weaving volume between the freeway-to-off-ramp and on-ramp-to-freeway volumes. A suggested approach would be to use the merge or diverge segment procedure when the volumes are particularly imbalanced. Additionally, more guidance is needed for complex weaving areas that may not adequately capture the capacity effects of lane changing if split into separate basic, merge, and diverge segments.

With an update of the *Highway Capacity Manual* (HCM) scheduled for 2015, now is a good time to revisit the freeway analysis procedures. In this paper, the following three areas for improvement are identified:

- Defining freeway segments,
- Capacity checkpoints, and
- Weaving segment procedure.

Recently released HCM clarifications and corrections (*1*) have provided additional guidance on selecting the appropriate analysis procedure for a given freeway segment. However, this guidance does not cover some common situations. While the manual discusses the overlap of a merge segment followed by a diverge segment, the overlap of influence areas for other segment types are not covered. An approach for handling adjacent segments separated by less than 1,500 ft is suggested based on the configuration and analysis results.

Capacity checkpoints are used in the merge and diverge segment procedures to determine if the ramp roadway, upstream freeway, or downstream freeway volumes exceed certain capacity thresholds. These checkpoints should be added to the weaving procedure since the same capacity constraints may occur. Since some segments that are initially assigned as merge, diverge, or weaving segments are actually analyzed using the basic procedure, the basic procedure should

also have the capacity checkpoints. In fact, the capacity checkpoints use general threshold values, so a better approach would be to use the basic segment procedure instead to determine if capacity is exceeded.

Despite the 2010 HCM update, the weaving segment procedure remains insensitive to the split in weaving volume between the freeway-to-off-ramp and on-ramp-to-freeway volumes. A suggested approach would be to use the merge or diverge segment procedure when the volumes are particularly imbalanced. Additionally, more guidance is needed for complex weaving areas that may not adequately capture the capacity effects of lane changing if split into separate basic, merge, and diverge segments.

DEFINING FREEWAY SEGMENTS

Chapter 10 in the HCM (*2*) provides guidance on dividing a freeway corridor into analysis segments. Merge, diverge, weaving, and basic segments are defined on page 10-2. Figure 1 shows the definition of the first three types. All other freeway segments are basic segments.

Pages 10-21 through 10-24 of the HCM provide additional guidance for defining freeway segments. In the first example, an on-ramp is followed by an off-ramp without a connecting auxiliary lane (2, Exhibit 10-12). Figure 2 shows the possible cases based on the ramp influence distance of 1,500 ft. Operations in the overlap segment are assigned from the worst of the merge and diverge analysis results. In the second example, weaving segments that do not meet a minimum threshold weaving length based on volume should be analyzed as basic segments (*1*).

Another situation is described in the Freeway Merge and Diverge Segments chapter. Segments with a single lane on-ramp that adds a freeway lane or a single lane off-ramp that drops a freeway lane should be analyzed as a basic segment (*1*).

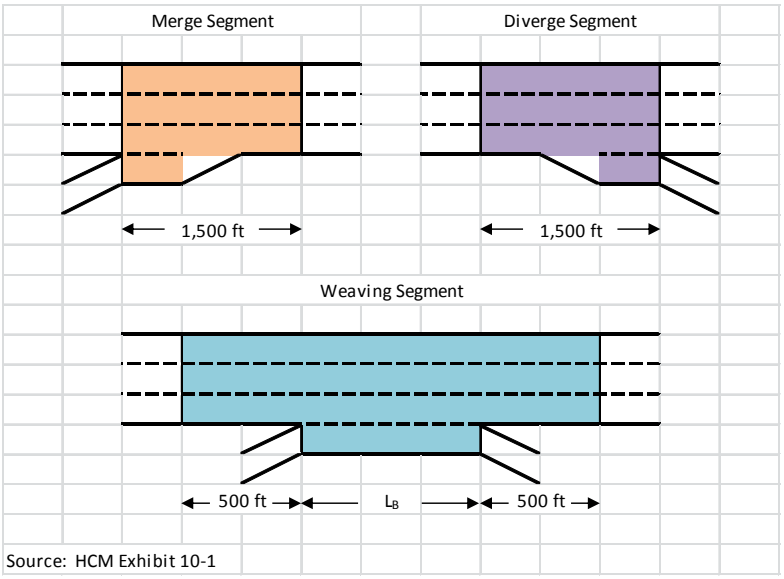

FIGURE 1 Freeway segment definitions.

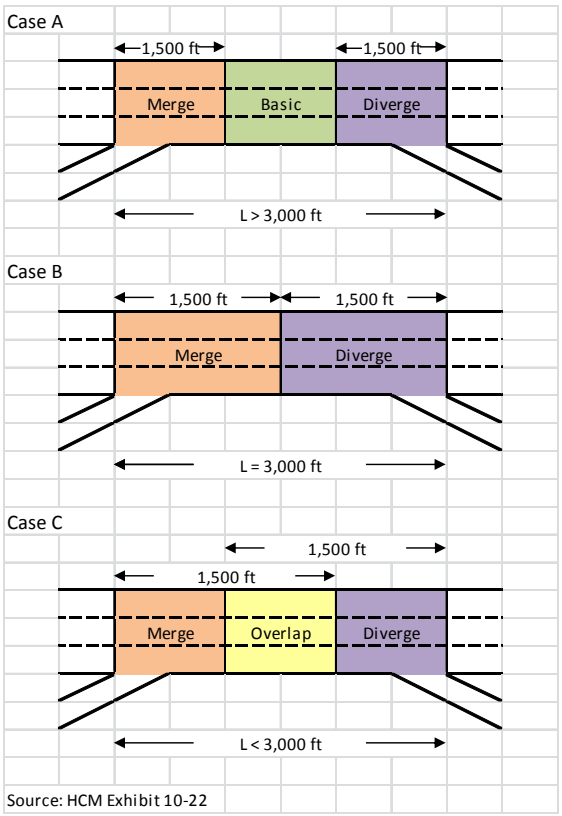

FIGURE 2 On-ramp followed by off-ramp.

While this guidance is useful, other freeway configurations exist that are not covered by these conditions. Several such conditions are described below with suggested approaches to defining the freeway segments.

The HCM defines the overlap of merge and diverge segments, but overlaps of two merge segments, two diverge segments, and merge or diverge with weaving segments also occur. Figure 3 shows the freeway segment definitions at adjacent on-ramps, which is similar to the on-ramp followed by off-ramp configurations in Figure 2. In Case C, the merge influence areas overlap. Thus, the overlap concept in Figure 2 potentially could be applied in this situation. However, this does not appear to be the intent of the procedure since the effect of adjacent ramps is accounted for in the merge and diverge analysis procedures (for three-lane freeways, see HCM Chapter 13). Therefore, the upstream merge segment is recommended to end at the downstream on-ramp gore and have a distance less than 1,500 ft. The cases for adjacent off-ramps would be similar.

Merge or diverge segments adjacent to weaving segments are more complicated. Weaving segments extend 500 ft upstream of the on-ramp gore and downstream of the off-ramp gore because field observation has shown that drivers anticipate the lane changes to be undertaken (*2*, p. 12-3). The upstream weaving influence area may overlap with a merge influence area, and the downstream weaving influence area may overlap with a diverge influence area. The suggested procedure would be to apply the overlap segment concept for overlapping merge and diverge segments. The assigned analysis result for the overlap segment would be the worst operating condition of the adjacent segments. If the distance from the merge segment's on-

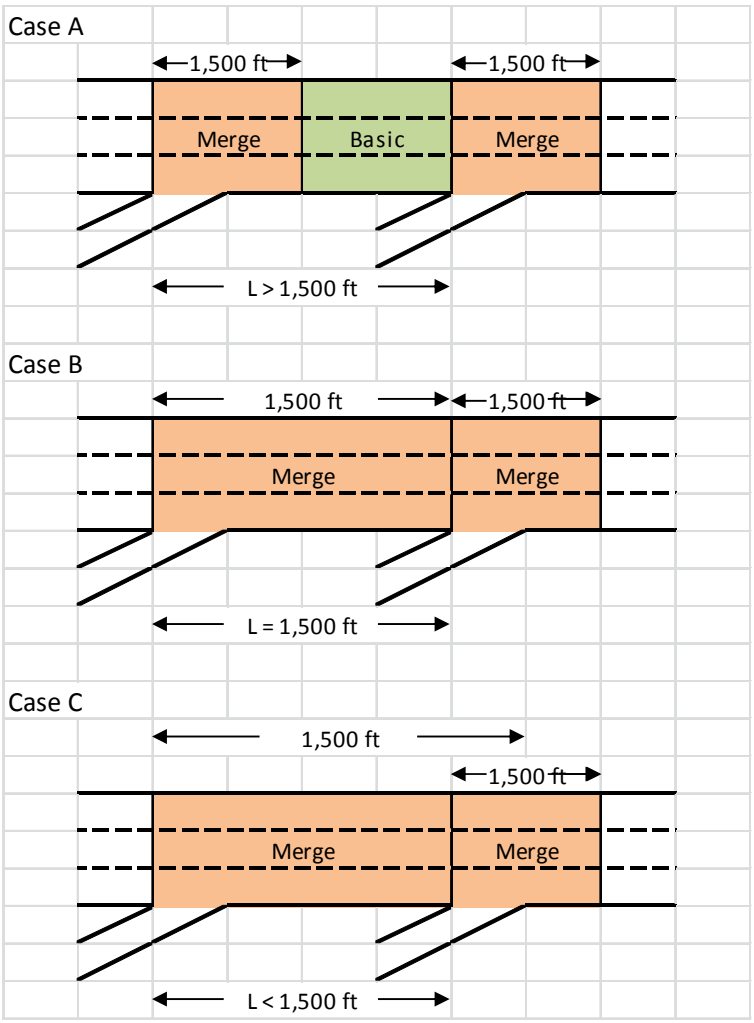

FIGURE 3 On-ramp followed by on-ramp.

ramp gore to the weaving segment's on-ramp gore were less than 1,500 ft, the merge segment would be shortened similar to the approach with adjacent on-ramps. Figure 4 shows the suggested approach. A similar approach would be applied to a weaving segment following a diverge segment.

While the suggested rules above would help to clarify how to define freeway segments, the distances used for merge, diverge, and weaving influence areas seem arbitrary. For some conditions, the actual merge influence area may be shorter or longer than 1,500 ft. Similarly, the weaving influence area may be more or less than 500 ft from the ramp gore. Whether a weaving segment is to be analyzed using the weaving or basic procedure depends on the freeway and ramp volumes. Similarly, volumes could be used to develop a procedure to estimate the ramp influence area distance.

Another approach would be to apply the overlap segment concept. For example, the 1,000-ft long segment at the boundary of merge and basic segments would be redefined as an overlap segment. This segment would be assigned the higher of the delay results for the adjacent segments (Figure 5). The determination of influence area length is suggested for further research.

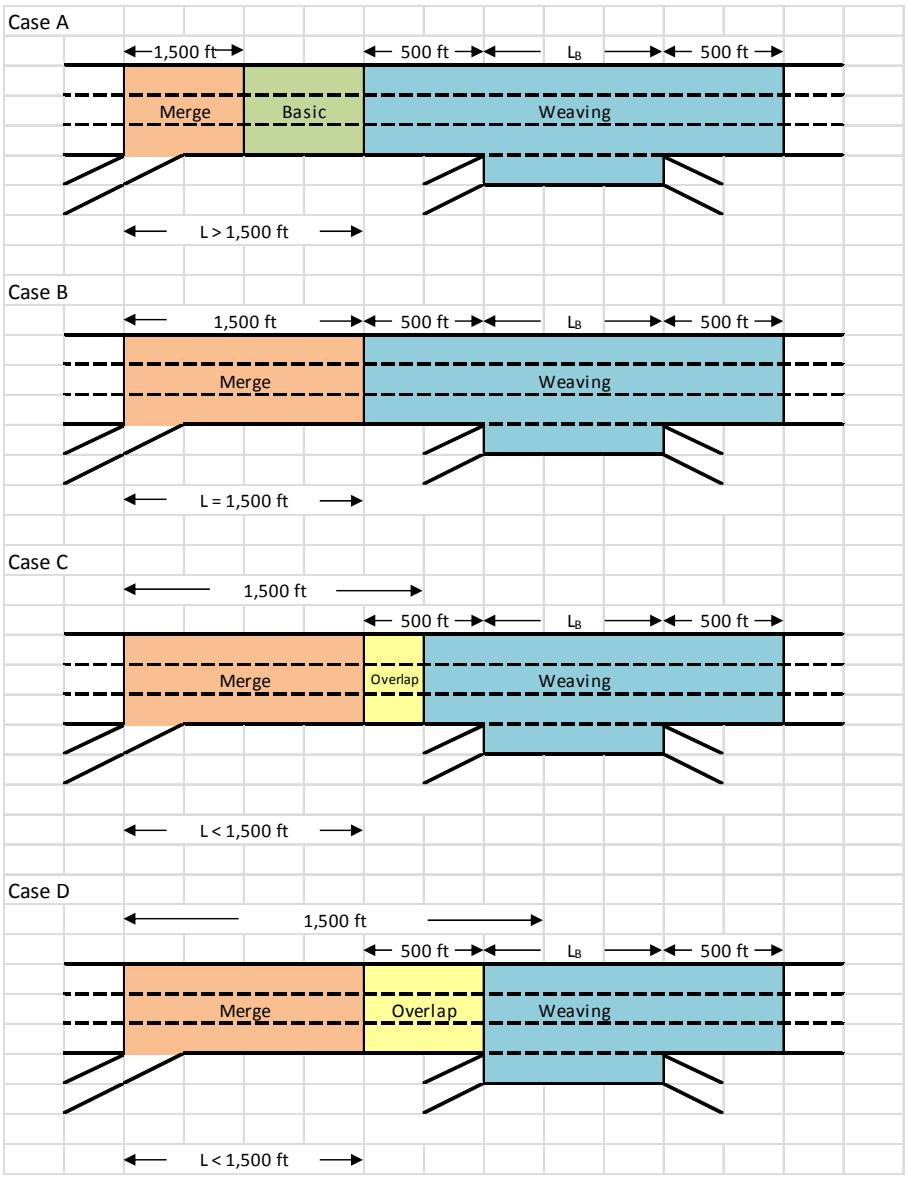

FIGURE 4 On-ramp followed by weaving segment.

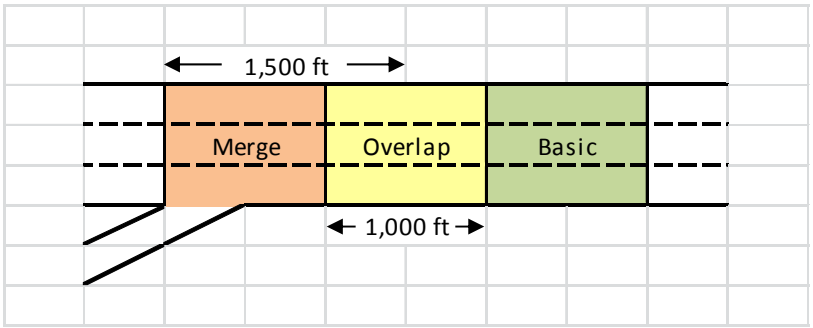

FIGURE 5 Potential overlap segment.

CAPACITY CHECKPOINTS

The merge and diverge segment analysis procedure includes capacity checkpoints: the exiting freeway volume at the merge segment (v_{FO}), the entering freeway volume at the diverge segment (v_F), and the ramp roadway (v_R). For ramp junctions with lane additions or lane drops, both the entering (v_F) and exiting (v_{FO}) freeway volume must be checked (*2*, pp. 13–18). Figure 6 shows the volumes that have checkpoints under the merge and diverge segment procedures.

Although weaving segments have similar features to ramp junctions (on-ramp, off-ramp, and entering and exiting freeway volumes), the weaving analysis procedure does not include capacity checkpoints. As a result, a ramp volume that is unreasonably high, for example, would not be flagged as a potential bottleneck in the weaving segment analysis. Similarly, there may be conditions where the on-ramp volume is high and the off-ramp volume is low such that the exiting freeway volume may be over capacity even though the weaving segment operates acceptably. It is recommended that capacity checkpoints be added to the weaving procedure.

Some freeway segments with ramps are analyzed using the basic segment procedure: at single lane ramps with a lane addition or drop and weaving segments where the weaving length is less than the critical weaving length. For these cases, the capacity checkpoints tests should still be conducted.

The capacity checkpoints for the freeway mainline use a lookup table based on free-flow speed. However, capacity decreases with increasing volume as shown in the Basic Segments chapter (*2*, Exhibit 11-2). To be more precise, the capacity checkpoints should be replaced with the basic segment procedure. So, the procedures for merge, diverge, and weaving segments would incorporate the basic segment to check input and output freeway segment capacity. As part of this recommendation, the ramp capacity checkpoint would be retained.

For merge and diverge segments, the basic procedure would be applied first using the entering and exiting freeway volumes (v_F and v_{FO}). For weaving segments, the basic procedure would also be applied for the volume in the weaving segment (the sum of v_F and v_R). If a capacity constraint were uncovered, the segment could be assigned as level of service (LOS) F and no further analysis would be performed. For the conditions noted above where the merge, diverge,

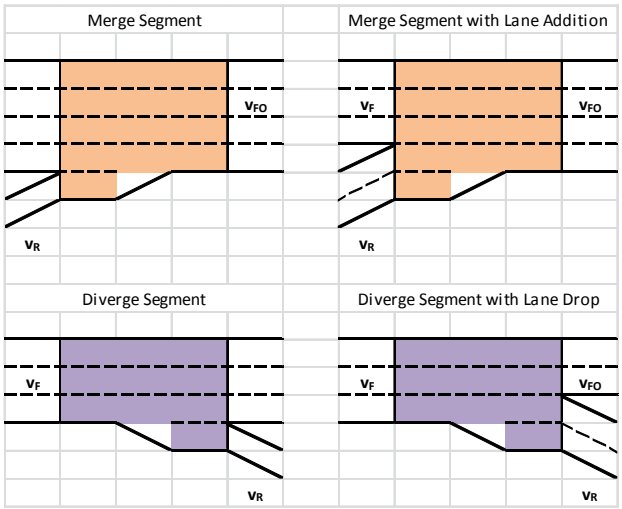

FIGURE 6 Capacity checkpoints.

or weaving segment would be analyzed as a basic segment instead, the segment could retain the initial definition and still have the appropriate analysis procedure. For example, all freeway segments with an on-ramp would be defined as a merge segment. This could clear up the confusion caused by segments with ramps that are analyzed using the basic segment procedure.

WEAVING SEGMENT PROCEDURE

The 2010 edition of the HCM introduced a new procedure for analyzing weaving segments. Although the procedure applies a different capacity equation, the input volume calculation is unchanged from the previous version. That is, the capacity equation uses the total weaving volume such that the relative split between freeway to ramp volume (v_{FR}) and ramp to freeway volume (v_{RF}) does not affect the analysis result. This limitation as it applies to the HCM 2010 procedure is described below.

Figure 7 shows an example weaving segment. In the procedure, the weaving volume ($v_W = v_{RF} + v_{FR}$) and nonweaving volume ($v_{NW} = v_{FF} + v_{RR}$) are determined. Then, the speed is estimated for these two flows. The final density estimate is based on a volume-weighted average of the weaving and nonweaving speeds. Because the freeway to ramp and ramp to freeway volumes are grouped, the effect of a relatively high volume for one of the two ramps is not taken into account. As a result, varying combinations of v_{RF} and v_{FR} yield about the same analysis result as long as the sum is constant.

Table 1 presents analysis results for an example weaving segment. The input parameters listed below the table remain the same across scenarios; only the distribution of weaving volume was changed. For the two cases where the freeway to ramp volume is higher, the diverge analysis results are presented. For the two cases where the ramp to freeway is higher, the merge analysis results are presented.

For the four cases presented in Table 1, the calculated weaving segment density varies by 0.2 vehicles per lane per mile. In contrast, the ramp junction results show more variability. In all

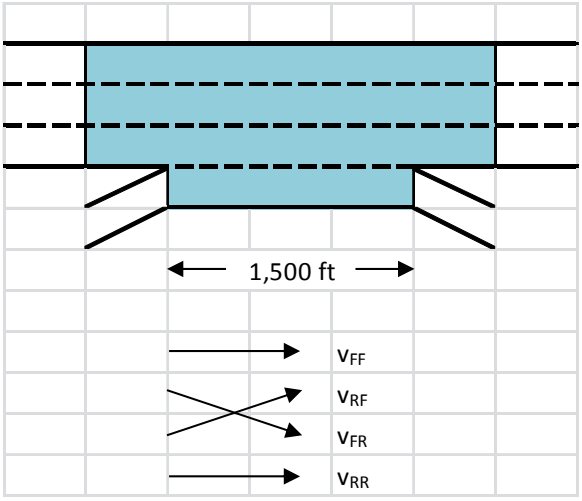

FIGURE 7 Example weaving segment.

TABLE 1 Example Analysis Results Comparison

Case	Weaving Volume		HCM Weaving		HCM Merge / Diverge	
	v_{FR}	v_{RF}	LOS	Density	LOS	Density
1	1,500	0	E	38.5	D	32.9
2	1,250	250	E	38.5	D	32.6
3	250	1,250	E	38.3	E	35.9
4	0	1,500	E	38.3	E	36.6

NOTE: Input parameters:

Lane configuration for weaving analysis = same as shown in Figure 7.
Lane configuration for merge/diverge analysis = deceleration/acceleration lane length of 1,000 ft.
Total segment volume = 6,500 vph.
Ramp-to-ramp volume (v_{RR}) = 0 vph.
Freeway free-flow speed = 65 mph.
Ramp free-flow speed = 45 mph.
Ramp and freeway terrain = level.
Ramp and freeway peak hour factor = 0.95.
Freeway truck and bus percentage = 6%.
Ramp truck and bus percentage = 3%.
Interchange density = 2 interchanges per mile.
Passenger car equivalents for trucks and buses = 1.5.
Driver population factor = 1.0.

cases, the density is higher in the weaving results. The crossing paths of vehicles in a weaving segment would have more turbulence. Ramp junctions have ramp traffic only in one direction, so it is reasonable that density would be lower. In the comparison of weaving and diverge calculations, the diverge analysis results are one LOS grade better.

For cases where the imbalance in freeway to ramp and ramp to freeway volume is relatively high, the merge or diverge segment procedure likely provides a better estimate of freeway operations. Threshold values for the relative percentage of the v_{FR} and v_{RF} to the total weaving volume could be used to determine whether the weaving or merge/diverge procedures should be applied. Further research would be needed to determine the threshold value.

As part of redefining weaving segments, the multiple weaving segment analysis procedure has been eliminated (*2*, pp. 12-23–12-24). The manual directs that the segments be defined according to the guidance in the other chapters; however, these other chapters do not specifically describe how to handle overlapping segments. This topic is addressed above, and another example is provided below.

The partial cloverleaf interchange—an off-ramp, a loop on-ramp, and a slip on-ramp in each direction—is a common configuration. When an auxiliary lane exists between the partial cloverleaf's loop on-ramp and the downstream off-ramp, the slip on-ramp must merge into the auxiliary lane, as shown in Figure 8.

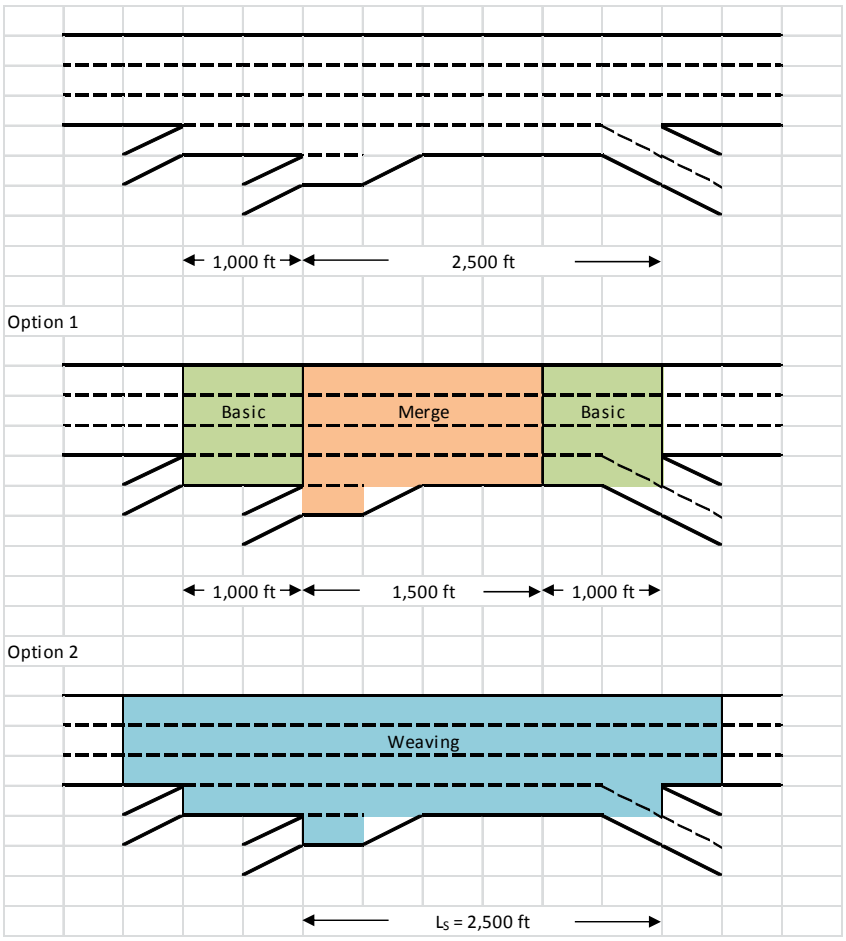

FIGURE 8 Example complex weaving segment.

The HCM definition of a weaving segment requires that the auxiliary lane connect successive on and off ramps. As a result, the weaving procedure would not be applied. Instead, the freeway segment would be divided into two basic segments and a merge segment as shown in Option 1. The loop on-ramp would be a basic segment rather than a merge segment because the on-ramp traffic is not required to merge with the mainline traffic. Similarly, the off-ramp would not be a diverge segment because a lane drops at the off-ramp.

Given the close spacing of the on-ramps and off-ramps, it is likely that both upstream on-ramp and downstream off-ramp traffic would change lanes in the merge segment. This turbulence would only be accounted for if the weaving procedure were used.

Option 2 in Figure 8 shows a potential application of the weaving procedure. In this option, the loop and slip on-ramp volume would be combined and considered to be a two-lane on-ramp. To be conservative, the weaving length would be the distance between the downstream on-ramp and the off-ramp, which assumes that the upstream on-ramp traffic does not change lanes until passing the downstream on-ramp. This application of the weaving procedure could serve as a check of the Option 1 analysis results, or the higher density of the two calculations could be reported.

CONCLUSIONS

This paper has presented several recommendations for clarifications, modifications, and extensions of the HCM freeway analysis procedures. The suggestions are summarized below.

- Adjacent merge or diverge segments separated by less than 1,500 ft should not overlap. Instead, the ramp gore point should be the dividing point.
- Adjacent merge–weaving or weaving–diverge segments should use overlap segments, but the ramp gore point should also be the dividing point.
- Rather than using fixed distances, the ramp and weaving influence areas may be dependent on volume. Overlap segments could be used to account for variable ramp influence areas.
- The capacity checkpoints used in the merge and diverge segment procedures should also be applied to the weaving segment procedure.
- Since some freeway segments with ramps are analyzed as basic segments, the basic procedure should also have the capacity checkpoints.
- The capacity checkpoints are imprecise, so a better approach would be to replace the checkpoints with basic segment analysis of the entering and exiting freeway volume.
- For weaving segments with imbalanced on-ramp and off-ramp volumes, the merge and diverge segment procedure should be applied instead. Further research is needed to determine what the volume threshold would be to switch from the weaving procedure to the merge or diverge procedure.
- Complex weaving segments should have alternate segment definitions so that the weaving procedure can be applied rather than the basic, merge, or diverge procedure, which may not capture the turbulence associated with closely spaced ramps.

REFERENCES

1. Approved Corrections and Clarifications to the HCM 2010, January 2013.
2. *Highway Capacity Manual 2010*. Transportation Research Board of the National Academies, Washington, D.C., 2010.

Operational Impacts of Auxiliary Lanes at Freeway Weaving Segments

YUBIAN WANG
RUEY LONG CHEU
The University of Texas at El Paso

YI QI
XIAOMING CHEN
Texas Southern University

A two-part study was conducted to assess the operational impacts of auxiliary lanes at freeway weaving segments. The first part of the study evaluated the improvements in traffic density and level of service at freeway segments between an on-ramp junction and an off-ramp junction before and after the addition of an auxiliary lane. The second part of the study developed recommendations on when to add auxiliary lanes at these freeway segments. The analyses were performed with the 2010 edition of the Highway Capacity Software, which follows the procedure prescribed in Chapters 12 and 13 of the *Highway Capacity Manual 2010*. The 2010 edition of the Highway Capacity Software was validated with field data collected at three freeway weaving segments in El Paso, Texas, prior to the analysis. The results show that adding an auxiliary lane at a freeway segment between on-ramp and off-ramp junctions reduces the traffic density in a range from 1.6 to 19.5 passenger car per mile per lane, or 4% to 50% while the level of service stays the same or improves. Higher improvements are obtained with shorter segment lengths combined with higher weaving volumes. This research has also developed charts, which contain recommendations on when to include auxiliary lanes under different combinations of freeway volume, weaving volume, and distance between the on-ramp and off-ramp.

AASHTO's *A Policy on Geometric Design of Highways and Streets*, a publication commonly known as the *Green Book*, defines an auxiliary lane (AL) as "the portion of the roadway adjoining the traveled way for speed change, turning, turning storage, weaving, truck climbing, and other purposes supplementary to through-traffic movement" (*1*). In freeway design, an AL typically refers to an added lane between an upstream on-ramp and a downstream off-ramp. Although the broader definition of AL includes acceleration lanes immediately downstream of isolated on-ramps, and deceleration lanes immediately upstream of isolated off-ramps, this paper only focuses on ALs in freeway weaving segments (FWSs).

Figure 1 shows a typical FWS with three main lanes and an AL. The AL added between the on-ramp and off-ramp can provide an improved weaving environment, rather than a forced or direct merge or diverge, for vehicles entering and departing the freeway facility. In other words, the AL provides additional longitudinal space for a vehicle to execute a mandatory lane change while entering or exiting the freeway. Although the length of the weaving segment (and the length of the AL) may be taken as the distance between the upstream on-ramp and the downstream off-ramp, the 2010 edition of *Highway Capacity Manual* (HCM 2010) (*2*) defines it as the distance between the end points of barrier markings

(solid white lines) that prohibit or discourage lane-changing. The length of a weaving segment, according to this HCM 2010 definition, is denoted by L_S in Figure 1. The terms weaving segment and AL appear throughout this article. It is important to note that a FWS refers to the freeway facility with all the lanes as shown in Figure 1 and, in the context of this research, an AL is the travel lane next to the right shoulder that connects an upstream on-ramp and a downstream off-ramp, as highlighted in the shaded area in Figure 1. According to Chapter 12 of HCM 2010, a FWS includes at least one AL (*2*). It also states that a freeway segment between an on-ramp and an off-ramp but without an AL should be analyzed as isolated merge and diverge junctions, respectively. It appears that HCM 2010 defines FWSs as facilities that include ALs. However, for simplicity and continuity in discussions for the rest of this paper, we regard that a FWS may be designed with or without an AL.

In past decades, more and more ALs have been constructed to facilitate traffic operations at ramp areas on freeways. The AASHTO *Green Book* (*1*) and several states' roadway design manuals (*3–6*) have so far included little detail as to the AL design, such as when to add an AL at a FWS. A recent survey conducted as part of a Texas Department of Transportation (DOT) project on engineers in 26 states in the United States has found that there was little guidance in the literature on when and how ALs should be incorporated in freeway design (*7*). Design engineers need to better understand the operational impacts of ALs, such as how adding an AL affects the speed, density, and level of service (LOS) in a freeway segment between an on-ramp and off-ramp under different traffic demands and geometric conditions.

A two-part study is reported to assess the operational impacts of ALs at FWSs. First, this research compared the density and LOS of FWSs with and without ALs, so as to provide insights into when an AL should be added. Second, recommendations on when to add ALs at FWSs were developed. All the calculations were performed using the procedure described in Chapter 12 of HCM 2010 through the Highway Capacity Software 2010 (HCS 2010) (*8*).

The organization of this paper is as follows. After this introduction, literature on the operational impacts of ALs at FWSs is reviewed. The literature review also includes the guidance provided in the AASHTO *Green Book* and the LOS analysis procedure in HCM 2010. Next, the average space–mean speed estimated by the HCM 2010 LOS analysis procedure is validated with field data collected at three FWSs in El Paso, Texas. This is followed by a description of the experimental scenarios. The results of HCS 2010 calculations are then analyzed and discussed, followed by tables to illustrate our recommendations. A summary of the findings is provided at the end of this paper.

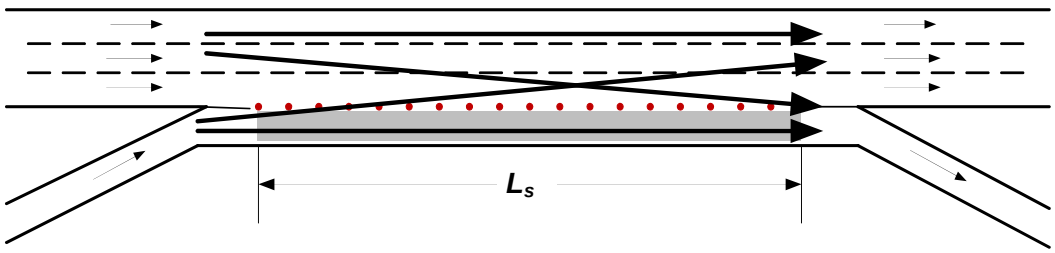

FIGURE 1 FWS with three main lanes and an AL.

LITERATURE REVIEW

AASHTO *Green Book*

The AASHTO *Green Book* (*1*) contains the standards for highway geometric design in the United States. Many state DOTs (and their design manuals) follow the standards and provisions in the AASHTO *Green Book*.

The *Green Book* states that the freeway operational efficiency may be improved by using a continuous AL between the an on-ramp and an off-ramp where (*a*) the interchanges are closed spaced; (*b*) the distance between the end of the taper on the entrance and the beginning of the taper on the exit is short; or (*c*) local frontage roads do not exist. When interchanges are widely spaced, it might not be practical or necessary to extend the AL from one interchange to the next. In such cases, the AL originating at a two-lane entrance should be carried along the freeway for an effective distance (minimum of 750 ft) beyond the merge point. An AL introduced for a two-lane exit should be carried along the freeway for an effective distance (minimum of 750 ft) in advance of the exit and extended onto the ramp. The AASHTO *Green Book* provides many drawings to illustrate how ALs may be incorporated into on-ramp terminals, off-ramp terminals, and in between.

The AASHTO *Green Book* provides guidance on AL designs at FWSs purely from geometric consideration. It does not mention the effect of traffic volume on operational efficiency within the vicinity of an AL.

Past Studies

Although ALs are often found in FWSs, only a few studies have been made with regards to the design of AL on traffic operations. Several studies focused on the operational effects while some other emphasized safety, or both. The documented studies on the operational effects are reviewed in this section.

Walters et al. (*9*) summarized 13 bottleneck removal projects in Texas, and presented before and after studies at four sites in more detail. The authors evaluated the effects of small geometric changes at four freeway bottlenecks in Dallas, Fort Worth, and El Paso. The geometric improvements involved adding or extending ALs. The operational benefits were quantified based on floating-car surveys (which measured speeds of different movements) before and after the ALs were constructed. The results of this study established that adding an AL could increase capacity and speed.

Sato et al. (*10*) conducted a field study at Higashi–Meihan Expressway in Nagoya, Japan, before and after ALs were added to connect upstream off-ramps and downstream on-ramps. The authors found that, after ALs were added, the capacity increased in the range of 3% to 6%. The total delay was reduced by an average of 33%.

In Bathenhorst and Gerken (*11*), the authors studied 20 FWSs in Dallas, Texas, each with an AL. The FWSs all have a one-lane on-ramp. However, for each location, traffic operations with a one-lane off-ramp and a two-lane off-ramp were compared by the analysis procedure of the 1997 edition of HCM, and by other two microscopic simulation software. They found that the one-lane off-ramp design consistently gave lower density than the two-lane off-ramp design. This finding is counter intuitive. The LOS analysis procedure of 1997 edition of HCM has since been revised and superseded by the procedure described in HCM 2010.

Roess and Ulerio (*12*) reported the development of new equations under NCHRP Project 3-75 to estimate (*a*) the weaving lane change rate; (*b*) the capacity of a weaving segment; and (*c*) the average speeds of weaving and nonweaving vehicles. The data were collected from 14 weaving sites in Arizona, California, Florida, Maryland, Ohio, and Oregon. In a companion paper, the same authors presented equations to calculate the capacity of FWSs, which were derived from the same set of data (*13*). They concluded that the capacity occurred when the traffic density was at 43 passenger cars per mile per lane (pcpmi/lane). They have also developed equations for ideal capacity of a FWS and maximum length of a FWS beyond which there is no operational improvement. The findings of these two studies have been incorporated into Chapter 12 of HCM 2010 (*2*) as part of the LOS analysis procedure for FWSs.

Highway Capacity Manual

Chapter 12 of HCM 2010 (*2*) is devoted to the LOS analysis of FWSs. This LOS analysis procedure is the outcome of NCHRP Project 3-75 (*14*). The procedure consists of eight steps, which estimates the average space mean speed of all vehicles (*S*), and converts it into density (*D*) before determining the LOS.

A FWS has four traffic movements: freeway-to-freeway, freeway-to-ramp, ramp-to-freeway and ramp-to-ramp (Figure 1). The freeway-to-ramp and ramp-to-freeway movements are weaving movements, while the freeway-to-freeway and ramp-to-ramp movements are non-weaving movements. Given a site's geometry and traffic volumes of the four movements, the analysis procedure starts with the examination of the minimum lane-changing rate for all vehicles (LC_{MIN}, in lane changes/h), and checked L_S (in feet) against the maximum length of a FWS. It then calculates the capacity of the FWS. This is followed by the estimations of lane changing rates of weaving and nonweaving vehicles.

The equivalent hourly lane-changing rate of weaving vehicles (in lane changes per hour) is determined from

$$LC_W = LC_{MIN} + 0.39\left[(L_S - 300)^{0.5} N^2 (1 + ID)^{0.8}\right] \quad (1)$$

in which N is the total number of lanes in the FWS (the sum of main lanes and AL); and ID is the interchange density (in interchanges per mile). The equivalent hourly lane-changing rate of nonweaving vehicles (LC_{NW}, in lane changes per hour) is calculated from a set of equations, depending on "a non-weaving vehicle index". The total lane-changing rate of all vehicles (LC_{ALL}, in lane changes per hour) is then

$$LC_{ALL} = LC_W + LC_{NW} \quad (2)$$

The analysis procedure next estimates the average speed of weaving vehicles (in mph) from

$$S_W = 15 + \left(\frac{FFS - 15}{1 + 0.226\left(\frac{LC_{ALL}}{L_S} \right)} \right) \quad (3)$$

where FFS is the free-flow speed of the freeway main lanes (in mph). The average speed of nonweaving vehicles (in mph) is

$$S_{NW} = FFS - (0.0072 LC_{MIN}) - \left(0.0048 \frac{v}{N}\right) \quad (4)$$

where v is the total volume (in passenger cars per hour) which is the sum of the weaving volume [v_W, in passenger cars per hour (pcph)] and nonweaving volume (v_{NW}, in pcph). The space–mean speed of all vehicles in the weaving segment (in mph) is

$$S = \frac{v_W + v_{NW}}{\left(\frac{v_W}{S_W}\right) + \left(\frac{v_{NW}}{S_{NW}}\right)} \quad (5)$$

The space–mean speed is converted into density (pcpmi/lane) by

$$D = \frac{1}{N}\left(\frac{v}{S}\right) \quad (6)$$

The LOS is then determined based on the value of D.

Chapter 13 of HCM2010 (*2*) is devoted to the LOS analysis of isolated on-ramps and off-ramps. The analyzed ramp influence area covers 1,500 ft downstream of the on-ramp, or 1,500 ft upstream of the off-ramp, in the two rightmost lanes on the freeway, plus the AL (if any).

This analysis procedure consists of the following steps:

1. Estimate the demand flow rate in the two rightmost lanes on the freeway (at the upstream end of the influence area);
2. Estimate the capacity of the merge or diverge area (in the two rightmost lanes on the freeway, plus the AL, if any) and compare the capacity with the demand flow rate; and
3. If the total demand flow rate is greater than capacity, LOS F is assigned; otherwise, estimate the density within the influence area and converting the density into LOS.

Summary of Literature Review

The AASHTO *Green Book* has only provided qualitative guidance on the implementation and geometric design of ALs. The few studies that analyzed field data have indicated that adding an AL improves speed, capacity and reduces delay at the FWS. However, these quantitative findings are too few to be generalized into design guidelines. Therefore, this study will quantify the operational benefits of adding ALs at FWSs under different combinations of traffic volume and geometric configurations, and then develop design recommendations on when to add ALs at FWSs.

MODELING TOOL

A recent survey (*7*) has found that the most popular tool used by state transportation engineers for analyzing operational impacts of auxiliary lanes is Highway Capacity Software (HCS). Therefore, this study used the 2010 version of HCS (HCS 2010) (*8*) to assess the operational impacts of auxiliary lanes.

The HCS 2010 follows the LOS analysis procedure prescribed in HCM 2010. The HCM 2010 LOS analysis procedure for FWSs has been developed based on data collected at 14 sites across United States (*12–14*). Prior to the application of HCS 2010 in this research, field data were collected at three independent FWSs in El Paso, Texas, to validate the HCS 2010 calculations.

Table 1 lists the three sites, dates and hours selected for data collection. Only these three sites in El Paso met the criteria of (*a*) having an AL; (*b*) having an L_A not exceeding the maximum length as specified in HCM 2010; (*c*) having lane markings that conform to the latest edition of *Manual of Uniform Traffic Control Devices* (*15*); (*d*) having at least a traffic surveillance camera with the necessary view for recording the video; and (*e*) not near any work zone. All the three sites have one auxiliary lane, a one-lane on-ramp and a one-lane off-ramp. Video recordings of traffic operations at the hours (usually the morning and afternoon peak hours) as listed in Table 1 were obtained from Texas DOT El Paso District's Transvista Traffic Management Center. The video recordings were replayed in the laboratory for data extraction. For each hour, traffic volumes of the four movements were counted. For each movement, the travel times of approximately 30 randomly selected vehicles between fixed markers were captured. The movement's space mean speed was then estimated from the sample.

For each hour of observation, the site geometry, traffic volumes and *FFS* were entered into HCS 2010 to predict *S*. At the same time, the observed S_W and S_{NW} were aggregated to form *S*, using the *Road Design Manual: Uniform Design Guide for MnDOT Projects* (*5*). Figure 2 plots the *S* values estimated by HCS 2010 against the *S* values obtained from the field data, for the 8 observed hours. The space mean speed was used as the performance measure during the validation because it was easier to measure speed than density from the video recordings. Furthermore, according to Washington State DOT's *Design Manual* (*6*), *D* is a deterministic function of *S*. The plotted data points in Figure 2 all scatter around the 45-degree line. The fitted line that passes through the origin has a gradient of 1.0028 which is very close to 1.0. A statistical test on

TABLE 1 Data Collection for Validation

Freeway	Upstream On-Ramp	Downstream Off-Ramp	L_S (ft)	*N*	Date	Time
US-54 SB	Hondo Pass Ave.	Hercules Ave.	752	4	2/23/2012	7:00–8:00 a.m. 12:00–1:00 p.m. 4:00–5:00 p.m.
US-54 NB	Hercules Ave.	Hondo Pass Ave.	680	3	3/13/2012	7:45–8:45 a.m. 3:00–4:00 p.m. 5:00–6:00 p.m.
I-10 EB	Artcraft Rd.	Redd Rd.	697	3	3/13/2012	9:00–10:00 a.m. 3:00–4:00 p.m.

NOTE: SB = southbound; ave. = avenue; NB = northbound; EB = eastbound; rd. = road.

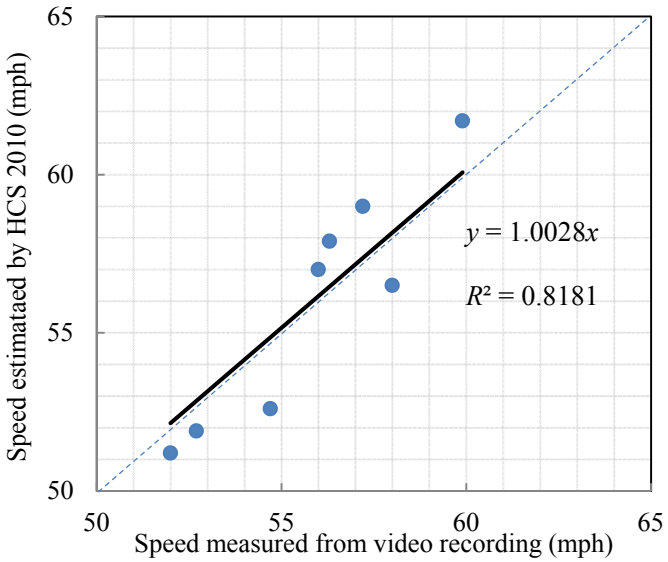

FIGURE 2 Comparison of space mean speeds.

the gradient of the fitted line showed that this value was not significantly different from 1.0 at 0.01 level of significance. Therefore, it was concluded that the HCM 2010 analysis procedure and the HCS 2010 software produced satisfactory estimates of *S*.

EXPERIMENTAL DESIGN

In this section, study scenarios under different traffic and geometric conditions at freeway weaving segments are described.

Figure 3 shows a FWS with three main lanes before and after the addition of an AL. A set of 147 scenarios have been designed for the geometric configurations as shown in Figure 3*a*. Another set of 147 scenarios have also been designed for the geometric configurations as shown in Figure 3*b*. The comparisons of the HCS 2010 outputs between the two sets of design (each with 147 scenarios) permitted the authors to determine the operational effects of adding an AL at the FWSs.

According to the HCM 2010 LOS analysis procedure, and based on site observations (from driving on freeways and observing the designed geometry in Google Earth), the following important factors were initially identified in the design of FWSs:

- Total number of lanes (main lanes plus AL) in the weaving segment, N;
- Number of AL, N_A;
- Number of lanes at the on-ramp, N_{ON};
- Number of lanes at the off-ramp, N_{OFF} ;
- Length of AL (also known as weaving segment length), L_S;

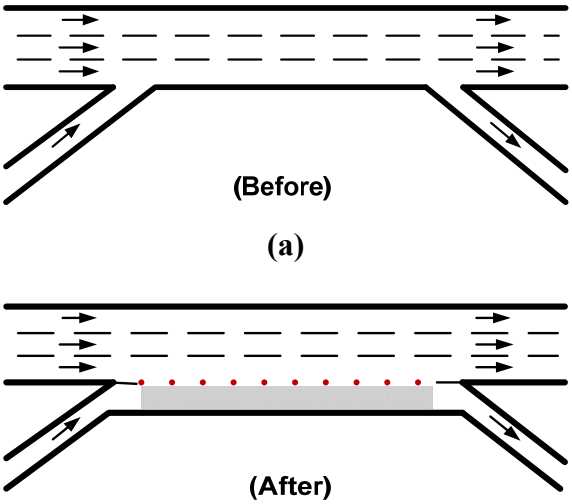

FIGURE 3 FWS before and after the addition of an AL: (*a*) $N_A = 0$ and (*b*) $N_A = 1$.

- Freeway-to-freeway volume, v_{FF};
- Weaving volume (sum of freeway-to-ramp and ramp-to-freeway volumes), v_W; and
- Ramp-to-ramp volume, v_{RR}.

The above factors were then assigned numerical values based on the following considerations:

- Most of the freeways in urban areas have at least three main lanes. According to a preliminary sensitivity test with HCS 2010, when there were three or more main lanes, the number of main lanes has no significant effect on *S* in the FWSs. Therefore, *N* was set to 3 without an AL and 4 with an AL (as depicted in Figure 3).
- Almost all the FWSs have at most one AL. Weaving segments with two ALs are almost nonexistent. Therefore, $N_A = \{0, 1\}$.
- Most of the on-ramps have only one lane that feeds traffic into the freeways. Therefore, $N_{ON} = 1$.
- Most of the off-ramps have one lane. Therefore, $N_{OFF} = 1$.
- For L_S, although the minimum distance of 1,500 ft is specified in the Texas DOT *Roadway Design Manual* (*3*), sites with shorter L_S have been found (see Table 1 for examples). Other states have used up to $L_S = 2{,}500$ ft (*7*). Depending on the traffic volume, the HCM 2010 LOS analysis procedure may consider an on-ramp and an off-ramp with $L_S > 3{,}000$ ft as isolated ramp junctions and so they should be analyzed with another procedure. Therefore, three L_S values have been assigned: $L_S = \{750, 1{,}500, 2{,}250\}$ ft.
- Based on the range of traffic count data collected in the previous section, $v_{FF} = \{500, 750, 1{,}000, 1{,}250, 1{,}500, 1{,}750, 2{,}000\}$ pcph/lane and $v_W = \{200, 400, 600, 800, 1{,}000, 1{,}200, 1{,}400\}$ pcph/lane.

- Since very few vehicles entered the on-ramp and exited immediately at the off-ramp (as observed in the data collected in the previous section), v_{RR} was set to 0 pcph/lane in all the scenarios, i.e, v_{RR} =0 pcph/lane.

Note that, other factors, such as *FFS* and *ID*, were found to have insignificant impact on the estimated *S*, *D* and LOS. Therefore *FFS* was set to 70 mph and *ID* set to 1 interchange/mi.

RESULTS

This paper reports a two-part study that assessed the operational impacts of having ALs at FWSs. Research analyses in the first part of the study assessed the operational performance of FWSs with and without an AL. The second part of the study developed recommendations on when to add ALs at FWSs, based on the findings in the first part of this research.

Effect of Adding an Auxiliary Lane

This part of the study compared the operational performance of the FWSs before and after the addition of an AL under different design scenarios. The performance measure selected was density, since in HCM 2010, the LOS of FWSs is directly determined by density.

Table 2 visualized density and LOS with and without ALs under different scenarios. Table 3 lists the reduction in density and percentage reduction in density.

The density with the presence of ALs is computed by the weaving module in HCS 2010. HCM 2010 defines a FWS in which vehicles in the freeway-to-ramp movement and ramp-to-freeway movements cross paths with each other. Therefore, the procedure described in Chapter 12 of HCM 2010 cannot be used to analyze a freeway segment between an on-ramp and an off-ramp without an AL. For the scenarios without auxiliary lanes, the freeway segment was treated as (*a*) an on-ramp with an adjacent downstream off-ramp and (*b*) an off-ramp with an adjacent upstream on-ramp respectively (see Figure 4). The densities and speeds are computed separately at the on-ramp junction and the off-ramp junction by the ramp module in HCS 2010. According to HCM 2010 (*2*), whenever a series of ramps on a freeway is analyzed, if the ramp influence areas overlap with each other, the operation in the overlapping region is determined by the ramp having the highest density. Therefore, the higher value among the on-ramp density and off-ramp density was selected to be the density without an AL.

It can be seen from Table 2 that after the addition of an AL, there is a reduction in density in every scenario. In addition, the changes in LOS are also compared by using colors codes in Table 2. With an AL, the LOS all became better or stayed the same. Table 3 shows that adding an AL can decrease the density in the range of 1.6 to 16.5 pcpmi/lane, or 4% to 50%. The density reduction is greater at shorter weaving segment length, i.e., at L_S = 750 ft.

TABLE 2 Comparison of Density and LOS with and without AL

Density in the Weaving Segment (pcpmi/lane)

Weaving Segment Length	Without Auxiliary Lane							With Auxiliary Lane						
	v_{FF} (pcphpl)	v_W (pcph/lane)							v_{FF} (pcphpl)	v_W (pcph/lane)					
		200	400	600	800	1,000	1,200	1,400		200	400	600	800	1,000	1,200	1,400
L_S = 750 ft	500	14.0	15.1	16.1	17.0	17.6	18.8	19.9	500	6.9	8.0	9.1	10.3	11.6	12.9	14.2
	750	18.2	19.9	21.4	22.8	23.6	23.6	24.5	750	10.1	11.3	12.6	13.9	15.2	16.7	18.1
	1,000	22.1	24.3	26.4	28.3	30.1	30.1	30.1	1,000	13.4	14.7	16.1	17.5	19.0	20.6	22.2
	1,250	25.9	28.3	30.9	33.4	35.8	36.5	36.5	1,250	16.8	18.3	19.8	21.3	23.0	24.7	26.5
	1,500	29.4	32.0	35.1	38.1	41.0	43.0	43.0	1,500	20.3	21.9	23.5	25.2	27.0	28.9	30.8
	1,750	32.8	35.2	38.9	42.5	45.9	49.2	49.4	1,750	24.0	25.6	27.4	29.3	31.2	33.2	35.4
	2,000	35.8	38.1	42.4	46.5	50.4	54.3	55.9	2,000	27.7	29.5	31.4	33.4	35.6	37.8	40.1
L_S = 1,500 ft	500	13.8	14.2	14.9	15.7	16.6	17.5	18.5	500	7.0	8.0	9.1	10.2	11.4	12.6	13.8
	750	18.0	18.5	19.4	20.3	21.1	21.8	22.4	750	10.1	11.3	12.5	13.7	15.0	16.4	17.7
	1,000	22.1	22.4	23.6	24.7	25.8	26.8	27.7	1,000	13.4	14.7	16.0	17.4	18.8	20.2	21.8
	1,250	25.9	26.0	27.4	28.8	30.1	31.4	32.6	1,250	16.8	18.2	19.6	21.1	22.7	24.3	25.9
	1,500	29.4	29.6	30.8	32.5	34.1	35.7	37.2	1,500	20.3	21.8	23.4	25.0	26.7	28.5	30.3
	1,750	32.8	32.9	33.8	35.8	37.7	39.6	41.3	1,750	23.9	25.6	27.3	29.0	30.9	32.8	34.8
	2,000	35.8	35.9	36.4	38.7	40.9	43.1	45.1	2,000	27.6	29.4	31.2	33.2	35.2	37.3	39.5
L_S = 2,250 ft	500	13.8	13.9	14.5	15.4	16.2	17.1	18.0	500	7.0	8.0	9.1	10.2	11.3	12.5	13.7
	750	18.0	18.2	18.7	19.4	20.0	20.7	21.7	750	10.1	11.3	12.5	13.7	14.9	16.2	17.5
	1,000	22.1	22.2	22.6	23.5	24.3	25.1	25.9	1,000	13.4	14.7	16.0	17.3	18.7	20.1	21.6
	1,250	25.9	26.0	26.2	27.2	28.3	29.2	30.2	1,250	16.8	18.2	19.6	21.1	22.6	24.1	25.7
	1,500	29.4	29.6	29.7	30.6	31.8	33.0	34.1	1,500	20.3	21.8	23.3	24.9	26.6	28.3	30.1
	1,750	32.8	32.9	33.0	33.5	35.0	36.3	37.7	1,750	23.9	25.5	27.2	28.9	30.7	32.6	34.5
	2,000	35.8	35.9	36.1	36.3	37.7	39.3	40.9	2,000	27.6	29.4	31.2	33.1	35.0	37.1	39.2

LOS	A	B	C	D	E	F
Density (pcpmi/lane)	≤10	10–20	20–28	28–35	>35	Demand exceeds capacity

TABLE 3 Reduction in Density After Adding ALs

Weaving Segment Length, L_S (ft)	Reduction in Density After Adding ALs	
	Reduction in Density (pcpmi/lane)	Percent Reduction
750	5.7–16.5	23–50
1,500	4.7–9.1	13–49
2,250	1.6–9.1	4–49

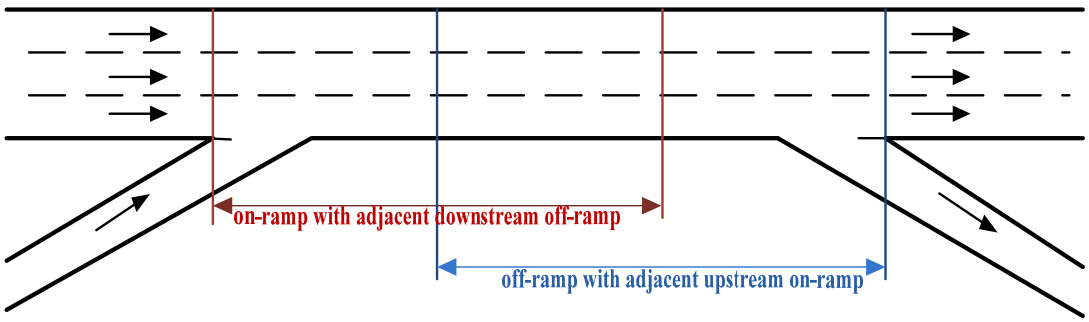

FIGURE 4 Weaving segment without ALs.

Recommendations on When to Add Auxiliary Lane

A recent survey (*7*) conducted as part of a Texas DOT research project on the design practice of ALs has found that state transportation engineers considered the use of ALs under the following conditions:

- When the ramp has high percentage of trucks;
- When the ramp has high volumes;
- When the traffic density is high;
- If there is safety or operational issues; or
- If the predicted LOS is D or worse for the design year peak-hour traffic.

The first four conditions are qualitative in nature. However, the condition based on LOS provides a clearer threshold. Therefore, the following criterions were set up to develop the quantitative recommendations for including ALs at FWSs:

1. If there is no AL, the LOS in the FWSs is D or worse; and
2. With the inclusion of an AL, the LOS in the FWSs becomes C or better.

The identification of scenarios that meet the LOS improvement criteria is illustrated in Table 4 with the use of Table 2. The scenarios that meet Criterion A are determined from the nested tables in the left column of Table 2 (without AL). For each nested table that represents a fixed L_S value, the combinations of v_W and v_{FF} values that result in LOS D or worse are outlined in red and shown in Table 4. In Table 4, the regions below the red lines represent LOS D or worst when no AL is included at the FWSs. The scenarios that meet Criterion B are determined

TABLE 4 Design scenarios in which auxiliary lanes should be added.

	v_{FF} (pcph/lane)	v_W (pcph/lane)						
		200	**400**	**600**	**800**	**1,000**	**1,200**	**1,400**
L_s = 750 ft	500							
	750							
	1,000							
	1,250							
	1,500							
	1,750							
	2,000							
	v_{FF} (pcph/lane)	v_W (pcph/lane)						
		200	**400**	**600**	**800**	**1,000**	**1,200**	**1,400**
L_s = 1,500 ft	500							
	750							
	1,000							
	1,250							
	1,500							
	1,750							
	2,000							
	v_{FF} (pcph/lane)	v_W (pcph/lane)						
		200	**400**	**600**	**800**	**1,000**	**1,200**	**1,400**
L_s = 2,250 ft	500							
	750							
	1,000							
	1,250							
	1,500							
	1,750							
	2,000							

in the same fashion from the nested tables in the right column of Table 2 (with AL). In Table 4, the regions above the blue lines represent LOS C or better after an AL has been included. Each shaded region between the red and blue line in Table 4 encloses the v_W and v_{FF} values that satisfy both criteria A and B. It represents the combinations of L_S, v_W, and v_{FF} values with which AL should be designed to improve the LOS from D or worst to C or better. AL is not recommended for the regions above the red lines in Table 4 because even without an AL, the LOS is always C or better. Likewise, AL is not recommended for the regions below the blue lines in Table 4 because even with an AL the LOS will not become C or better. This implies that other geometric improvement options, e.g., increasing the number of freeway lanes, should be considered.

The application of Table 4 in combination with Table 2 may be illustrated through the following example. If a FWS has L_s = 750 ft, design volumes of v_{FF} = 1,250 pcph/lane and v_W = 600 pcph/lane, according to the first chart in Table 4, an AL should be added. By doing so, the LOS is expected to be B (from the first nested table in the right column of Table 2). For the same Ls = 750 ft but no AL is provided, LOS D is expected (from the first nested table in the left column of Table 2). However, if the site geometry permits, L_S may be extended to 1,500 ft

without having to add an AL, as recommended by the second chart in Table 4. Under this option, the LOS will, however, be C (from the second nested table in the left column of Table 2).

CONCLUSIONS

This research has assessed, by means of HCS 2010, the operational impacts of AL at FWSs. Before conducting the experiment, the space–mean speed estimated by HCS 2010 was validated with field data collected at three FWSs in El Paso, Texas. A total of 294 scenarios were designed for FWSs with different freeway-to-freeway volume (v_{FF}), weaving volume (v_W), weaving segment length (L_S), and with and without an AL (N_A). The density and LOS were used as the operational performance measures. Based on the analysis of traffic density and LOS in the FWSs with and without AL, the operational benefits of adding ALs at FWSs are visualized and quantified (see Tables 2 and 3). The results of this study show that adding an AL reduces traffic density by 1.6 to 19.5 pcpmi/lane or 4% to 50%. A higher percentage reduction in density can be achieved when L_S is shorter and v_W is higher.

This research has also developed charts (Table 4) which contain recommendations on when to add ALs at FWSs under different combinations of freeway volume, weaving volume and weaving segment length.

ACKNOWLEDGMENTS

This research is supported in part by Texas Department of Transportation under Contract 0-6706. The authors thank Wade Odell, the Project Director; Jane Lundquist, the Project Advisor; and members of the Project Management Committee for their advice and assistance. This research is also supported in part by the National Science Foundation under Grant #1137732. The contents of this report reflect the views of the author, who are responsible for the facts and the accuracy of the data presented. The contents do not necessarily reflect the official view or policies of the Texas Department of Transportation. This article does not constitute a standard, specification, or regulation.

REFERENCES

1. AASHTO. *A Policy on Geometric Design of Highways and Streets.* American Association of State Highway and Transportation Officials, 2004.
2. *Highway Capacity Manual 2010*. Transportation Research Board of the National Academies, Washington, D.C., 2010.
3. *Roadway Design Manual*. Texas Department of Transportation, May 2010.
4. *Highway Design Manual*. California Department of Transportation, May 2012.
5. *Road Design Manual: Uniform Design Guide for MnDOT Projects*. Minnesota Department of Transportation, May 2012.
6. *Design Manual*. Washington State Department of Transportation, March 2012.
7. Design and Scope of Impact of Auxiliary Lanes. *Technical Memorandum for Task 2—Survey Transportation Engineers*. Project 0-6707. Texas Department of Transportation, 2011.
8. McTrans. HCS 2010 Weaving Version 6.1. *Highway Capacity Software 2010*. Center for Microcomputers in Transportation, University of Florida, 2010.

9. Walters, C. H., S. A. Cooner, and S. E. Ranft. Reconsidering Freeway Bottlenecks: Case Studies of Bottleneck Removal Projects in Texas. *Transportation Research Record: Journal of the Transportation Research Board, No. 1925,* Transportation Research Board of the National Academies, Washington, D.C., 2005, pp. 66–75.
10. Sato, H., J. Xing, S. Tanaka, and K. Morikita. Examining the Effect of Connecting Auxiliary Lanes on Mitigation of Expressway Traffic Congestion. *International Journal of ITS Research*. Vol. 9, 2011, pp. 55–63.
11. Bathenhorst, R. A., and J. G. Gerken. Operational Analysis of Terminating Freeway Auxiliary Lanes with One-Lane and Two-Lane Exit Ramps: A Case Study. *Proc., Mid-Continent Transportation Symposium 2000*, Washington, D.C., 2000, pp. 77–76.
12. Roess, R. P., and J. M. Ulerio. Level of Service Analysis of Freeway Weaving Segments. *Transportation Research Record: Journal of the Transportation Research Board, No. 2130,* Transportation Research Board of the National Academies, Washington, D.C., 2009, pp. 25–33.
13. Roess, R. P., and J. M. Ulerio. Capacity of Freeway Weaving Segments. *Transportation Research Record: Journal of the Transportation Research Board, No. 2130,* Transportation Research Board of the National Academies, Washington, D.C., 2009, pp. 34–41.
14. Roess, R. P., J. M. Ulerio, E. S. Prassas, J. Schoen, M. Vandehey, W. Reilly, and W. Kittelson. *Analysis of Freeway Weaving Sections*. NCHRP Project 3-75, Polytechnic University and Kittelson & Associates, Inc., 2008.
15. *Manual of Uniform Traffic Control Devices*, 2009 Edition. FHWA, U.S. Department of Transportation, 2009.

Vehicle Trajectory Analysis System for Estimating HCM-Compatible Performance Measures

BIN LU
Southwest Jiaotong University, China, and University of Florida

SCOTT S. WASHBURN
University of Florida

Vehicle trajectory analysis is recommended as a technique to calculate performance measures consistent with those defined by the *Highway Capacity Manual 2010* (HCM). This paper presents a vehicle trajectory analysis system referred to as VTAPE (vehicle trajectory analysis for performance estimation), which is intended for the visualization and analysis of vehicle trajectory data provided by microscopic simulation programs and field observations. Thus, simulation program users can verify the consistency of the outputs with the HCM performance measure definitions by using VTAPE to directly process the vehicle trajectory file generated by the simulation program. Likewise, for vehicle trajectories obtained from field observations, VTAPE can be used to calculate HCM-compatible performance measures. By employing a uniform database structure and source-specific data transformation, VTAPE is able to read different arrangements of vehicle trajectory data from simulation programs such as CORSIM and NGSIM, and then produce HCM-compatible performance measures, of which the computational procedures are described in this paper. VTAPE is also built on an extensible software architecture, which allows researchers and developers to cooperatively expand the range of capabilities to support more types of data and analysis methods. Examples of analyses for estimating performance measures performed by VTAPE are presented to show the effectiveness of the proposed computational procedures.

Traffic analysis methods generally range from deterministic and macroscopic to stochastic and microscopic. The most significant resource for deterministic, macroscopic traffic analysis methods is the *Highway Capacity Manual 2010* (HCM) (*1*). Since the first edition of the HCM in 1950, the methods in the HCM have increased in scope and complexity over the years. Meanwhile, over the past 20 years, stochastic, microscopic traffic simulation has seen significant advances in capabilities and execution speed, making it a commonly used tool for traffic analysis projects (*2*). Given that the HCM analysis methods are commonly defined as the standard for traffic analysis by governmental transportation agencies, a subject that has been generating considerable discussions recently is how to compare the performance measure outputs of simulation to those of the HCM. It is not uncommon for users of microscopic simulation programs (e.g., CORSIM, VISSIM, AIMSUN, PARAMICS) to use the outputs from these programs with the level of service (LOS) tables of the HCM to report a LOS value. However, if the simulation program does not calculate the value of a performance measure, say density, in the same manner that it is calculated in the HCM, then using this measure to report an HCM LOS value is potentially misleading, at best. This area was preliminarily broached by Courage et al. in NCHRP Project 3-85 (*3*). One of the key recommendations for how to deal with comparing simulation output to HCM output from this project is to apply vehicle trajectory analysis, which will be discussed further in this paper. The basic premise of the

recommendation was that the HCM would serve as the standard reference for the definitions of any or all performance measures used in analyzing traffic performance. The corresponding calculation procedures to generate these performance measures consistent with the definitions, from vehicle trajectory data, would also be provided in the HCM. In this manner, the vehicle trajectory data output by microscopic traffic simulation programs can be processed according to the HCM standard definitions. If the results of this process generate performance measure values that are the same as that output by the simulation program itself, then the consistency of the simulation program's outputs to the HCM definitions is verified.

In this paper, a vehicle trajectory analysis system for estimating performance measures referred to as VTAPE, is developed and intended for the visualization and analysis of vehicle trajectory data from various sources (e.g., microscopic simulation programs or field observations) by applying a uniform database structure and source-specific data transformation. Specially, VTAPE is able to calculate various performance measures in a manner consistent with the definitions of these performance measures in the HCM. Thus, for simulation program users, they can verify the consistency of the outputs with the HCM performance measure definitions by using VTAPE to directly process the vehicle trajectory file generated by the simulation program (e.g., .ts0 from CORSIM or .fzp from VISSIM). Likewise, for vehicle trajectories obtained from field observations, VTAPE can be used to calculate HCM-compatible performance measures. The remainder of this paper is organized as follows: a review of the characteristics of vehicle trajectory data that influenced the development of VTAPE from both a graphical and mathematical perspective; a description of the database structure and data transformation used in VTAPE; a description of the computational procedures implemented to estimate performance measures; an overview of the software architecture and user interface aspects of the VTAPE; and presentation of two analysis examples.

VEHICLE TRAJECTORY DATA

Vehicle trajectory data, at its simplest level, generally consists of spatiotemporal locations of all individual vehicles within a given small time interval (usually 1 s or less), and can be depicted as a series of vehicle coordinates in a two-dimensional space. Additional vehicle-specific measurements may also be part of the vehicle trajectory data, such as velocity, acceleration, and so on. With these data, vehicle-movement phenomena such as car following, lane changing, and gap acceptance can be well explained in the field of traffic flow theory (*4–6*).

An example of vehicle trajectory data is plotted in terms of a time–space diagram in Figure 1*a*, which illustrates a simple queue accumulation and discharge process at a signalized intersection. In addition, Figure 1*b* depicts a typical freeway situation with multiple lanes of operation in which vehicles follow their own leaders according to a certain car-following regulation. In this situation, vehicle trajectory lines can cross one another as vehicles overtake their leaders through lane changing.

Although the plots shown in Figure 1 provide a good visual understanding for the movement of vehicles, they do not support any quantitative assessments. To conduct performance measurements from vehicle trajectories, it is necessary to describe them mathematically through a set of properties that are associated with each vehicle at each time step and position. Theoretically, each trajectory point of the vehicle can be quantified by a list of the properties as shown in Figure 1*c*.

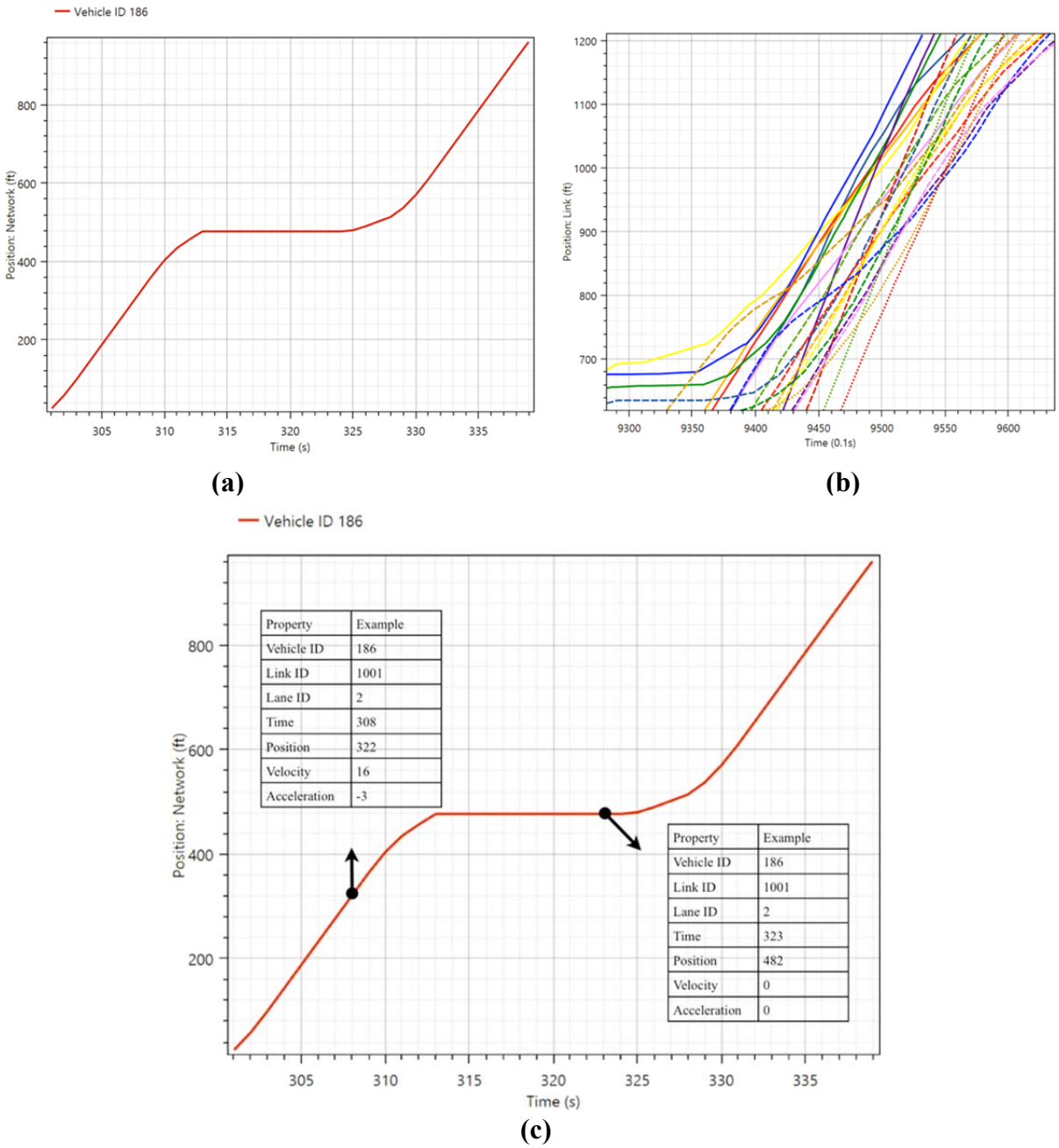

FIGURE 1 Examples of (*a*) and (*b*) vehicle trajectory and (*c*) quantitative properties in vehicle trajectory.

DATABASE STRUCTURE AND DATA TRANSFORMATION

To develop performance measures from different arrangements of vehicle trajectory data, it is necessary that the data elements in the vehicle trajectory dataset contain sufficient detail to implement calculations for a variety of performance measures regardless of the source. Thus, a uniform database structure specifying those vehicle trajectory properties must be established.

There is little documentation in the literature of previous efforts to establish a database structure for vehicle trajectory analysis. However, one was developed by the FHWA to support the Surrogate Safety Analysis Model (SSAM) (*7*). Basically, the database structure established for SSAM was designed to support the analysis of safety measures. Using SSAM as the basis, additional data elements were proposed in the NCHRP 3-85 project for better serving the calculation of traffic performance measures, such as vehicle classification type, distance from the upstream and downstream link end, and so on.

The structure of CORSIM's time step data output file is also an alternative as CORSIM itself is widely used by many transportation professionals (*8*, *9*). It indicates properties of vehicle trajectory data like the position of the vehicle on the link and driver type for each vehicle that are lacking from SSAM but necessary for performing calculating some of the performance measures. In addition, the essential properties used for presenting vehicle trajectories are defined natively in the database structure of CORSIM, which include vehicle ID for keeping track of all vehicles, link ID for each link, and lane ID for each lane on a specific link.

Besides CORSIM, other microscopic simulation programs such as VISSIM also provide a database structure with a different level of focus and detail (*10*). Additionally, FHWA's Next Generation Simulation (NGSIM) effort produced several vehicle trajectory datasets based on field observations, of which the structure can also be used for reference (*11*).

Considering that the database structure of SSAM is still not widely followed by microscopic simulation programs in the market, and even the database structures of microscopic simulation programs themselves are not compatible with each other, ideally, the profession will work towards establishing a common database structure that will be utilized in the various providers or sources of vehicle trajectory data.

At a minimum, it is suggested that the data elements shown in Table 1, which is referred to as basic data, should be included in a common vehicle trajectory database definition. Although this minimum set of elements is not sufficient to determine all required HCM-compatible performance measures, they are sufficient for presenting vehicle trajectory plots. As long as the basic data is available from the source, the vehicle trajectory data output from the source can be imported into VTAPE. Each row in Table 2 shows the mapping relationship between the basic data of VTAPE and the different sources mentioned previously.

Based on the basic data elements, some other data elements can be derived. For example, follower ID can be determined through vehicle ID, leader ID, and time in the dataset. From those elements, the value of spacing between consecutive vehicles can be derived from leader ID, follower ID, and their positions, and so on. This type of data is referred to as derived data. It should be noted, however, that the calculation of derived data from basic data could be a time-consuming procedure. Thus, the more elements included in the basic dataset, the more efficient VTAPE can be.

With basic data and derived data, VTAPE may still not have sufficient information to compute performance measures. The additional data that allows VTAPE to compute all required performance measures is referred to as extended data. Given the current lack of consistency in vehicle trajectory datasets provided by the various sources, predefined interfaces implemented in VTAPE are designed for each source, which provide one-to-one and many-to-one data transformation rules that convert the extended data into VTAPE's database structure. For example, desired speed is an extended data element that is essential for computing delay-related measures. The value of desired speed is included in the vehicle trajectory file of VISSIM and can be simply retrieved by VTAPE though one-to-one mapping. But this value is not provided by

TABLE 1 Database Structure of VTAPE's Basic Data

Property	Data Type	Description
Vehicle ID	Integer	Vehicle identification number
Time	Double	Time step identification number
Position (link)	Double	Distance traveled by the vehicle from the upstream end of the link
Velocity	Double	Instantaneous velocity of the vehicle
Acceleration	Double	Instantaneous acceleration of the vehicle
Link ID	Unsigned integer	Link identification number
Link length	Double	Link longitudinal length
Lane ID	Unsigned integer	Lane identification number
Vehicle length	Double	Vehicle longitudinal length
Leader ID	Integer	Vehicle ID of the leader vehicle in car-following movement

TABLE 2 Data Mapping Between VTAPE and Different Sources

VTAPE	CORSIM	VISSIM	NGSIM
Vehicle ID	Global vehicle ID	Vehicle number	Vehicle ID
Time	Simulation time	Simulation time	Frame ID
Position (link)	Vehicle position	Link coordinate	Local Y
Velocity	Velocity	Speed	Vehicle velocity
Acceleration	Acceleration	Acceleration	Vehicle acceleration
Link ID	Instance ID	Link number	Link ID[a]
Link length	Link length[a]	Link length[a]	Link length[a]
Lane ID	Lane ID	Lane number	Lane identification
Vehicle length	Vehicle length	Length	Vehicle length
Leader ID	Leader vehicle ID	Leading vehicle	Preceding vehicle

[a] Properties can be found in network geometry files provided by the source.

CORSIM. In this situation, a predefined interface was set up in VTAPE for CORSIM to specify a method which implements a transformation of desired speed from link free-flow speed and driver type. The work flow of the transformation of extended data is shown in Figure 2.

HCM-COMPATIBLE PERFORMANCE MEASURES

The preceding sections have discussed how vehicle trajectory data can be visualized graphically and analyzed mathematically. This section will address the development of the computational procedures that estimate the HCM-compatible performance measures from vehicle trajectory data.

Four commonly used categories of performance measures defined in the HCM are queue-related measures, stop-related measures, delay-related measures, and density-related measures. These measures and the computational procedures implemented in VTAPE to calculate them in a manner consistent with the HCM definitions are described in the following subsections.

Before introducing the calculation methods, the definitions of the variables used throughout the rest of the discussion are presented here:

- $s(t)$ is the position of the vehicle from the upstream link end at time step t, in feet.
- $v(t)$ is the velocity of the vehicle at time step t, in ft/s.
- $vl(t)$ is the velocity of the vehicle's leader at time step t, in ft/s.
- $vd(t)$ is the desired (target) speed of the vehicle at time step t, in ft/s.
- $a(t)$ is the acceleration of the vehicle at time step t, in ft/s^2.
- Δt is the time step interval, in seconds.
- t_{beg} is the beginning time step of analysis period, in seconds.
- t_{end} is the ending time step of analysis period, in seconds.
- gap(t) is the gap between the following vehicle and its leader at time step t, where
  - gap(t) is calculated as $s_l(t) - s_f(t)$, in feet;
  - $s_l(t)$ is the position of the leader at time step t, in feet; and
  - $s_f(t)$is the position of the follower at time step t, in feet.
- $s_{stop}(i)$ is the position of stop line located on link i, relative to the upstream end of the link, in feet.

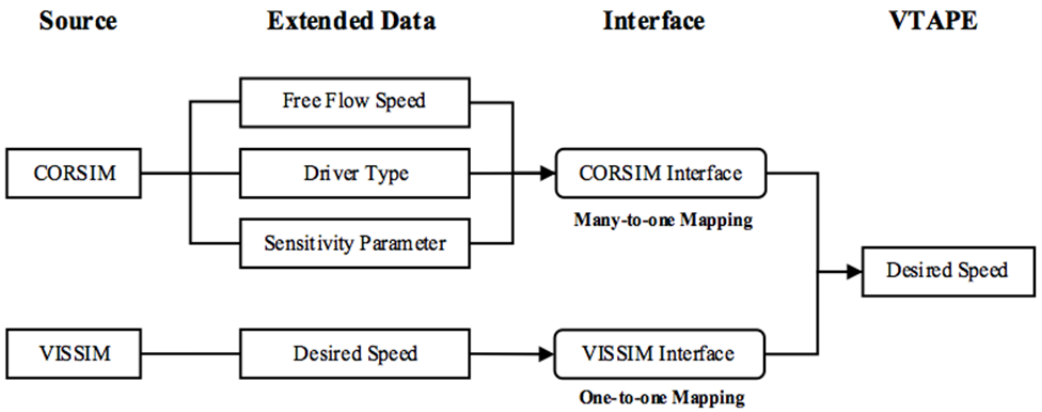

FIGURE 2 Example of transformation of extended data through interfaces.

- $k(t_{beg}, t_{end}, i)$ is the density on link i during the analysis period ($t_{end} - t_{beg}$), in vpmpl.
- L_{veh} is the length of the vehicle, in feet.
- $L_{boq}(t, i)$ is the back of queue at time step t on link i, in feet.
- $L_{link}(i)$ is the length of link i, in feet.
- $ID_{link}(t)$ is the identification number of the link the vehicle is occupying at time step t.
- $ID_{lead}(t)$ is the identification number of the vehicle's leader at time step t, which is equal to null if the vehicle does not have a leader.
- $QS(t)$ is a Boolean variable that indicates the queued state of the vehicle at time step t, where true corresponds to vehicle in queue and false corresponds to vehicle not in queue.
- $SS(t)$ is a Boolean variable that indicates the stopped state of the vehicle at time step t, where true corresponds to vehicle in a stopped state and false corresponds to vehicle releasing from stopped state.
- $SS_{sub}(t)$ is a Boolean variable, where true represents the vehicle is still in a subsequent stopped state at time step t.
- $D_{ts}(t)$ is the time step delay of the vehicle at time step t, in seconds.
- $D_{ts}(t_{beg}, t_{end})$ is the time step delay of the vehicle during the analysis period ($t_{end} - t_{beg}$), in seconds.
- $D_{seg}(i)$ is the time step delay of the vehicle accumulated on the link–segment i, in seconds.
- $D_{que}(t)$ is the queue delay of the vehicle at time step t, in seconds.
- $D_{que}(t_{beg}, t_{end})$ is the queue delay of the vehicle during the analysis period ($t_{end} - t_{beg}$), in seconds.
- $D_{stop}(t)$ is the stopped delay of the vehicle at time step t, in seconds.
- $D_{stop}(t_{beg}, t_{end})$ is the stopped delay of the vehicle during the analysis period ($t_{end} - t_{beg}$), in seconds.
- $N_{stop}(t_{beg}, t_{end})$ is the number of stops accumulated during the analysis period ($t_{end} - t_{beg}$).
- $N_{veh}(t, i)$is the total number of vehicles present on link i at time step t.
- $N_{lane}(i)$ is the number of through lanes on link i.

It should be noted that the logic provided in the flowcharts in this section comes directly from the HCM 2010, either the facility-specific analysis chapters or Chapter 24. While the logic presented in these flowcharts might be debatable, since the intent of VTAPE is to generate performance measures consistent with the HCM performance measure definitions, the logic provided in the HCM 2010 was not modified when implemented into VTAPE.

Queue-Related Measures

Queue-related measures are used in HCM Chapter 10 Freeway Facilities, Chapter 18 Signalized Intersections, Chapter 19 Two-Way Stop-Controlled (TWSC) Intersections, Chapter 20 All-Way Stop-Controlled (AWSC) Intersections, Chapter 21 Roundabouts, and Chapter 22 Interchange Ramp Terminals. These measures mainly consist of queue delay and queue length estimation, the latter being used to indicate the number of vehicles in the queue and the distance of the last vehicle in the queue from the downstream end of the segment or link (BOQ).

The key to estimating any of queue-related measures from vehicle trajectory data is identifying the queued state of a vehicle; that is, when the vehicle joins a queue and when it exits a queue. The logic for determining the queued state of a vehicle is described in Figure 3*a*, which consists of two steps. The first step is to check the beginning of the queued state for both uninterrupted and interrupted flow conditions as shown in Figure 3*b*. If the vehicle has already entered into a queue, the second step is to identify when the vehicle has left queued state occurred, which is described in Figure 3*c*.

By estimating the queued state through the procedure given above for each vehicle at each time step within the analysis period, the BOQ at any time step can be determined by the position of the farthest upstream vehicle that is in the queued state. BOQ can be updated by looping through the function below until the last vehicle in a queued state on the link has been processed.

$$L_{boq}(t,i) = s_{stop}(i) - s(t) + L_{veh} \quad (1)$$

The estimation of queue delay will be given in detail in delay-related measures.

Stop-Related Measures

Stop-related measures are used in HCM Chapter 17 Urban Street Segments, Chapter 18 Signalized Intersections, and Chapter 31 Signalized Intersections. The two main stop-related measures are estimations of number of stops and stopped delay.

Before performing stop-related measures, the stopped state of a vehicle needs to be determined. According to the definition of the stopped state described in HCM, a speed less than 7.33 ft/s (5 mph) is simply applied as the threshold to check if a vehicle has stopped. A vehicle is considered to have left a stopped state if it accelerates to a velocity of one-third or more of its desired velocity. The time between when a vehicle enters a stop status and leaves a stop status is counted as a single stop, regardless of the length of the stop. For each vehicle within the analysis period, the number of stops on any segment–link can be determined by checking the number of times the vehicle's stop status changed while on the segment–link. The details of the logic are shown in Figure 4. The estimation of stopped delay will be given in detail in delay-related measures.

Delay-Related Measures

Delay-related measures are used in HCM Chapter 10 Freeway Facilities, Chapter 11 Basic Freeway Segments, Chapter 12 Freeway Weaving Segments, Chapter 13 Freeway Merge and Diverge Segments, Chapter 18 Signalized Intersections, Chapter 19 TWSC Intersections, Chapter 20 AWSC Intersections, Chapter 21 Roundabouts, and Chapter 31 Signalized Intersections Supplemental. The various measures consist of time step delay, segment delay, queue delay, stopped delay, and control delay.

Delay is the additional time spent on a segment–link due to situations that hinder the vehicle traveling at its desired speed. Theoretically, it can be determined by the time difference between actual travel time and a reference travel time, typically travel time at the desired speed.

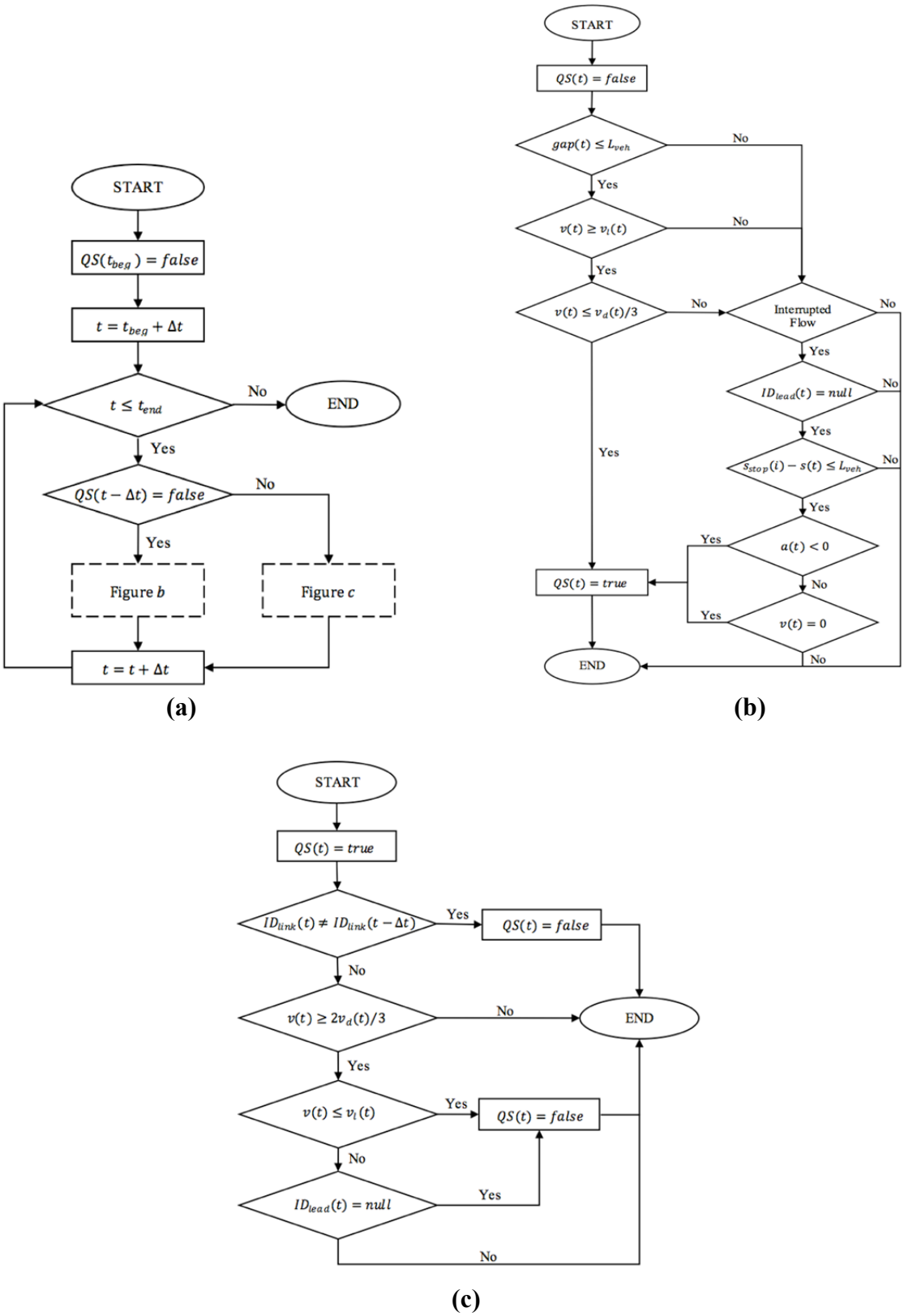

FIGURE 3 (*a*) Flowchart of logic to identify (*b*) when a vehicle joins a queue or (*c*) when a vehicle exits a queue.

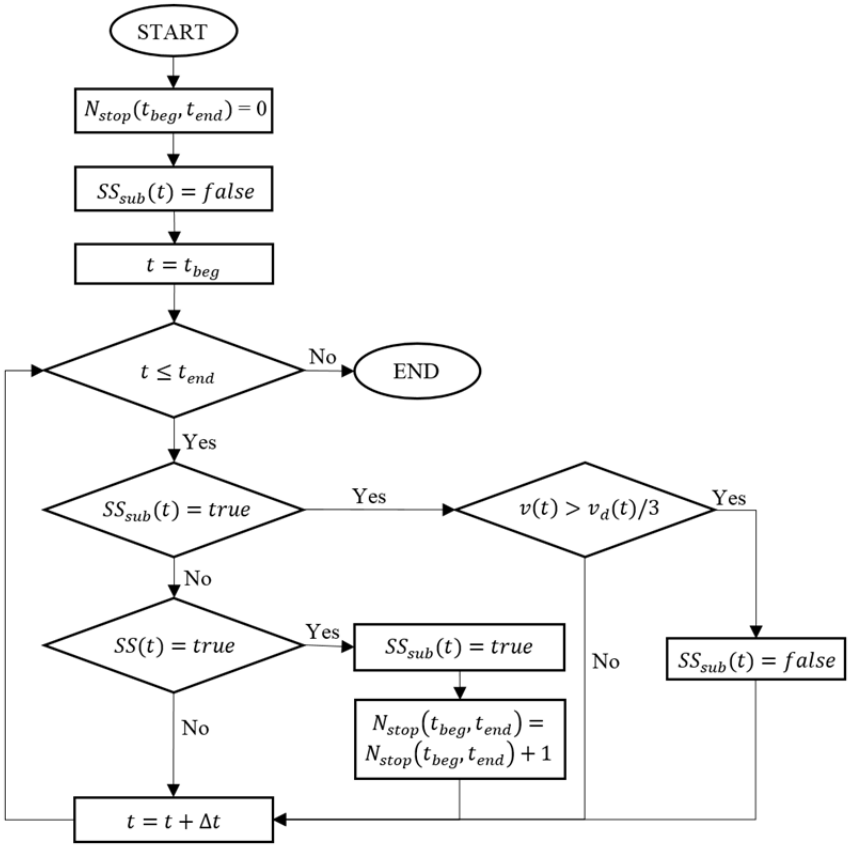

FIGURE 4 Flowchart of logic to estimate the number of stops.

Time step delay is the basis for determining the rest of the delay measures presented in this section. Time-step delay at any time step can be expressed as the time difference between the travel time actually taken and the reference travel time, as follows

$$D_{ts}(t) = \Delta t - \Delta t[v(t) / v_d(t)] \tag{2}$$

In addition, the total time step delay is the sum of time step delays during analysis period. For example, the time step delay from time step t_{beg} to t_{end} can be expressed as

$$D_{ts}(t_{beg}, t_{end}) = \sum_{t=t_{beg}}^{t_{end}} \Delta t - \Delta t[v(t) / v_d(t)] \tag{3}$$

Segment delay is the total time step delay accumulated on a specific segment/link. Suppose a vehicle is present on segment/link i from time step t_{beg} to t_{end}, the segment delay can be expressed as

$$D_{seg}(i) = D_{ts}(t_{beg}, t_{end}) \tag{4}$$

Queue delay is the time step delay at any time step that the vehicle is in a queued state. The estimation procedure of queue delay is shown in Figure 5*a*. Stopped delay, of which the computational procedure is similar with that of queue delay, is represented by time-step delay accumulated over all time steps that the vehicle is in the stopped state. The determination of stopped delay is presented in Figure 5*b*.

Conceptually, the relationship between segment delay, queue delay, and stopped delay is

$$D_{seg}(i) = D_{ts}(t_{beg}, t_{end}) \geq D_{que}(t_{beg}, t_{end}) = \sum_{t=t_{beg}}^{t_{end}} D_{que}(t) \geq D_{stop}(t_{beg}, t_{end}) = \sum_{t=t_{beg}}^{t_{end}} D_{stop}(t) \quad (5)$$

In addition, according to the definition of HCM, control delay can be calculated as an approximation of queue delay if it is a traffic control device causing the queue delay.

Density-Related Measures

Density-related measures are used in HCM Chapter 10 Freeway Facilities, Chapter 11 Basic Freeway Segments, Chapter 12 Freeway Weaving Segments, and Chapter 13 Freeway Merge and Diverge Segments.

Link–segment density can be determined by counting the number of vehicles present on each lane on a specific link–segment during the analysis period.

$$k(t_{beg}, t_{end}, i) = \sum_{t=t_{beg}}^{t_{end}} N_{veh}(t,i) / (t_{end} - t_{beg}) / N_{lane}(i) / L_{link}(i) \quad (6)$$

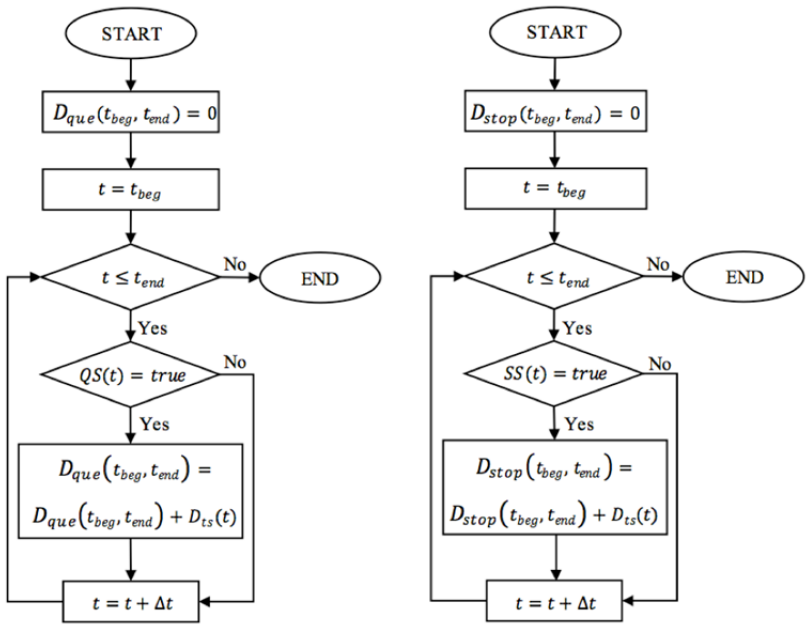

(a) **(b)**

FIGURE 5 Flowchart of logic to determine (*a*) queue delay and (*b*) stopped delay.

VTAPE SYSTEM

VTAPE was developed to be able to analyze vehicle trajectory data for determining HCM-compatible performance measures. VTAPE has also been developed with the intent of being a useful tool for the evaluation and verification of microscopic simulation vehicle-movement models, but this topic is beyond the scope of this paper. An earlier prototype of VTAPE was developed by Courage as a part of the NCHRP 3-85 project, but it was much more limited, both in terms of functionality and software architecture, than the version described here (*3*). The new version of VTAPE takes advantage of the latest software technologies from Microsoft, such as the .NET Framework, the C# programming language, and the Windows Presentation Foundation. A general overview of the features and software architecture of VTAPE are as follows.

- Visualization and analysis of vehicle trajectory data provided by different simulation programs and field observations. Currently, VTAPE supports data provided by CORSIM, VISSIM, and NGSIM.
- Flexibility in filtering vehicle trajectory data, as users can locate any vehicles and links they prefer for analysis.
- Estimation of HCM-compatible performance measures and generating an analysis report for consistency verification. Currently, VTAPE is able to estimate queue-related, stop-related, delay-related, stop-related, and density-related performance measures.
- Extensibility based on expandable software architecture and open-source codebases for allowing researchers and developers to cooperatively expand the range of capabilities of VTAPE, such as reading trajectory data from additional sources and supporting more analysis methods.

VTAPE is built on a flexible architecture, which consists of three separate layers as presented in Figure 6*a*. The presentation layer provides the functionality of visualizing vehicle trajectories and presenting analysis reports based on the binding data transferred from the interaction layer operated by the VTAPE user. In the interaction layer, the VTAPE user can inspect and filter different types of vehicle trajectory data processed in the model layer. The model layer consists of two sublayers, which implement the data transformation and data analysis. The model layer is designed for modularity. It is able to fulfill the needs of processing more types of data and make the process of data analysis more adaptive to change. The functionality of the data transformation sublayer is to convert data from different sources and import them into a uniform database structure introduced in Section 3. The data analysis sublayer performs the calculation of various performance measures defined in the HCM as described in Section 4.

The workflow of VTAPE is shown in Figure 6*b*. VTAPE imports vehicle trajectory files given by sources and extracts basic data and derived data that are used to generate vehicle trajectory plots. Additionally, VTAPE applies extended data which is mapped from source files through predefined source-specific interfaces to calculate HCM-compatible performance measures. Finally, VTAPE produces the analysis report containing the outputs of performance measure calculations. For illustration purpose, screenshots of the vehicle trajectory visualization window and the analysis report window were taken from VTAPE, which are shown in Figure 6*c* and 6*d*.

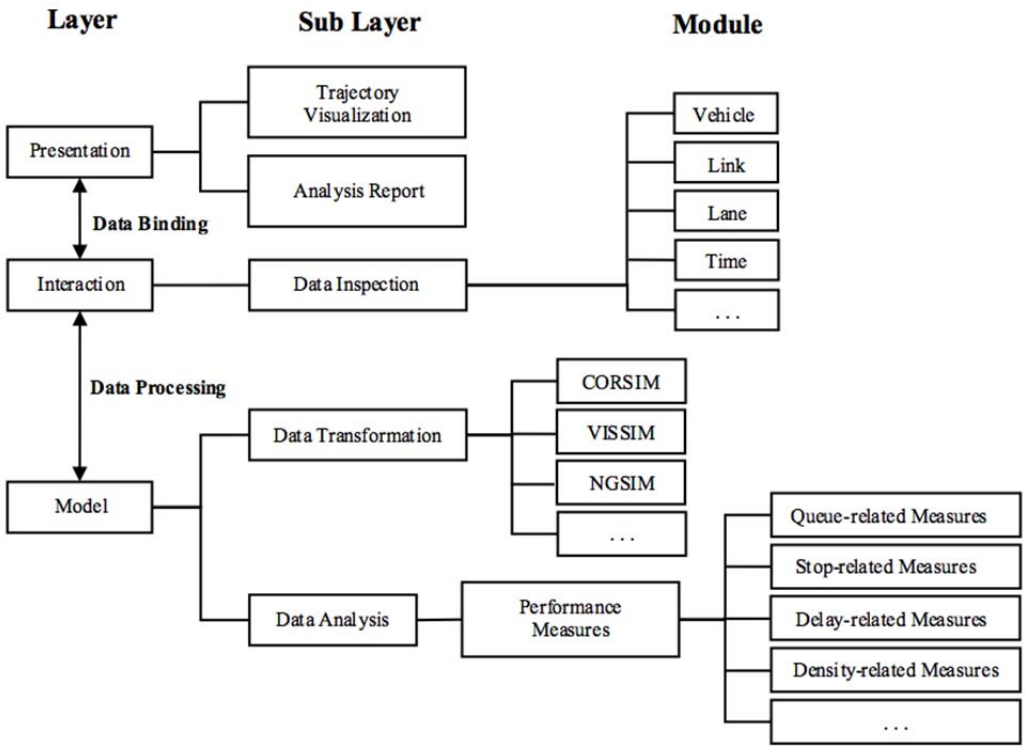

(a)

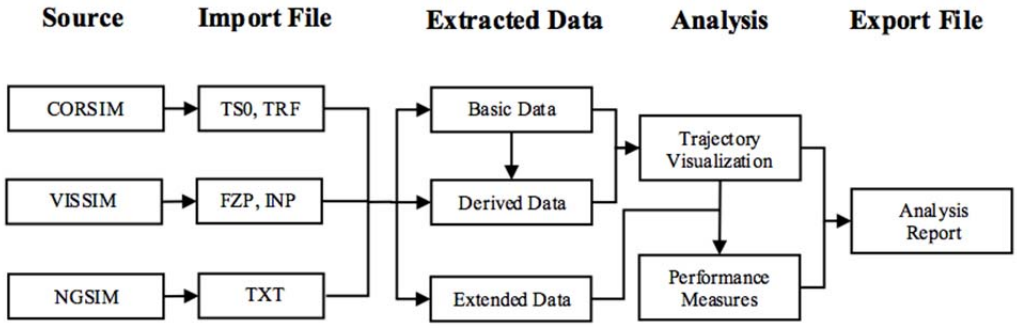

(b)

FIGURE 6 (*a*) The software architecture of VTAPE; (*b*) the workflow of VTAPE.

(continued on next page)

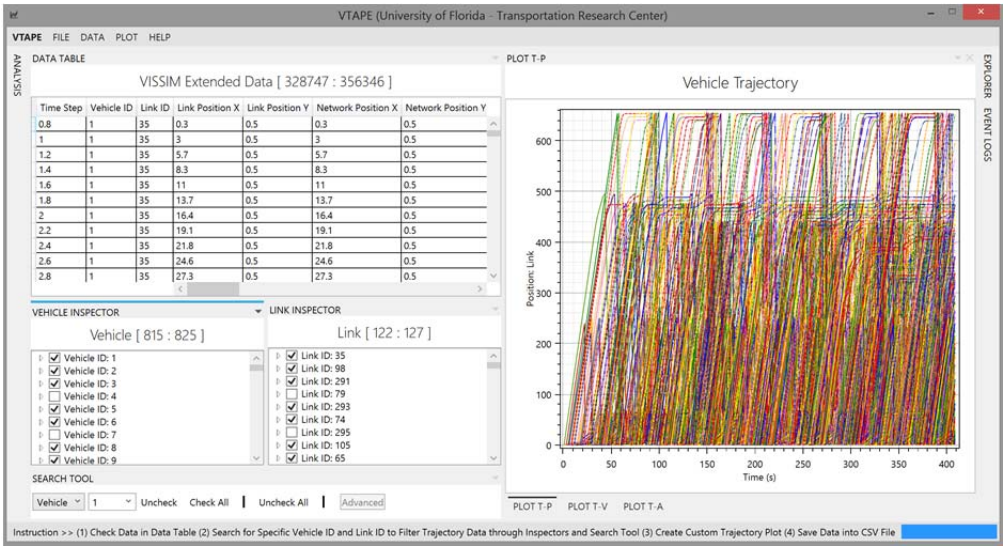

(c)

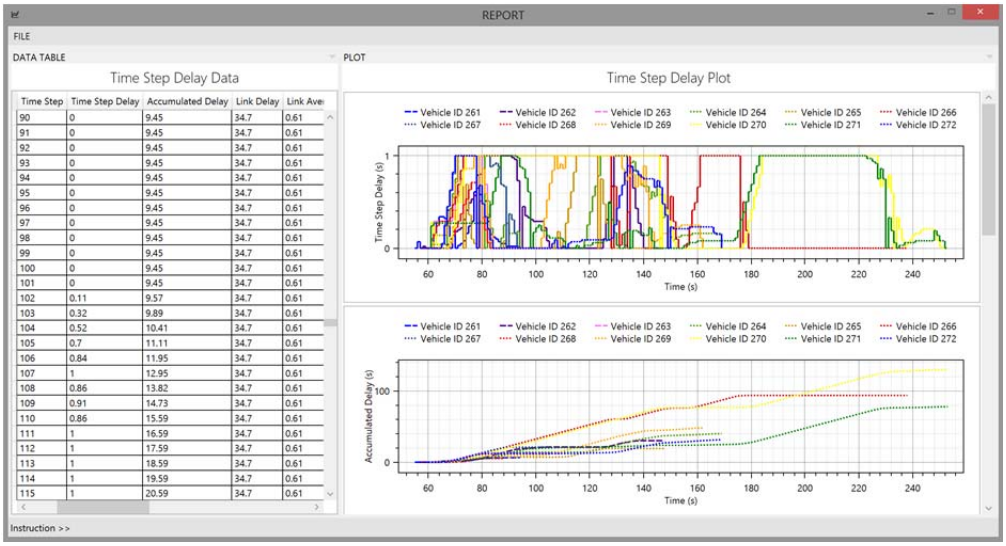

(d)

FIGURE 6 (*continued*) (*c*) The vehicle trajectory visualization window; and (*d*) the analysis report window.

VEHICLE TRAJECTORY ANALYSIS USING VTAPE

Freeway Analysis with Field Data

The vehicle trajectory dataset used for this freeway analysis example comes from the NGSIM project. This dataset was collected from an approximately 1,650-ft segment of I-80 in Emeryville, California, from 4:00 to 4:15 p.m. on April 13, 2005 (*12*). Figure 7*a* shows the entire set of trajectories from 2,052 vehicles, resulting in 1,262,678 trajectory records. It is apparent from Figure 7*a* that traffic congestion appears spontaneously every 3 min in the last 10 min of

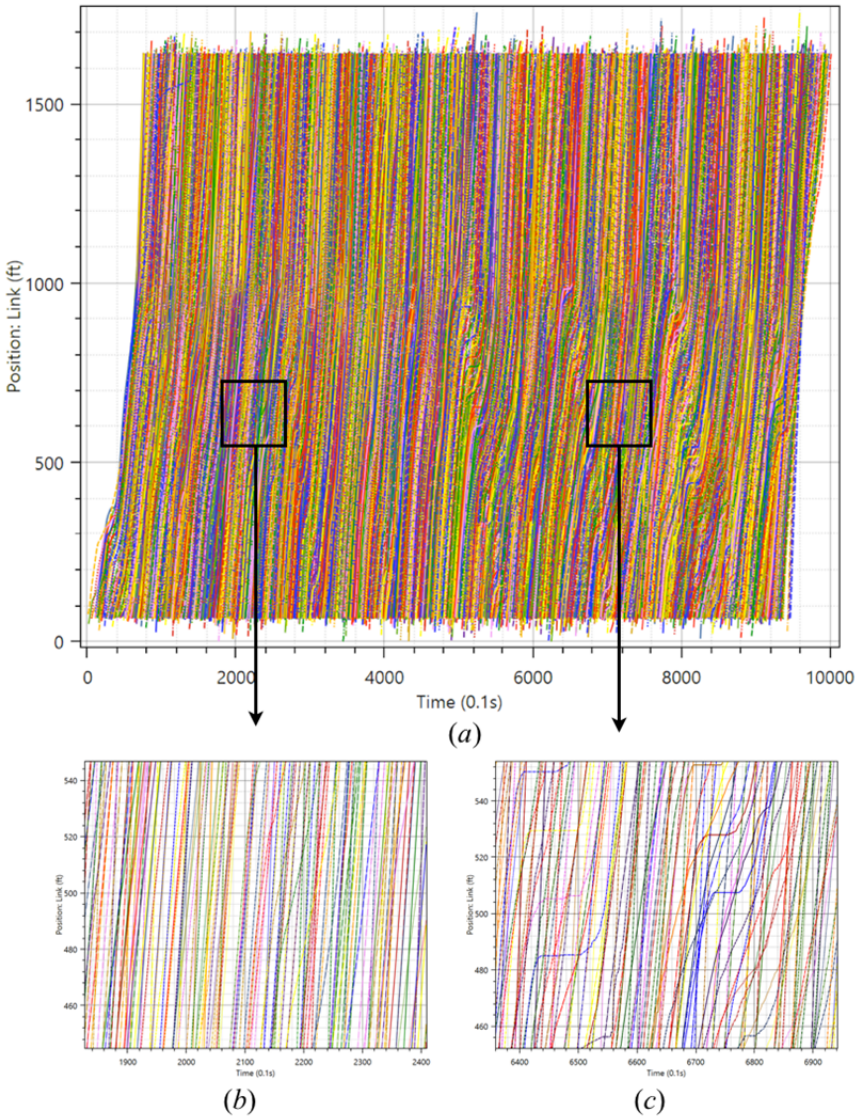

FIGURE 7 Illustrations of (*a*) the entire vehicle trajectories; (*b*) the vehicle trajectories in free flow condition; and (*c*) the vehicle trajectories in congestion.

the analysis period as the lines of vehicle trajectories cross each other when in congestion and are more non-linear than those vehicles in a free-flow condition. The difference in trajectory lines can be seen clearly from Figure 7*b* and Figure 7*c*, which are zoomed in excerpts from Figure 7*a*.

For further investigating the variance of vehicle trajectories in a congestion condition, a typical vehicle with ID 2108 is selected from Figure 7*c* for performing delay-related measures described in Section 4. First, the vehicle trajectory plots are generated by VTAPE, as shown in Figure 8*a*, *b*, *c*, and *d*.

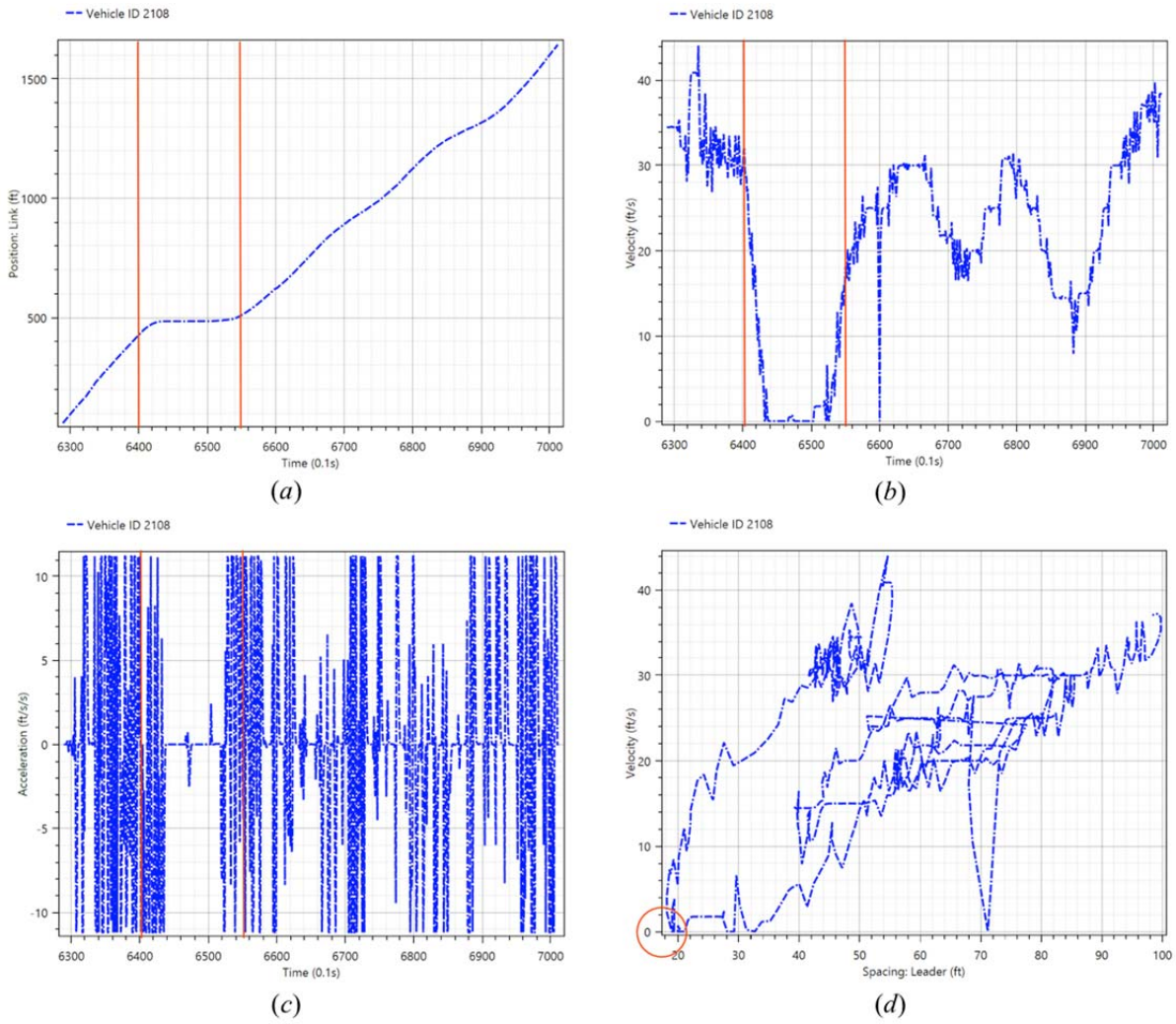

FIGURE 8 The vehicle trajectory plots of vehicle 2108 in terms of (*a*) time–space diagram; (*b*) time–velocity diagram; (*c*) time–acceleration diagram; and (*d*) spacing–velocity diagram.

It is implied by the vehicle trajectory plots that the vehicle is severely constrained by the congestion as the vehicle trajectory line, from the time–space diagram shown in Figure 8*a,* tends to be flat between time steps 6,400 and 6,550, while its velocity shown in Figure 8*b* decreases dramatically from 30 ft/s to 0 and the spacing between the vehicle and its leader becomes less than approximately 20 ft, as shown in Figure 8*d*.

It should be noted that the potential impact of measurement errors from field trajectory data on the results can be significant, as Figure 8*c* illustrates (i.e., unlikely acceleration values). At this time, VTAPE does not have the capability to identify and filter noisy or erroneous data. This type of data preprocessing is the responsibility of the analyst (*13*).

The delay-related measures, such as time step delay, queue delay, and stopped delay for each time step are computed by VTAPE, as depicted in Figure 9, where t'_{beg} indicates the time

step in which the vehicle joins the queue, while t'_{end} and t''_{end} represent the time step the vehicle exits from the queued and stopped states, respectively.

By comparing the constitution of the different delays in Figure 9, equation (5) can be verified by observations, as follows:

$$D_{seg} = D_{ts}(t_{beg}, t_{end}) > D_{ts}(t'_{beg}, t'_{end}) = D_{que}(t'_{beg}, t'_{end}) > D_{que}(t'_{beg}, t''_{end}) = D_{stop}(t'_{beg}, t''_{end}) \quad (6)$$

$$D_{que}(t'_{beg}, t'_{end}) \approx D_{que}(t_{beg}, t_{end}) \quad (7)$$

$$D_{stop}(t'_{beg}, t''_{end}) \approx D_{stop}(t_{beg}, t_{end}) \quad (8)$$

Note that no control delay is produced since the vehicle is on an uninterrupted flow link.

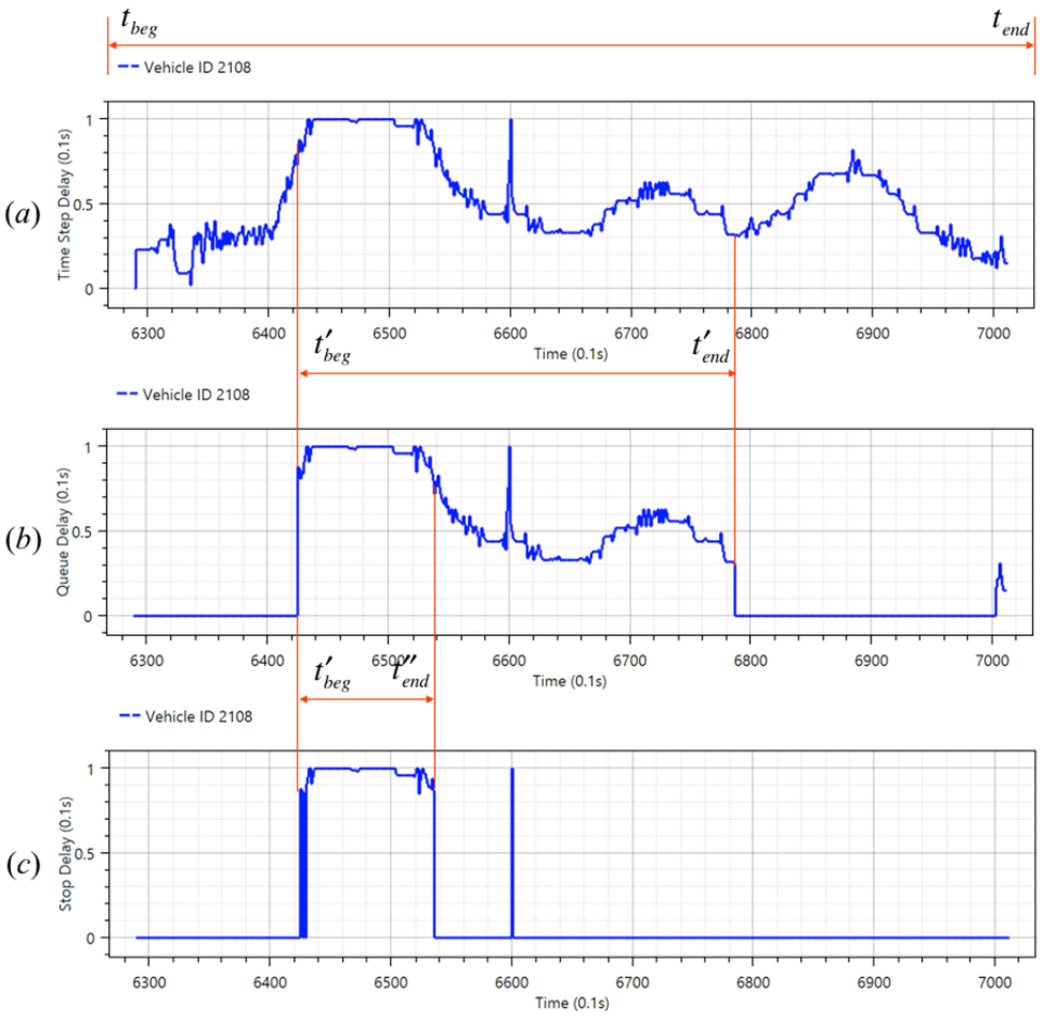

FIGURE 9 Estimations of (*a*) time step delay, (*b*) queue delay, and (*c*) stopped delay of vehicle 2108.

Arterial Analysis with Simulation Data

The dataset used for arterial analysis was generated by CORSIM, of which the road network is depicted in Figure 10*a* (*14*). An eastbound arterial route consisting of eight links is selected for estimating performance measures. The total length of the route is about 4,400 ft, and the analysis period is set up for 600 s. Segment-specific density results can be calculated for the analysis period. The results generated by VTAPE are presented in Figure 10*b*.

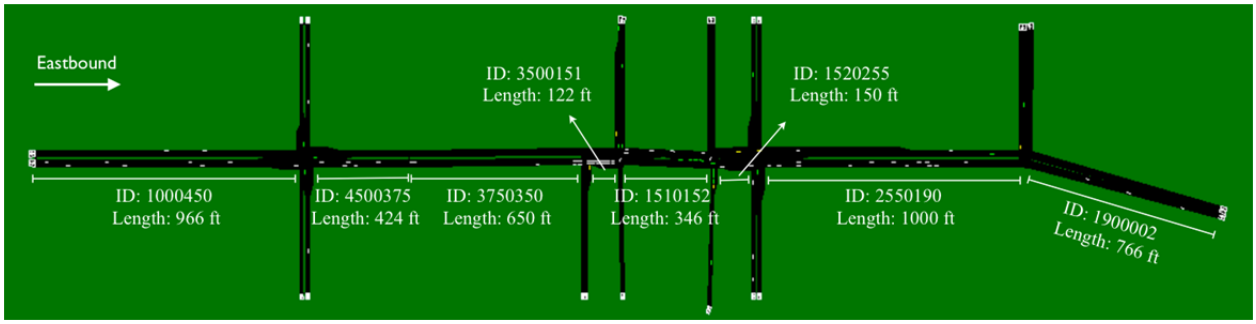

(a)

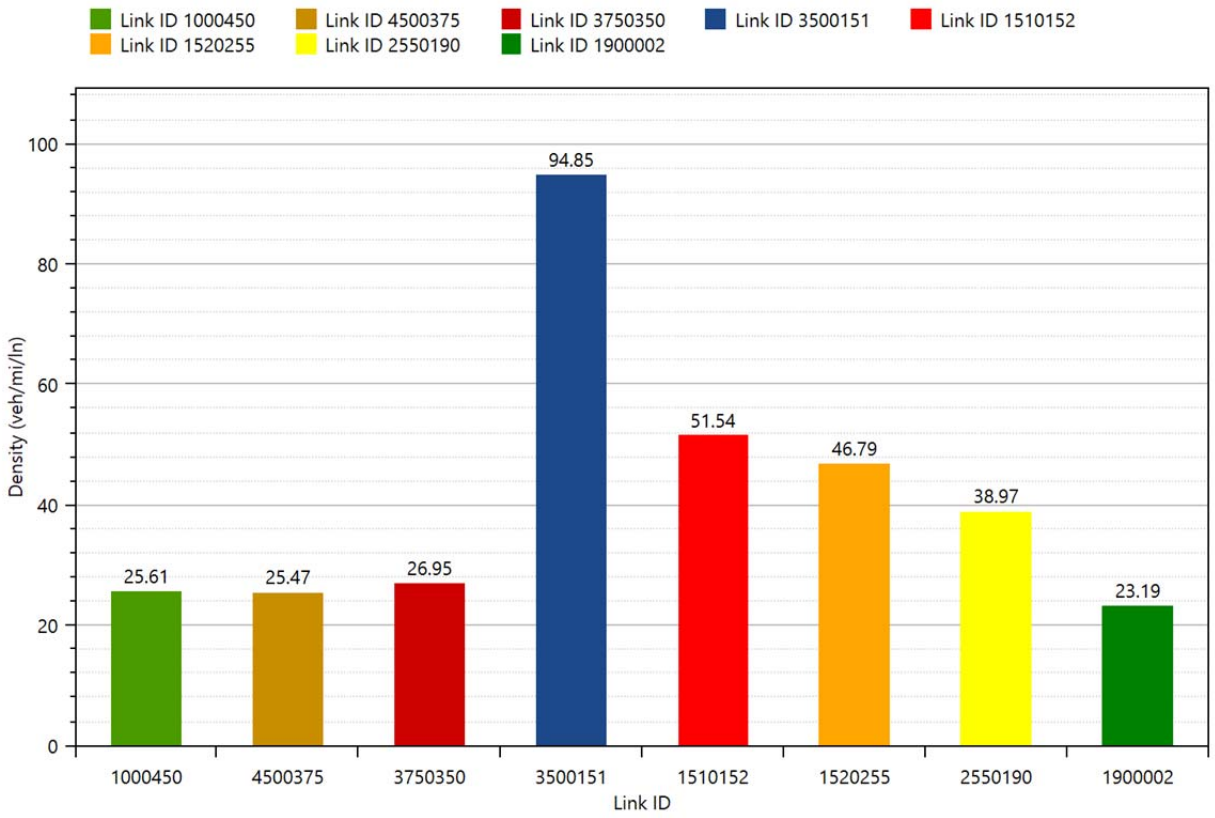

(b)

FIGURE 10 Illustrations of (*a*) the road network geometry and (*b*) the density calculation results.

TABLE 3 Comparison of Networkwide Performance Measures Outputs (per vehicle)

	Time Step Delay (s)	Queue Delay (s)	Stopped Delay (s)
CORSIM	58.94	35.04	32.77
VTAPE	58.21	35.86	33.14

In addition, vehicles in a platoon within a given time period can be chosen for displaying performance measures. Here, the vehicles in a platoon with IDs 578, 580, 583, 587, 588, 595, and 605 are selected and corresponding stop-related performance measure calculations are conducted by VTAPE. The results of stopped delay and number of stops for each vehicle are shown in Figure 11*a*, *b*, *c*, and *d*. Other results of delay-related measures are also calculated by VTAPE and summarized in Figure 11*e*.

Table 3 shows the networkwide performance measure outputs (per vehicle) from CORSIM and VTAPE respectively. Note that the results of VTAPE are based on the HCM calculation procedures. Regarding the time step delay, queue delay, and stopped delay, the calculation results show that the CORSIM and VTAPE values are similar, but not identical. Thus, it can be concluded that the CORSIM calculation methods for these performance measures are not 100% consistent with the HCM-defined calculation methods.

SUMMARY

This paper presented the VTAPE software program, a vehicle trajectory analysis system that is able to visualize and analyze the vehicle trajectory data provided by microscopic simulation programs and field observations. A uniform database structure and expandable software architecture have been developed to make VTAPE capable of supporting various types of vehicle trajectory datasets and analysis methods. In addition, the computational procedures to generate HCM-compatible performance measures from vehicle trajectory data are discussed in detail in this paper. Finally, the analysis examples show the effectiveness of the computational procedures and reliable results that encourage future development.

ACKNOWLEDGMENT

The authors acknowledge Ken Courage for his initial work in this area.

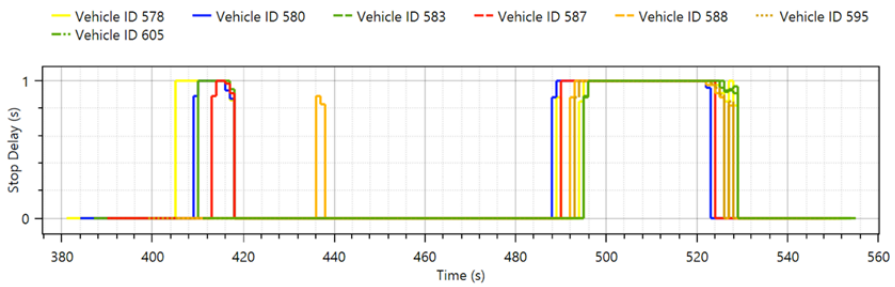

(*a*)

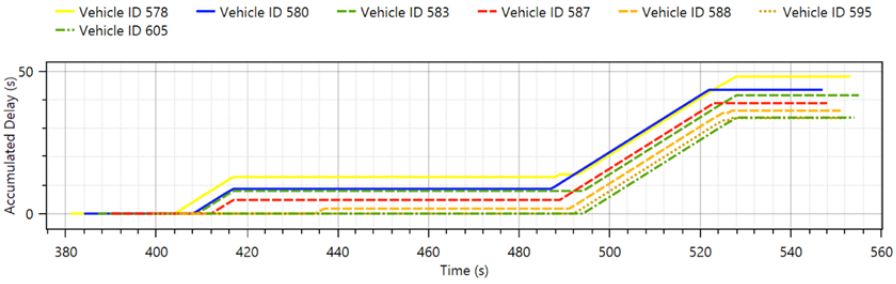

(*b*)

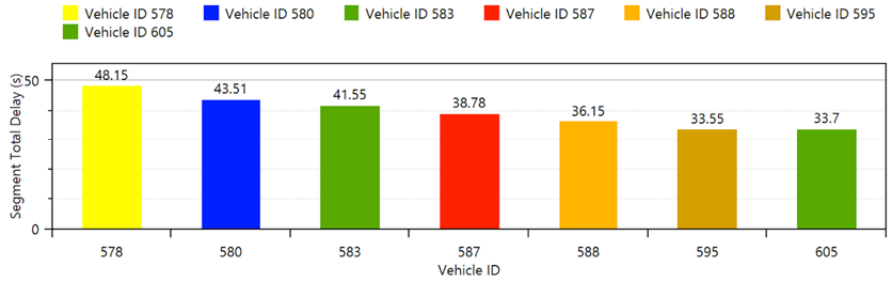

(*c*)

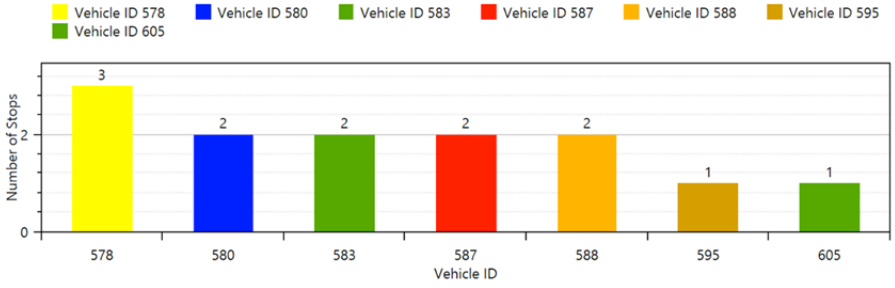

(*d*)

	Time Step Delay (s)	Queue Delay (s)	Stopped Delay (s)	Number of Stops
Total	407.26	308.39	275.39	13
Average	58.18	44.06	39.34	1.86

(*e*)

FIGURE 11 Illustrations of (*a*) stopped delay at each time step; (*b*) accumulated stopped delay; (*c*) stopped delay on entire segment; (*d*) number of stops; and (*e*) summary of analysis results.

REFERENCES

1. *Highway Capacity Manual 2010*. Transportation Research Board of the National Academies, Washington D.C., 2010.
2. Dowling, R., A. Skabardonis, and V. Alexiadis. Traffic Analysis Toolbox. FHWA-HRT-04-040. FHWA, U.S. Department of Transportation, 2004.
3. Courage, K. G., S. Washburn, L. Elefteriadou, and D. Nam. Guidance for the Use of Alternative Traffic Analysis Tools in Highway Capacity Analyses. NCHRP Project 3-85 Final Report. University of Florida, Gainesville, 2010.
4. Brackstone, M., and M. McDonald. Car-Following: A Historical Review. *Transportation Research Part F*, Vol. 2, 1999, pp. 181–196.
5. Yeo, H., and A. Skabardonis. Oversaturated Freeway Flow Algorithm for Use in Next Generation Simulation. In *Transportation Research Record: Journal of the Transportation Research Board, No. 2088,* Transportation Research Board of the National Academies, Washington, D.C., 2008, pp. 68–79.
6. Chen, D., J. Laval, Z. Zheng, and S. Ahn. A Behavioral Car-Following Model That Captures Traffic Oscillations. *Transportation Research Part B*, Vol. 46, 2012, pp. 744–761.
7. Siemens Energy and Automation, Inc. Surrogate Safety Assessment Model and Validation: Final Report. FHWA-HRT-08-051. FHWA, U.S. Department of Transportation, 2008.
8. CORSIM User's Guide Version 6.3. University of Florida, 2012.
9. TRAFVU File Description Document. University of Florida, 2008.
10. VISSIM 5.40 User Manual. PTV Vision, Karlsruhe, Germany, 2012.
11. Next Generation Simulation. FHWA, U.S. Department of Transportation. Available at http://ops.fhwa.dot.gov/trafficanalysistools/ngsim.htm. Accessed July 2, 2013.
12. Interstate 80 Freeway Dataset. FHWA, U.S. Department of Transportation. Available at http://www.fhwa.dot.gov/publications/research/operations/06137/index.cfm. Accessed July 7, 2013
13. Punzo, V., M. Borzacchiello, and B. Ciuffo. On the Assessment of Vehicle Trajectory Data Accuracy and Application to the Next Generation SIMulation Program Data. *Transportation Research Part C*, Vol. 19, 2011, pp. 1243–1262.
14. McTrans. Trafvu Viewer. Available at http://mctrans.ce.ufl.edu/featured/tsis/TRAFVUViewer.htm. Accessed July 9, 2013.

Field Evaluation of Traffic Performance Measures for Two-Lane Highways in Spain

ANA TSUI MORENO
CARLOS LLORCA
Universitat Politècnica de València, Spain

TAREK SAYED
University of British Columbia, Canada

ALFREDO GARCÍA
Universitat Politècnica de València, Spain

Two-lane highway operations have been extensively studied. Many of these studies state that the current *Highway Capacity Manual 2010* (HCM) procedure is difficult to measure in the field. Several promising alternative measures have been proposed which are easy to measure in field, such as follower density, percent impeded, or freedom of flow. Nevertheless, some of these measures are based on hypotheses that may only be applicable to local driver behavior. Moreover, the previous field studies that compared some of the performance measures had very limited traffic flow range. The present field study calibrates and evaluates 10 performance measures in Spanish two-lane highways. The data was collected using video recordings in 10 sites on two-lane rural highways. Observed two-way traffic volumes ranged from 120 to 1,000 vehicles per hour and traffic flows were mainly balanced. From this data, time headways, average travel speed and platooning variables were calculated. The studied performance measures included: average travel speed, average travel speed of passenger cars, percent free-flow speed, percent free-flow speed of passenger cars, percent followers, follower density, percent impeded, average platoon length, traffic intensity, and freedom of flow. The results indicated that the follower density had the strongest correlation with traffic variables, with a coefficient of determination of 94%, and it is recommended as a major performance measure. The estimations were compared with previous models and they were alike within their observation range. The second best performance measure was the percent followers and the estimates were very similar to the models in Finland. The HCM 2010 overestimated the percent followers at low traffic flows, which could indicate that the extrapolation of medium-high traffic volume driver behavior was not too accurate at our observation range. Other platooning-related variables had lower correlations, while the speed-related measures presented the weakest correlation with traffic variables.

Two-lane highways constitute about 70% of all roads in Spain. Their unique characteristics, derived from the level of interaction between vehicles traveling in the same and in opposing direction, make the evaluation of their traffic operations a complex process. Currently, the *Highway Capacity Manual 2010* (HCM 2010) of TRB (*1*) is used for the analysis of the operation on these roads, not only in the United States but also in Spain (*2*).

The HCM 2010 provides an analysis procedure for directional segments of two-lane highways based on the average travel speed (ATS) and percent time spent following (PTSF). The level of service (LOS) for Class I two-lane highways depends on both values, while the LOS for

Class II two-lane highways depends only on PTSF. The percentage of followers (PF), defined as the percentage of vehicles with time headways smaller than 3 s, may be used as a surrogate measure for the PTSF (*1*). The percent of free-flow speed (PFFS) is introduced as a performance measure for the new Class III two-lane highways, following recommendations from Washburn et al. (*3*).

Romana and Perez (*4*) proposed a threshold speed to determine whether it is more appropriate to define the LOS based on the ATS or on the PTSF. On the other hand, Luttinen et al. (*5*) stated that the performance measures should be easy to measure and estimate and should correlate with the traffic conditions in a meaningful way. However, the HCM performance measures are difficult to measure in the field (*5–10*) and some authors have developed alternative performance measures to overcome this problem as discussed below.

LITERATURE REVIEW

Speed-Related Performance Measures

The speed-related performance measures include the ATS, the ATS of passenger cars (ATS_{PC}), the PFFS and the PFFS of passenger cars ($PFFS_{PC}$).

The ATS is the output mean speed and is one of two performance indicators used by the HCM 2010 and in Brazil (*11*). However, several researchers indicated that it fails to provide an accurate indication of traffic performance (*8–10*). The ATS_{PC} is used in Germany as a major performance measure (*12*) and it replaces the ATS in Finland (*3*, *13*), however this speed-related measure was hardly sensitive to traffic flow in some field studies (*8–10*). Moreover, they also reported weak relationships between ATS, ATS_{PC}, and the flow rate (R^2 between 10% and 13%), and the PFFS and $PFFS_{PC}$ and flow rate (R^2 lower than 1%). Eight-second headway criterion was used to determine free-flow conditions.

Platooning-Related Performance Measures

In addition to the PTSF and the PF that are defined at the HCM 2010, more performance measures have been developed and calibrated with field data. These measures are: follower density (FD), percent impeded (PI), average platoon length (APL), traffic intensity (ρ), and freedom of flow (η).

The PTSF is the performance measure defined by the HCM, but it is difficult to measure in the field and the PF is used as its surrogate measure. Theoretically, low traffic levels could still have high PFs if speed dispersion is relatively high and passing opportunities are limited; therefore it can be misleading (*14*). Previous field studies showed good relationship between the percent followers and the flow rate, with coefficient of determination of 73% (*7*), 79% (*8*), 30% (*10*), 93% (*16*), and 61% (*18*). The high difference on the study in Egypt (*10*) may be caused by the low traffic volumes or more specific driving behavior. However, the previous field studies only observed low traffic flows (*7*, *8*, *10*, *16*).

The FD is the major performance measure in South African highways (*14*) and in Japanese expressways (*15*). It is defined as the number of followers per kilometer per lane and is calculated as the PF multiplied by the traffic flow and divided by the travel speed. It showed the best correlation with traffic variables in all the field evaluations (*8–10*) compared to the speed-

related measures and the PF (R^2 between 75% and 98%). Besides, this measure had some degree of correspondence with the analysis of freeways and multilane highways (*5*, *14*).

The PI estimates the PTSF using a probabilistic approach (*7*). It is calculated by multiplying the probability of being part of a platoon and the probability of being impeded. The 3-s headway platoon definition is used to calculate the probability of being part of a platoon. The probability of being impeded is calculated at the percentile of the desired speed distribution for all the vehicles that is equal to the average speed of slow-moving vehicles. Platoon leaders are used as the slow-moving vehicles while the distribution of desired speed is calculated using vehicles outside of platoons (6-s headway). This measure presented stronger correlation to traffic flow than the percent followers but it was not compared to other platooning measures. In Egypt, the relationship between percent impeded and flow rate was disperse (R^2 = 22%) (*10*).

The final three performance measures are based on queuing theory (*16*) and depend on the average number of headways inside platoons and between platoons (Equations 1 and 2). Platoons are identified using 3-s headway. The APL is the number of vehicles including the leading vehicle, while the traffic intensity (ρ) is the ratio between the average time spent in the first position when waiting for an appropriate gap and the average interarrival times at the back of the queue and it represents how busy the system is. The freedom of flow (η) is the ratio between the average travel time between platoons and the expected value of the time interval between the arrival of a fast vehicle into a position behind the slow vehicle and the time when the passing maneuver starts; and it reflects an individual driver's undisturbed travel time versus the delay in first position resulting from inability to pass. The measures were calibrated to Israel field data (*17*, *18*) and the correlation to traffic flow of the freedom of flow was strong (R^2 = 93%) while the traffic intensity presented a fair correlation (R^2 = 62%). The theoretical model assumes that (*a*) all drivers are rational and are always willing to pass a slower vehicle and that (*b*) only the first impeded is performing a passing maneuver at one time. This disagrees with actual passing maneuvers field data of other countries that reported considerable number of multiple passing maneuvers (*19–22*) or faster vehicles' speed accommodation to the slower vehicle's speed (*22*, *23*).

$$\rho = 1 - \frac{1}{Q_0} \tag{1}$$

$$\eta = \frac{N_0}{\rho} \tag{2}$$

where

ρ = traffic intensity;
Q_0 = average number of headways inside platoons;
η = freedom of flow; and
N_0 = average number of headways between platoons.

Passing-Related Performance Measures

The HCM 2010 provides a qualitative definition of the LOS depending on driver expectations and perceptions of service, which are influenced by the passing capacity and passing demand balance. The passing ratio (or overtaking ratio) was defined by Morral and Werner as the number of passes achieved by the number of passes desired (*24*) and was considered as a possible performance measure to be included in the 2000 HCM. However, passing ratio would be complicated to measure directly in the field and it was not rated high by HCM users (*25*).

Research Motivation

Two-lane highways operation has been extensively studied. Many studies state that the current HCM procedure is difficult to measure in field and they propose alternative promising measures which are easy to measure in field, such as the FD, PI, or freedom of flow. However, some of the measures are based on hypotheses that may only be applicable to local driver behavior. Moreover, the previous field studies that compared some of the performance measures had very limited traffic flow range. The present field study calibrates and evaluates all the defined performance measures using data from Spanish two-lane highways.

OBJECTIVES AND INITIAL HYPOTHESES

The objective of the paper was to calibrate and evaluate performance measures for two-lane rural highways in the same data set. The relationships between the performance measures and the traffic variables were estimated for 10 sites from three Spanish two-lane rural highways.

The performance measures include: ATS, ATS_{PC}, PFFS, $PFFS_{PC}$, PF, FD, PI, APL, ρ, and η. Besides, ATS deviation (ATS_{dev}) would also be evaluated to confirm the hypothesis of high-speed dispersion at low traffic flow.

Based on the literature, the following hypotheses were established:

- Speed-related measures will present weaker relationships with traffic variables compared to platooning-related measures.
- FD will present the best correlation with traffic variables.
- Speed dispersion will be higher at low traffic flow.
- Spanish drivers may behave more aggressively than U.S. drivers. Therefore, the percent of followers, follower density or percent impeded may be lower.
- APL will fail to represent traffic performance because it misinterprets the actual platoon distribution.
- Freedom of flow and traffic intensity will not represent accurately traffic performance as the theoretical hypotheses differ with Spanish driver behavior.

METHODOLOGY

Field Study

Data were collected in 10 sites of three highways in the province of Valencia, Spain. The sites were located at the beginning of passing zones. The highways were classified as Class II two-lane highway, according to the HCM 2010, and were selected to cover as much range of passing zone length, traffic volume, and percentage of heavy vehicles as possible. Passing zones' characteristics were included as selection criteria for another study (*23*).

Data was collected using two coordinated high definition video cameras located at the beginning and ending of the passing zones. They were at the roadside and were not perceived by drivers. At some sites, the whole passing zone was covered with the camera and accepted and rejected gaps, passing times, and time-to-collision could be calculated (*26*). The sites characteristics are summarized in Table 1 and the directional splits were mainly balanced: directional splits higher than 40/60 were observed in a 15% of the sample and higher than 30/70, in 1.7%.

Data Reduction

Traffic volumes, vehicles type, headways and ATS were obtained from the videos. The counting period was 5 min and the results were aggregated in 15 min as the sum of three overlapping consecutive 5-min period in order to skip the error of peak 15-min period overlapped on two 15-min counting periods (*27*). Then, equivalent hourly data were calculated based on the 15-min data. The 15-min period was chosen over hourly period times in order to better represent passing maneuvers, as peak traffic volumes and traffic proportion are smoothed on hourly periods.

To calculate the ATS of each vehicle, the travel time between the beginning and the end of the passing zone was divided by the passing zone length. Platooning measures considered the headways criteria indicated before. To calculate the percent impeded, the average speed of slow-moving vehicles and the speed distribution of isolated vehicles were obtained. The percentile that corresponds to the average was then multiplied by the PF.

STATISTICAL ANALYSIS

Preliminary Analysis

Preliminary analysis of each variable was carried out in order to obtain the probabilistic distribution that best fitted the data. The normal distribution is preferred, as many non-normally distributed dependent variables can distort relationships and significance parametric tests (*28*). If the variable failed to be normally distributed, they were transformed to the lognormal or inverse to check their normality. The analysis should be carried out by site and across-sites.

A total of 240 preliminary analyses were carried out. Two-way traffic flow, directional traffic flow, opposing traffic flow and follower density were adjusted as lognormal distributions, while the average platoon length and the freedom of flow were inverse distributions and the number of following vehicles followed a negative binomial distribution. The remaining variables were normally

TABLE 1 Sites Characteristics

ID	Highway	Speed Limit (km/h)	AADT (vpd)	Station (km)	Bound	Passing Zone Length (m)	Two-Way Traffic Volume (vph)	Duration (h)	Total Directional Traffic Flow (veh)
1	N-225	100	5,925	5.5	Vall	265	120–900	9:30	1,614
2					Teruel	510			1,624
3				6.1	Vall	1,270			1,614
4					Teruel	1,050			1,624
5	CV-405	80	15,342	12.0	Monserrat	895	520–1,000	2:30	791
6					Torrent	895			1,073
7	CV-35	100	5,797	46.5	Casinos	1,690	200–450	2:50	445
8					Losa	1,860			497
9				42.8	Casinos	780			445
10					Losa	1,135			497
Total								**55:20**	**10,224**

NOTE: ID = identification; AADT = annual average daily traffic; vpd = vehicles per day; vph = vehicles per hour.

distributed. Based on the results of the preliminary analysis, the variables were adjusted to the most suitable proability distribution, that was normal, lognormal, or inverse (Table 2).

Statistical Differences

Once the variables were adequately described and the outliers were identified and removed from the sample, we tested whether the dependent variable was statistically different considering each independent variable. As all the variables (or transformed variables) were normal or almost normal, the parametric test (ANOVA) could be applied grouping the variables in levels with approximately equal sample. Besides, the residuals were also normally distributed. The percentage of no passing zones failed to provide statistical differences on most of the platooning variables and the PFFS, while the ATS_{dev} was uniform for all the traffic flows, which disagrees with the theoretical misleading of PTSF estimation of LOS at low traffic flows (*14*).

Simple Linear Relationships

Simple linear relationships were tested between the dependent variables and the independent variables, one-to-one. Only the statistically significant variables were tested. The analysis of the residuals plot allowed verifying the normality of the residuals and homocedasticity. Consequently, the assumptions of the linear regression were fulfilled in all the cases.

The platooning measures were more correlated to the traffic variables than the speed-related measures as their R^2 varied between 31% and 76% and between 3% and 9%, respectively. On the other hand, using the directional traffic flow provided higher correlations than the two way traffic flow (R^2 increased between 2% and 8%).

TABLE 2 Adjusted Distribution of Each Variable, Across-Site Examination

Variable		Better Adjustment	Normal		Transformed Scale	
			Average	Standard Deviation	Average	Standard Deviation
Two-way traffic flow	Log(V)	Lognormal	220	47.92	4.624	0.414
Traffic proportion	Prop	Normal	49.94	7.31	—	—
Direct traffic flow	Log(Vd)	Lognormal	55.38	25.46	3.918	0.438
Opposing traffic flow	Log(Vo)	Lognormal	55.53	25.55	3.921	0.438
Percentage trucks	%HGV	Normal	14.58	9.47	—	—
Average travel speed$_{100}$	ATS_{100}	Normal	101.19	5.49	—	—
Average travel speed$_{80}$	ATS_{80}	Normal	75.94	2.30	—	—
Average travel speed PC_{100}	$ATSpc_{100}$	Normal	102.77	6.20	—	—
Average travel speed PC_{80}	$ATSpc_{80}$	Normal	76.22	2.42	—	—
Percent free flow speed	PFFS	Normal	0.98	0.04	—	—
Percent free flow speed PC	$PFFS_{pc}$	Normal	1.00	0.03	—	—
Following vehicles	NB(FV)	Negative binomial	22.09	17.19	—	—
Percent followers	PF	Normal	35.03	13.52		
Follower density	Log(FD)	Lognormal	0.24	0.27	–1.807	0.895
Percent impeded	PI	Normal	23.64	13.08	—	—
Average platoon length	1/APL	Inverse	2.72	0.54	0.381	0.068
Traffic intensity	ρ	Normal	0.36	0.18	—	—
Freedom of flow	1/μ	Inverse	18.74	25.43	0.130	0.092

Multiple Regression Analysis

The last phase of the statistical analysis was the multiple regression. The regression models would be trustworthy if the *p*-value of the *F*-statistic is lower than 0.05, at a level of confidence of 95%. Moreover, the *p*-value of the *F*-statistic of each one of the independent variables must be lower than 0.05 and the residuals must be normally distributed. Considering the previous analysis, all the assumptions would be fulfilled and the regression models would be valid. The multiple regression analyses were carried out considering two approaches: directional traffic flows and two-way traffic flows; so the results can be compared and discussed with previous research.

Directional Analysis

The directional analysis considers as independent variables the directional traffic flow, opposing traffic flow, percentage of trucks and percentage of no-passing zones in the analysis segment travel direction. The multiple regression models were fitted using forward stepwise selection. Table 3 shows the equations obtained from the multiple regression analyses.

TABLE 3 Directional Analysis Multiple Regression Models

Variable	Equation	R^2 (%)	R^2_{adj} (%)
ATS_{100}	$ATS_{100} = 129.265 - 6.03 \cdot \ln(Vd) - 0.314 \cdot \%HGV$	16.54	16.14
ATS_{80}	$ATS_{80} = 87.644 - 2.606 \cdot \ln(Vd)$	9.19	7.48
$ATSpc_{100}$	$ATSpc_{100} = 140.12 - 8.555 \cdot \ln(Vd) - 0.288 \cdot \%HGV$	16.62	16.22
$ATSpc_{80}$	$ATSpc_{80} = 89.295 - 2.912 \cdot \ln(Vd)$	10.22	8.56
PFFS	$PFFS = 1.233 - 0.056 \cdot \ln(Vd) - 0.002 \cdot \%HGV$	18.36	18.01
PFFSpc	$PFFSpc = 1.113 - 0.030 \cdot \ln(Vd) + 0.001 \cdot \%HGV$	34.12	34.84
FV	$FV = \exp(-3.0834 + 1.5308 \cdot \ln(Vd) - 0.0051 \cdot \%HGV)$	96.61	96.30
PF	$PF = -60.6933 + 24.4293 \cdot \ln(Vd)$	62.65	62.57
FD	$\ln(FD) = -9.5670 + 1.9610 \cdot \ln(Vd) + 0.0051 \cdot \%HGV$	85.72	85.65
	$FD = -0.2083 + 0.0080 \cdot Vd - 0.0003 \cdot Vo + 0.0012 \cdot \%HGV$	94.84	94.81
PI	$PI = -36.728 + 15.7086 \cdot \ln(Vd) - 0.1123 \cdot \%HGV$	58.99	58.73
APL	$\frac{1}{APL} = 0.663 - 0.093 \ln(Vd)\ 9 + 0.001 \cdot \%NPZ$	36.00	35.73
ρ	$\rho = -0.117 + 0.174 \cdot \ln(Vd) - 0.002 \cdot \%HGV - 0.003 \cdot \%NPZ$	33.80	33.34
μ	$1/\mu = -0.325 + 0.145 \cdot \ln(Vd) - 0.002 \cdot \%NPZ$	49.90	49.67

NOTE: Where

ATS_{100} = average travel speed at highways with 100 km/h speed limit (km/h);
ATS_{80} = average travel speed at highways with 80 km/h speed limit (km/h);
$ATSpc_{100}$ = average travel speed of passenger cars at highways with 100 km/h speed limit (km/h);
$ATSpc_{80}$ = average travel speed of passenger cars at highways with 80 km/h speed limit (km/h);
PFFS = percent of free-flow speed;
$PFFS_{pc}$ = percent of free-flow speed of passenger cars;
FV = followers per period (followers/15 min);
PF = percent followers per period (followers/veh/15 min);
FD = follower density per period (veh/km/15 min);
PI = percent impeded (%/15 min);
ρ = traffic intensity;
μ = freedom of flow;
Vd = *traffic volume on the direction of analysis (veh/15-min);*
Vo = traffic volume on the opposing direction (veh/15-min);
%HGV = percentage of trucks and recreational vehicles (%);
%NPZ = percent no passing zones in the analysis segment (%).

The follower density presented the best adjustment to the field data (Figure 1) as the coefficient of determination of the models presented 85% and 94%, respectively. The first model was conducted for the transformed variable, while the second model was carried out for the original variable. The residuals of the model were normally distributed, so the main assumptions of the multiple regression analysis were fulfilled and the model was valid. The FD increased as the directional traffic flow and the percentage of trucks increased and the opposing traffic flow decreased, which is in agreement with previous models and hypothesis. Based on the simple regression analysis, the most influential variable was the directional traffic flow, as expected. The relatively high correlation between direct and opposing traffic flow may explain the low increase on the coefficient of correlation of the overall model when the opposing traffic flow was added as variable.

The PF and the PI were the second best group of measures, according to the coefficient of determination, 62% and 58%, respectively. Both models did not depend on the opposing traffic flow, which could be due to the correlation between direct and opposing traffic flow.

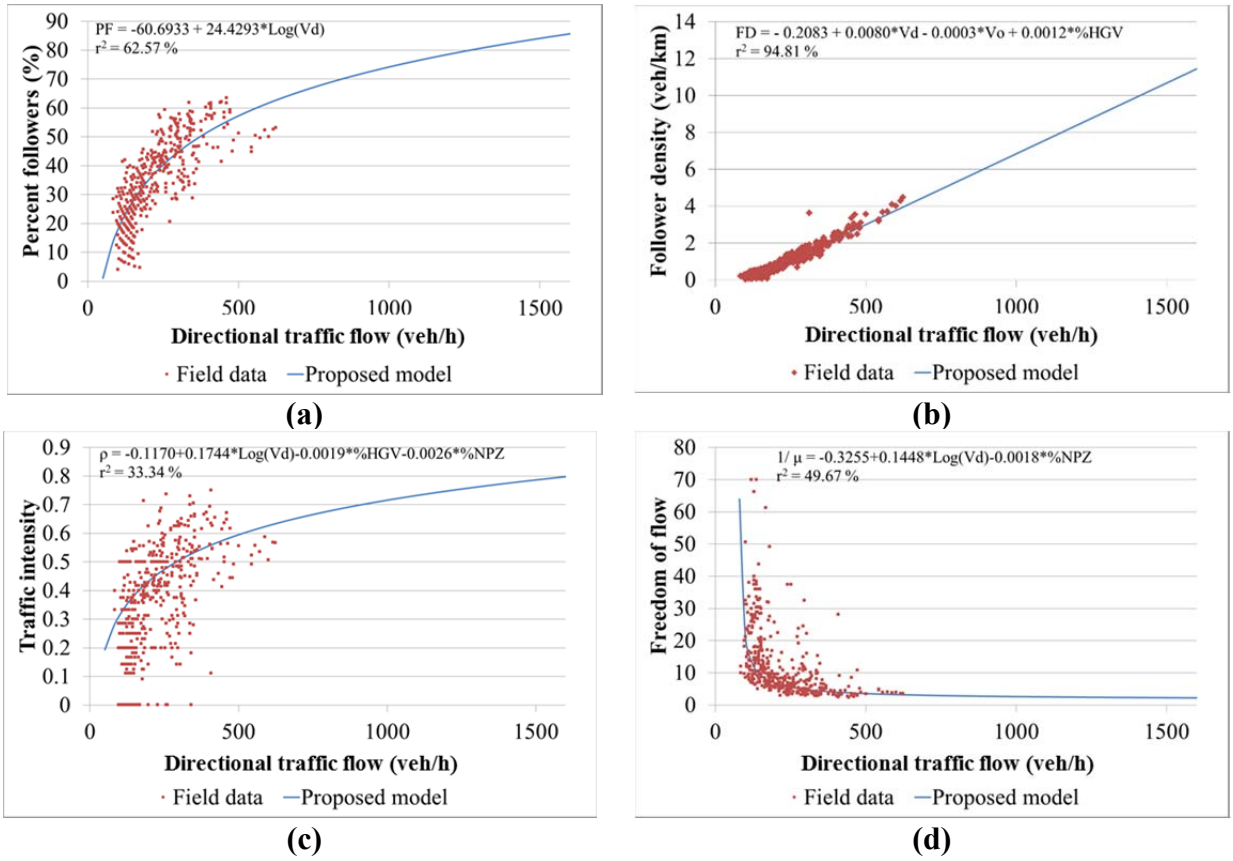

FIGURE 1 Platooning performance measures models adjustment to field data: (*a*) FD; (*b*) PF; (*c*) traffic intensity; and (*d*) freedom of flow.

The deviation of ATS was uniform, which is in accordance with the low PFs at very low traffic volume. The PI was supposed to improve the correlation to traffic but it failed to provide better results than the PFs. This measure assumes that the slow-moving vehicles are platoon leaders, but the platoon may be headed by a fast vehicle followed by another fast vehicle traveling close to its desired speed. Similarly, fast vehicles are characterized as vehicles outside platoons, and one truck traveling alone can be identified as a fast vehicle even though its speed can be very low. These two hypotheses may influence the accuracy of the results, as desired speeds may be lowered and slow-moving average speed may be overestimated. The probability of being impeded varied between 33.5% and 83.5%, with an average value of 67%.

The third group was composed of Polus and Cohen's measures (R^2 between 34% and 50%). This may be caused because the variables were defined based on theoretical models and the assumptions were not met in field. For example, 22% of passes were multiple and the models assumed that all vehicles in the queue would be willing to pass. Besides, 7.5% of the sample was removed to calculate the traffic intensity and the freedom of flow because they had a division by zero. After removing those periods from the sample, the freedom of flow presented lower dispersion than the average platoon length and traffic intensity. The freedom of flow decreased as the traffic flow increased, which meant that the system was busier. The traffic intensity shows similar conclusions.

The models with lowest coefficient of determination corresponded with the speed-related measures, with R^2 between 8% and 16%. The results were better for the highways with speed limit of 100 km/h, mainly because only two sites with speed limit of 80 km/h were observed and the traffic volume range was narrower. Generally, only passenger cars slightly improved the correlation.

Two-Way Analysis

The two-way analysis considers as independent variables the two-way traffic flow, traffic proportion, percentage of trucks, and percentage of no-passing zones. The multiple regression models were fitted using forward stepwise selection, as the directional analysis. Table 4 shows the equations obtained from the multiple regression analyses. The results were similar to the directional analysis, in fact, the coefficient of determination were within 1% lower than the directional analysis. Moreover, the opposing traffic flow was not statistically significant in many of the models which will suggest that the directional analysis may not be that relevant.

DISCUSSION

The 10 performance measures models obtained from the statistical analysis were compared to the HCM 2010 estimates and to previous field studies. The field data were used as input data of the models, and directional or two-way models were selected according to the analysis considered on the previous studies. The 15-min period results from the models were converted to equivalent hourly data. Adequate adjustments for heavy vehicles and grade were used to convert the observed flow rates to the equivalent base conditions of the HCM 2010. Then, the HCM estimation procedure was applied to each period considering the percent of no-passing zones. On the other hand, a comparison between the directional and the two-way analysis was carried out.

TABLE 4 Two-Way Analysis Multiple Regression Models

Variable	Equation	R^2 (%)	R^2_{adj} (%)
ATS_{100}	$ATS_{100} = 139.394 - 5.745 \cdot \ln(Vt) - 0.146 \cdot P - 0.308 \cdot \%HGV$	16.68	16.08
ATS_{80}	$ATS_{80} = 95.160 - 3.696 \cdot \ln(Vt)$	10.95	9.27
$ATSpc_{100}$	$ATSpc_{100} = 154.295 - 8.185 \cdot \ln(Vt) - 0.200 \cdot P - 0.279 \cdot \%HGV$	16.61	16.00
PFFS	$PFFS = 1.328 - 0.055 \cdot \ln(Vt) - 0.001 \cdot P - 0.002 \cdot \%HGV$	18.61	18.09
PFFSpc	$PFFSpc = 1.164 - 0.028 \cdot \ln(Vt) - 0.001 \cdot P - 0.001 \cdot \%HGV$	34.33	33.91
FV	$FV = \exp(-6.066 + 1.581 \cdot \ln(Vt) + 0.032 \cdot P)$	95.81	95.50
PF	$PF = -102.564 + 24.313 \cdot \ln(Vt) + 0.504 \cdot P$	62.71	62.55
Log(FD)	$\ln(FD) = -12.922 + 1.989 \cdot \ln(VT) + 0.037 \cdot P + 0.006 \cdot \%HGV$	85.90	85.81
PI	$PI = -55.572 + 15.616 \cdot \ln(Vt) + 0.352 \cdot P - 0.112 \cdot \%HGV - 0.167 \cdot \%NPZ$	58.99	58.65
1/APL	$\frac{1}{APL} = 0.807 - 0.096 \cdot \ln(Vt) + 0.001 \cdot P - 0.004 \cdot \%NPZ$	36.33	35.92
ρ	$\rho = -0.756 + 0.252 \cdot \ln(Vt) + 0.003 \cdot \%HGV - 0.003 \cdot \%NPZ$	34.83	34.42
1/μ	$\frac{1}{\mu} = -0.607 + 0.151 \cdot \ln(Vt) + 0.003 \cdot P - 0.002 \cdot \%NPZ$	51.38	51.07

NOTE: Where *Vt* = two-way traffic volume (veh/15 min); *P* = traffic proportion on the direction of analysis (%). The other variables have been previously defined.

Speed-Related Performance Measures

The ATS was compared to the HCM 2010 (*1*) estimate, as the previous field studies failed to provide a statistically significant model for the same speed limit highways (Figure 2). The ATS obtained on field was similar to the HCM estimate in highways with 100 km/h speed limit but the estimates were 9 km/h lower than the field data for 80 km/h highways. The larger differences may suggest that the adjustments for no-passing zones for ATS of 55 mph may not be as accurate as the adjustments for no-passing zones for ATS equal to 65 mph. It can also be observed that the average travel speed was hardly sensitive to traffic flow, as the reductions on the model were lower than 5 km/h, and that the deviation of ATS was almost uniform regardless the traffic flow.

The ATS_{PC} was compared to Luttinen's models (*13*) developed for 100 and 80 km/h speed limit Finnish two-lane highways. The Finnish models depended on the directional traffic flow and the opposing traffic flow, and they presented higher ATS_{PC} than our field data in highways with 80-km/h speed limit. The values were lower at highways with 100 km/h. Their model was less sensitive to traffic flow than the current study, which may be caused by a lower interaction of platooned vehicles.

On the other hand, the PFFS was compared to the HCM 2010 estimates, and they were higher than the HCM 2010 estimates. This performance measure was slightly more sensitive to traffic flow than ATS. However, the follower criterion was different and the observed highways were classified as Class II highways, where the PFFS is not considered as performance measure.

Platooning-Related Performance Measures

As the PF is the surrogate measure for PTSF, both HCM 2010 PTSF estimates and PF were compared. As observed in Figure 3, the estimated PTSF was similar to the PF obtained in the field data and the PF model developed in the current research. The average difference between the model prediction and the HCM 2010 estimation was 6%; while the extreme differences were –3.8% and 28%, respectively. The larger differences were produced mainly in the CV-405, where the posted speed limit was 80 km/h, which may suggest that the adjustments for no-

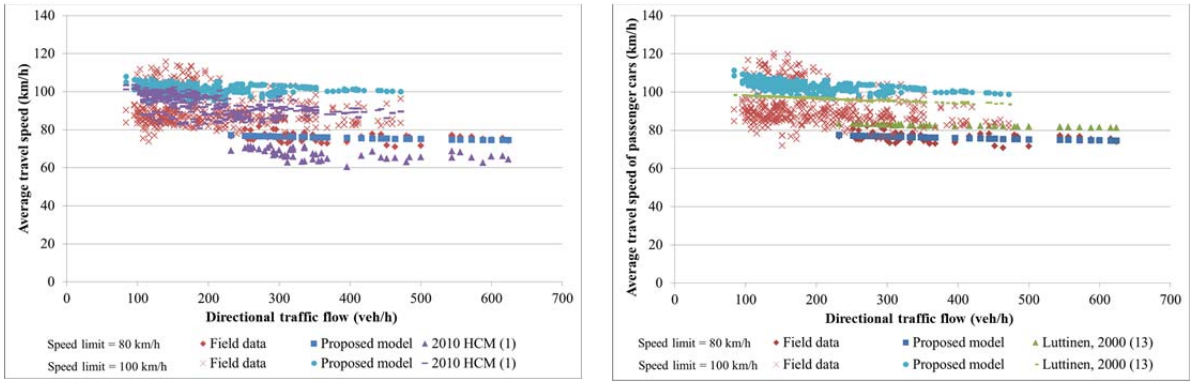

(a) **(b)**

FIGURE 2 Speed-related measures comparison: (*a*) ATS and (*b*) ATS_{PC}.

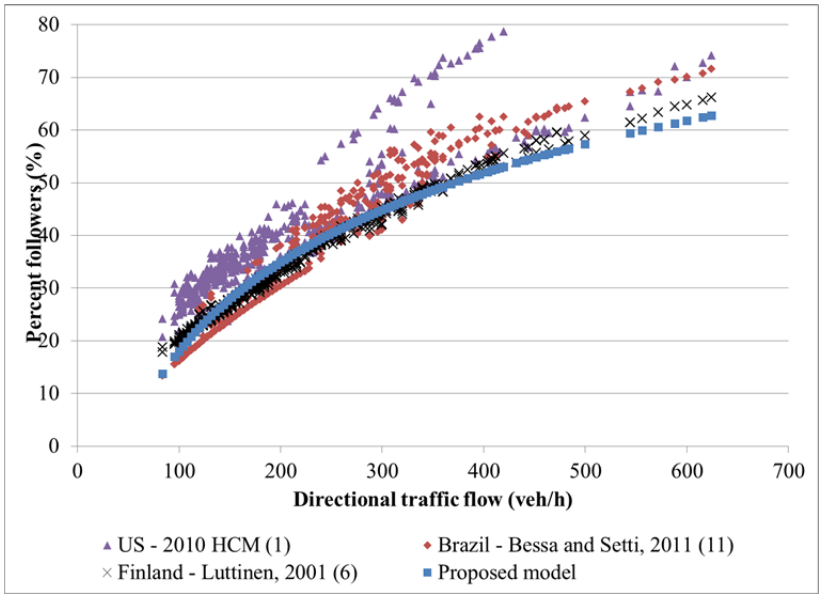

(a)

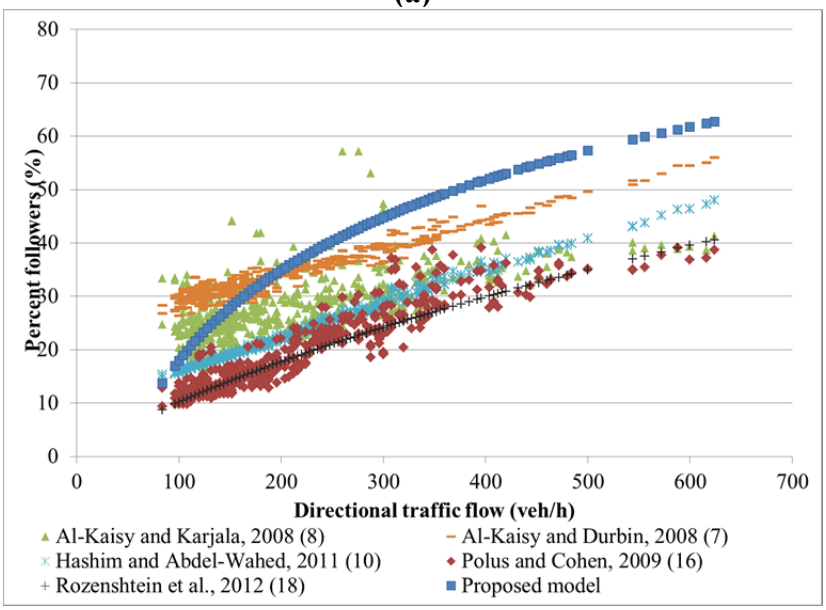

(b)

FIGURE 3 *PF* comparison: (*a*) guidelines and (*b*) field studies.

passing zones for FFS of 55 mph may not be as accurate as the adjustments for no-passing zones for FFS equal to 65 mph, as for ATS. Besides, more differences were observed at traffic flows lower than 250 vehicles per hour (vph), which would indicate that the extrapolation of their medium-high traffic volume field data was not too accurate for our observed low traffic flows.

As observed, the PF estimation of the current study was practically equal to the Finnish guidelines (*6*) even though their model depended on both direct and opposing traffic flow, the percentage of no passing zones and the percentage of heavy vehicles. Some minor differences could be observed for directional traffic flows higher than 500 vph, however they observed a maximum one-way traffic volume of 1,600 vph (*13*). The second closest guideline was the

Brazilian (*11*), followed by the HCM 2010 (*1*). The Brazilian model underestimated the PF at traffic flows lower than 200 vph and overestimated the value for higher traffic flows. Even though the correlation of their model was high, many of the scenarios were generated using traffic simulation and no characteristics of the observed data were given (*11)*.

The current model and previous field studies that considered the PF using the 3-s headway criterion were also compared. The studies in Montana (*7*, *8*) estimated similar PF to the current study only at their observed traffic flows (between 100 and 200 vph). The better adjustment of their second model (*8*) is caused by the presence of the standard deviation of the free-flow speed of the period on the model, which was obtained from our field data and could be slightly different than theirs. On the other hand, the models from Israel (*16*, *18*) and Egypt (*10*) estimated much lower PF than our model, which indicates a lower impact of platooning. This could be caused by a more aggressive behavior of the Israeli and Egyptian drivers or different road characteristics, such as the low percent of heavy vehicles and speed limit of 60 km/h in Egypt. On the other hand, the PF was calculated using the theoretical model and one of the hypotheses was that all vehicles that were at a platoon were willing to pass and they would perform a passing maneuver, which would lead to lower PF.

The follower density was compared to previous field studies in Montana, Oregon, and Egypt, as other studies did not provide the model equation (Figure 4). The prediction of the Oregon model (*9*) was similar to our model, especially for high traffic flows, while for low traffic flows it provided consistently higher FD than our observed field data. Reversely, Al-Kaisy and Karjala's model (*8*) presented good fit at their observed low traffic flow and their estimate for higher traffic flows was much higher than our observations. The results confirm that the Spanish driver platooning behavior was similar to the observed in U.S. drivers. Similarly to the PF, the study from Egypt (*10*) estimated the lowest FD and their prediction was negative for one-way traffic flows lower than 200 vph, which is a common traffic flow for two-lane rural highways in Spain.

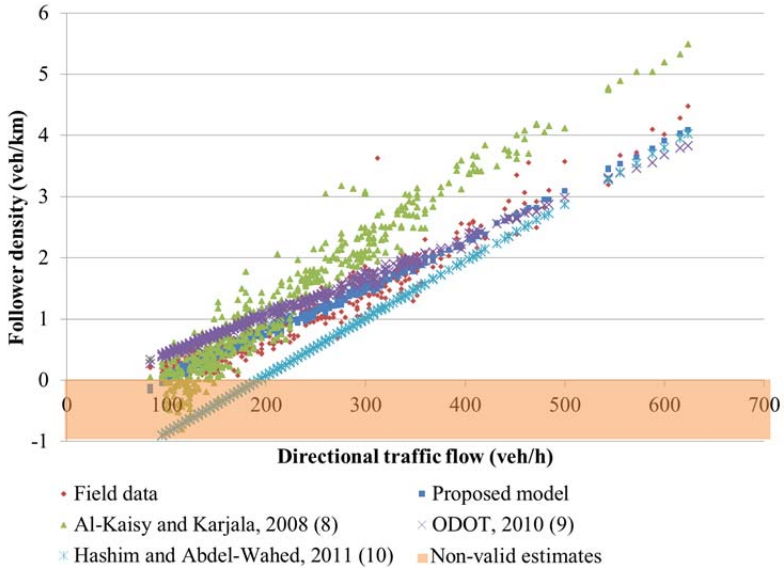

FIGURE 4 FD comparison.

The PI was compared to previous models and the results were very different. Firstly, the Egyptian model (*10*) estimates were lower than the other models and our field data, which can be explained because of the different driver behavior. On the other hand, the differences between the Al-Kaisy and Durbin's model (*7*) could be caused by an incorrect report of the model equation due to the high variability of the results, considering that their observations had a coefficient of determination of 98% and the same data set was used to calculate the PF, which was more similar to our field data.

The last comparisons were on the performance measures proposed by Polus and Cohen (*16*). The average platoon length from the current study was very similar to the Polus and Cohen's model, but the variable presented a high dispersion in the present study. Our freedom of flow was lower than their predictions (*16*) and our traffic intensity was higher (*16*, *18*), which supports the hypothesis that Spanish drivers were more affected by platooning than Israeli drivers.

Directional Versus Two-Way Analysis

All the 10 performance measures were calculated using the directional models and the two-way models and then the results were compared.

The directional distribution produced similar coefficients of determination as the two-way analysis, mainly because the observed balanced flows: directional splits higher than 40/60 were observed in a 15% of the sample and higher than 30/70, in 1.7%. The estimates from both analyses were very similar and the opposing traffic flow was only statistically significant on the follower density. For higher traffic flows, the predictions of the two-way analysis were higher than the field data and the directional analysis. The results partially support Luttinen's hypothesis that the directional analysis include the possible dependence of the performance measures on the opposing traffic flow (*13*).

CONCLUSIONS

Several authors have pointed out the shortcomings of the HCM 2010 procedure to characterize traffic performance on two-lane rural highways, and they have defined alternative performance measures that are easier to measure in field, such as the FD or the traffic intensity. This study calibrates 10 performance measures identified in the literature for the same data set. The recording time was 55 h, with more than 10,000 vehicles identified.

The studied performance measures included: ATS, ATS_{PC}, PFFS, $PFFS_{PC}$, PF, FD, PI, APL, traffic intensity, and freedom of flow. Both directional and two-way analyses were considered and the differences between them were very low, especially at the platooning variables.

The results of the analysis indicated that the FD had the strongest correlation with traffic variables, with a coefficient of correlation of 94%. The best-fitted model depended on the directional traffic flow, the opposing traffic flow, and the percent of heavy vehicles. The estimations from the present model were compared with the estimations of previous models and they were similar within their observation range, which can verify that Spanish drivers' behavior is comparable with U.S. drivers' behavior.

The next performance measures were the PF and the PI, with coefficients of correlation of 62% and 58%, respectively. The PF observed in this field study were very similar to Lutinnen's model (*6*) and slightly lower than the HCM 2010 estimates. Some differences with the HCM 2010 were produced at the highway with posted speed limit of 80 km/h, which may suggest that the adjustments for no-passing zones may not be as accurate as for the 100-km/h speed limit highways. However, the larger differences were detected for directional traffic flows lower than 250 vph. This could indicate that the extrapolation of the HCM 2010 for low traffic flows is not too accurate and provides higher PF than observed in the field. Reversely, previous U.S. linear models had similar results at low traffic flows, where their data was observed. This could indicate that the driver behavior in Spain was similar to the United States and supports the HCM 2010 overestimation of PF for low traffic flows.

The platooning-related performance measures defined by Polus and Cohen (*16*) presented higher dispersion and correlations with traffic variables between 33% and 49%, which could indicate that the observed driver behavior was more disperse and may have more influence on the results than their theoretical model expected. Moreover, they predicted less platooning for all their variables than observed in field, which could be caused by the incompliance of assumptions in their theoretical model (all drivers will perform a passing maneuver when possible) or by a more aggressive behavior in Israel. Finally, the speed-related measures presented the weakest correlation with traffic variables, and in some cases they were hardly sensitive to traffic flow, which agrees with previous field studies.

The conclusions of this study support the follower density selection as major performance measure, as it presents the strongest correlation to the traffic variables for the observed conditions and it is easy to measure and estimate. This performance measure combines the percent of followers, the average travel speed and the traffic flow. Even though the favorable results may be caused by the dependence of the follower density on the traffic flow, the measure can better represent the overall traffic performance than the PTSF or its surrogate, the PF. The conclusions may be limited to the observed conditions and two-way traffic flows higher than 1,000 vph. Directional traffic flows higher than 600 vph could provide different results, as well as skew directional distributions or two-way highways with speed limits different than 80 or 100 km/h; however, they could be used to develop two-lane highway simulation models and analytical methodologies to establish levels of service based on the follower density or better adjustments to the HCM 2010 procedure.

ACKNOWLEDGMENTS

This report has been partially developed as a result of a mobility stay at the University of British Columbia (UBC) funded by the Erasmus Mundus Programme of the European Commission under the Transatlantic Partnership for Excellence in Engineering–TEE Project.

The authors thank the Spanish Ministry of Science and Innovation that subsidizes the research project with reference code TRA2010-21736, and the Spanish General Directorate of Traffic and Spanish Ministry of Public Works, for their collaboration during the field study.

REFERENCES

1. *Highway Capacity Manual 2010*. Transportation Research Board of the National Academies, Washington, D.C., 2010.
2. Romana, M. Country Report, Spain. Presented at 6th International Symposium on Highway Capacity and Quality of Service, Stockholm, 2011.
3. Washburn, S. S., D. S. McLeod, and K. G. Courage. Adaptation of "Highway Capacity Manual 2000" for Planning-Level Analysis of Two-Lane and Multilane Highways in Florida. In *Transportation Research Record: Journal of the Transportation Research Board*, *No. 1802*, Transportation Research Board of the National Academies, Washington, D.C., 2002, pp. 62–68.
4. Romana, M. G., and I. Perez. Measures of Effectiveness for Level-of-Service Assessment of Two-Lane Roads: An Alternative Proposal Using a Threshold Speed. In *Transportation Research Record: Journal of the Transportation Research Board*, *No. 1988*, Transportation Research Board of the National Academies, Washington, D.C., 2006, pp. 56–62.
5. Luttinen, T., M. Dixon, and S. Washburn. Two-Lane Highway Analysis in HCM 2000. Draft White Paper, 2003. Available at https://people.sunyit.edu/~lhmi/ahb40/meetings/2005-07/White.pdf. Accessed May 5, 2013.
6. Luttinen, R. T. Percent Time-Spent-Following as Performance Measure for Two-Lane Highways. In *Transportation Research Record: Journal of the Transportation Research Board*, *No. 1776*, TRB, National Research Council, Washington, D.C., 2001, pp. 52–59.
7. Al-Kaisy, A., and C. Durbin. Evaluating New Methodologies for Estimating Performance on Two-Lane Highways. *Canadian Journal of Civil Engineering,* Vol. 35, 2008, pp.777–785.
8. Al-Kaisy, A., and S. Karjala. Indicators of Performance on Two-Lane Rural Highways: Empirical Investigation. In *Transportation Research Record: Journal of the Transportation Research Board*, *No. 2071*, Transportation Research Board of the National Academies, Washington, D.C., 2008, pp. 87–97.
9. Oregon Department of Transportation. Modeling Performance Indicators on Two-Lane Rural Highways: The Oregon Experience, 2010. Available at http://www.oregon.gov/ODOT/TD/TP/docs/reports/modelingperf.pdf. Accessed May 5, 2013.
10. Hashim, I., and T. A. Abdel-Wahed. Evaluation of Performance Measures for Rural Two-Lane Roads in Egypt. *Alexandria Engineering Journal,* No. 50, 2011, pp. 245–255.
11. Bessa, J. E., and J. R. Setti. Deviation of ATS and PTSF Functions for Two-Lane, Rural Highways in Brazil. Presented at the 6th International Symposium on Highway Capacity and Quality of Service, Stockholm, 2011.
12. Brilon, W., and F. Weiser. Two-Lane Rural Highways: The German Experience. In *Transportation Research Record: Journal of the Transportation Research Board*, *No. 1988*, Transportation Research Board of the National Academies, Washington, D.C., 2006, pp. 38–47.
13. Luttinen, R. T. Level of Service on Finnish Two-Lane Highways. In *Transportation Research Circular E-C018: Fourth International Symposium on Highway Capacity*, TRB, National Research Council, Washington, D.C., 2000, pp. 175–187.
14. Van As, S. C., and A. Niekerk. The Operational Analysis of Two-Lane Rural Highways. Presented at 23rd Southern African Transport Conference, 2003.
15. Catbagan, J. L., and H. Nakamura. Evaluation of Performance Measures for Two-Lane Expressways in Japan. In *Transportation Research Record: Journal of the Transportation Research Board*, *No. 1988*, 2006, Transportation Research Board of the National Academies, Washington, D.C., pp. 111–118.
16. Polus, A., and M. Cohen. Theoretical and Empirical Relationships for the Quality of Flow and for a New Level of Service on Two-Lane Highways. *Journal of Transportation Engineering*, Vol. 135, No. 6, 2009, pp. 380–385.
17. Cohen, M., and A. Polus. Estimating Percent-Time-Spent-Following on Two-Lane Rural Highways. *Transportation Research Part C,* No. 19, 2011, pp. 1319–1325.

18. Rozenhstein, S., A. Polus, and M. Cohen. Models for Estimating Drivers Following on Two-Lane Rural Highways. In *Transportation Research Record: Journal of the Transportation Research Board*, *No. 2286*, Transportation Research Board of the National Academies, Washington, D.C., 2012, pp. 68–75.
19. Kaub, A. R. Passing Operations on a Recreational Two-Lane, Two-Way Highway. In *Transportation Research Record 1280*, TRB, National Research Council, Washington, D.C., 1990, pp. 156–162.
20. Romana, M. G. Passing Activity on Two-Lane Highways in Spain. In *Transportation Research Record 1678*, TRB, National Research Council, Washington, D.C., 1999, pp. 90–95.
21. Llorca, C., and A. García. Evaluation of Passing Process on Two-lane Rural Highways in Spain with New Methodology Based on Video Data. In *Transportation Research Record: Journal of the Transportation Research Board*, *No. 2262*, Transportation Research Board of the National Academies, Washington, D.C., 2011, pp. 42–51.
22. Carlson, P. J., J. D. Miles, and P. K Johnson. Daytime High Speed Passing Maneuvers Observed on Rural Two-Lane, Two-Way Highway: Findings and Implications. In *Transportation Research Record: Journal of Transportation Research Board*, *No. 1961*, Transportation Research Board of the National Academies, Washington, D.C., 2006, pp. 9–15.
23. Moreno, A. T., C. Llorca, A. García, and A.-M. Pérez-Zuriaga. Operational Effectiveness of Passing Zones Depending on Length and Traffic Volume. In *Transportation Research Record: Journal of the Transportation Research Board, No. 2395*, Transportation Research Board of the National Academies, Washington, D.C., 2013, pp. 57–65.
24. Morrall, J. F., and A. Werner. Measuring Level of Service of Two-Lane Highways by Overtakings. In *Transportation Research Record 1287*, TRB, National Research Council, Washington, D.C., 1990, pp. 62–69.
25. Harwood, D., A. May, I. Anderson, L. Leiman, and R. Archilla. Capacity and Quality of Service of Two-Lane Highways, 1999.
26. Llorca, C., A. T. Moreno, A. Garcia, and A. M. Perez-Zuriaga. Daytime and Nighttime Passing Maneuvers on Two-Lane Rural Road in Spain. In *Transportation Research Record: Journal of the Transportation Research Board, No. 2358*, Transportation Research Board of the National Academies, Washington, D.C., 2013, pp. 3–11.
27. Luttinen, T. Uncertainty in the Operational Analysis of Two-Lane Highways. TL Consulting Engineers, 2001.
28. Osborne, J., and E. Waters. Four Assumptions of Multiple Regression That Researchers Should Always Test. *Practical Assessment, Research & Evaluation*, Vol. 8 No. 2, 2002.

Highway Capacity Planning Application and Development of Default Values in North Carolina

DANIEL J. FINDLEY
JEFFREY C. CHANG
CHRISTOPHER L. VAUGHAN
BASTIAN J. SCHROEDER
ROBERT S. FOYLE
North Carolina State University

DAVID M. ALFORD
North Carolina Department of Transportation

The North Carolina level of service (NCLOS) methodology provides a planning-level assessment of transportation facilities through a generally faithful implementation of the *Highway Capacity Manual 2010* (HCM 2010) to derive service volume estimates and performance expectations, with a few minor deviations from the HCM 2010. Implemented in the NCLOS software tool, the method gives a visual representation of traffic volume plotted against the various measures of effectiveness for each facility type. The graphical output shows the feasible performance range from the best to the worst case scenarios for each facility type in North Carolina based on different default values, as well as an average default scenario. The user-defined subject facility is evaluated within that range of values to give the user a direct assessment of the performance. The user can conduct a sensitivity analysis of various scenarios by altering the input values to represent possible design considerations for a particular highway. The tool also enables the user to produce a numerical report detailing the results of the analysis, as well as the ability to export the calculated capacity to transportation planning software and travel demand models. The main contributions of this paper are the NCLOS methodology itself, as well as extensive work on default value development. The paper further provides an example application to an urban street segment case and a two-lane highway facility, with the latter offering interesting insights in the behavior of the three different performance measures in that method. Overall, NCLOS is a powerful tool to allow quick planning-level assessment of the capacities of various road segments.

The Transportation Planning Branch of the North Carolina Department of Transportation (DOT) is responsible for working with outside planning agencies in providing engineering and planning assistance for the current, proposed, and potential highway network in North Carolina. This branch is charged with identifying future highway needs through the transportation planning process. This process requires the use of modeling and forecasting techniques to determine potential needs and improvements in the transportation system. Accurate travel demand modeling requires appropriate values for roadway capacities and service volumes at various levels of service (LOS). Tools such as the *Highway Capacity Manual* (HCM) are valuable for performing detailed analyses of facilities and corridors given a series of input data. However, the scarcity of information typically available at the planning stages, coupled with the relative complexity of the HCM product, make direct use of the HCM impractical or inefficient

for forecasting applications. The HCM is primarily designed for operational analyses; traditionally, it is not particularly well suited to the reverse process of determining acceptable roadway demands for various maximum service volumes or capacities at LOS thresholds. In early 2011, the *Highway Capacity Manual 2010* (HCM 2010) was available for transportation facility analyses (*1*). There are significant and important improvements for many of the methodologies in the HCM 2010 based on the most recent national research, including the presentation of planning-level service volume tables. As with previous editions of the manual, HCM 2010 is the standard for determining the capacity of most highway facilities in the United States.

The North Carolina DOT commissioned the development of the North Carolina Level of Service (NCLOS) software, a transportation planning application, based off the HCM in 2006 (*2*). It used the HCM 2000 edition's operational analysis methodologies and service volume calculations to determine capacities for each LOS—A through E—for freeways, multilane highways, two-lane highways, and arterial streets. When HCM 2010 was officially released in spring 2011, there were adjustments to the highway facilities methodologies and revisions in analysis; this also included several new facility types, enhanced capabilities, and additional quantitative service measures. As a result, the NCLOS software required updates to programming the HCM methodology, input definitions, and default values. The concepts and considerations taken into account may have use beyond North Carolina DOT's software and could help other practitioners apply the HCM operational analytics for planning applications.

BACKGROUND

NCLOS is used extensively in planning applications within North Carolina DOT and is delivered through a web-based service to business units at North Carolina DOT. Output capacities are used in travel demand forecasting models and in developing comprehensive transportation plans. Output values can also be used in the statewide travel demand model now under development by North Carolina DOT. Currently, the tool is also used to provide data for the performance metrics dashboard and as a scoring component in the strategic prioritization process and urban loop prioritization process. Practitioners from the North Carolina DOT prioritization office implement the tool for analysis required for statewide planning, in addition to engineers and planners inside and outside the agency who desire an automated tool for highway capacity planning. This tool is used primarily as a high-level analysis for making comparison across the state or amongst projects. Detailed operational analysis using the HCM 2010 would supersede the planning level results delivered by NCLOS, particularly as more data becomes available that would supplant default values.

The application is unique in that it provides a graphical display of qualitative LOS measures, based from quantitative service measures, plotted against the capacity, or annual average daily traffic (AADT), for a given highway facility under specified conditions. The program uses traffic and roadway parameters, or input values, to produce a capacity table for various conditions. The software has sets of input values for best case, worst case, and default conditions for each highway facility. These capacities are plotted automatically. NCLOS also allows users to define input values and plot a curve with the three aforementioned conditions. The user-defined curve shifts relative to the default case depending on the variations of input

values, and generally remains between the best-case and worst-case curves, unless the user has valid reasons to deviate beyond these boundary conditions.

The input fields and calculations are derived from the HCM 2010 methodologies. NCLOS is applicable for freeway, multilane highway, two-lane highway, and arterial facilities, thus corresponds with Chapter 11: Basic Freeway Segments; Chapter 14: Multilane Highways; Chapter 15: Two-Lane Highways; and Chapter 17: Urban Street Segments, respectively. Significant changes between the HCM 2000 and HCM 2010 methodologies are outlined.

Basic Freeway Segments

- Changes to speed–flow curves and the free-flow speed (FFS) equation that affect the analysis of the operational methodology (*3–7*):
  - The procedure recommends using the nearest 5-mph FFS increment for quantitative analysis, thus eliminating the need for interpolating between any of the pre-defined 5-mph curves.

Multilane Highways

- Changes to speed–flow curves:
  - The procedure recommends using the nearest 5-mph FFS increment for quantitative analysis, thus eliminating the need for interpolating between any of the pre-defined 5-mph curves.

Two-Lane Highways

- Elimination of the bidirectional analysis procedure:
  - HCM 2000 provided procedures for one-way analysis for climbing and passing lanes and bidirectional analysis for all other segments; one-way analysis used for mountainous terrain and the latter for level and rolling terrain. The inconsistencies between the two procedures led to the elimination of bidirectional analysis in HCM 2010. The one-way capacity of a two-lane highway remains at 1,700 passenger cars per hour (pcph) consistent with HCM 2000, while the two-way capacity is limited at a flow of 3,200 pcph;
- Revisions to basic characteristic curves and tables; and
- Introduction of Class III Two-Lane Highway type based on a Florida DOT analysis procedure (*3*, *8*, *9*).

Urban Street Segments

- Elimination of the four classes of arterials (I, II, III, and IV);
- Individual urban street segments can have a signalized, roundabout, or all-way stop-controlled (AWSC) intersection at a segment begin–end point (*5*, *10*, *11*):
  - Lengthier segments can be divided into unsignalized sections and
  - The basic signals can be actuate to vary effective green times per cycle unless all cycles are operating at capacity.

METHODOLOGY

NCLOS needed to be updated to incorporate the new methodologies in HCM 2010 and other enhancements to remain current with the state of practice (*12*). The most critical steps in the methodology implemented in NCLOS was the development of default values, the actual coding and implementation of the HCM 2010 methodologies, and the generation of the graphical user output. The development of default values is discussed in this section, while the programming of methodologies and plotting of LOS and AADT is discussed in the Implementation section.

Default Values

The data used for default value development were based on North Carolina traffic volume data, recommendations from NCHRP Report 599 (*3*), the HCM 2010, and professional judgment, which is briefly discussed in the Results section of this paper. This planning level method required the development of many defaults, ranging from hourly, directional, and peak-hour factors, to FFS defaults, to more complicated defaults for signal timing and platooned arrivals at intersections. Consequently, a significant effort was required to analyze the North Carolina traffic data.

Data were collected by North Carolina DOT beginning in 1988 and included information up until 2011. Data analysis showed no significant differences between earlier and later data, so all data were included in the full analysis. Detailed data from automated traffic recorder (ATR) stations were obtained from the North Carolina DOT Traffic Surveys Group in the form of a database. The first step of the process was to geocode 7,863 traffic volume data points, a step necessary to match volume information with a geographic information system inventory of roadway facilities and facility types for the state. Of the 7,863 points, 867 were automatically geocoded and 6,996 required manual geocoding. Another effort required the classification of roadways in terms of their functional classification and area type (urban, suburban, or rural). Table 1 details the selection process used to categorize each of the roadway types. At the conclusion of the geocoding, the data points were then classified based on the functional classification shown below using geospatial referencing. Once this was completed, default values specific to North Carolina for each classification were established. This extensive effort ensured that the default values produced in the NCLOS program were accurate based on typical North Carolina traffic volume data.

RESULTS

Following the geocoding and categorization process, the available traffic characteristics of the peak hour factor, hourly *K*-factor, and directional *D*-factor were graphed and analyzed. The peak-hour factor (PHF) describes the amount of peaking within the peak hour, the *K*-factor represents the proportion of the total daily traffic that travels during the peak hour, and the *D*-factor characterizes the directional split of traffic. The figures show a frequency distribution of all data points for a given factor, separated by roadway type, and separated by area type using the definitions for urban, rural, and suburban in Table 1. The corresponding tables in each figure tabulate statistical values of sample size (*N*), mean, median, and mode for each roadway type. *N* represents the number of traffic volume data points available for each roadway classification. The data represent the most current count data available at locations across North Carolina,

TABLE 1 North Carolina Roadway Classification Definitions

Roadway Type	General Classification	Setting	Selection Criteria
Arterials	Selection by facility type and speed limit Facility is within an MPO or smoothed urbanized area boundary	Urban	Roadway has speed limit of 35 mph or less
		Suburban	Roadway has speed limit of 36 mph or greater
		Rural	No roadways exist in this category
Two-lane highways	Selection by number of lanes Facility is outside an MPO or smoothed urbanized area boundary	Urban	No roadways exist in this category (roadway classified as arterial)
		Suburban	No roadways exist in this category (roadway classified as arterial)
		Rural	Class I = primary routes Class II = secondary routes Class III = no roadways exist in this category (roadway classified as arterial)
Multilane highways	Selection by facility type and area type	Urban	Roadway is within a MPO and a smoothed urbanized area boundary
		Suburban	Roadway is within a MPO, but outside smoothed urbanized area boundary or vice versa
		Rural	Roadway is outside any MPO and outside any smoothed urbanized area boundary
Freeways	Selection by facility type and area type	Urban	Roadway is within a MPO and a smoothed urbanized area boundary
		Suburban	Roadway is within a MPO, but outside smoothed urbanized area boundary or vice versa
		Rural	Roadway is outside any MPO and outside any smoothed urbanized area boundary

NOTE: MPO = metropolitan planning organization.

which includes 23 years of observations from sensor stations across the state. Mean is the statistical average, median is the numerical value separating the higher and lower halves of the data, and mode is the value occurring most often. The median values were selected as the default value for each parameter and rounded appropriately, along with national data suggested by the HCM 2010 and NCHRP Report 599.

Overall, the values show little variability among the roadway type dimensions considered in this evaluation. The majority of data on PHF presented in Figure 1 are within a range from 0.8 to 1.0, with an overall mean and median of 0.87 and 0.88, respectively. The distinction between urban, suburban, and rural facilities generally shows little difference in the distributions. Comparing PHF across facility types, both rural freeways and two-lane highways suggest a more dispersed distribution than arterials and freeways, with a greater frequency of low PHFs (traffic more focused within a 15-min period).

The distribution of the hourly *K*-factor in Figure 2 shows most of the data were contained in a range of 0.07 to 0.13, with an overall mean and median of 0.095 and 0.091, respectively.

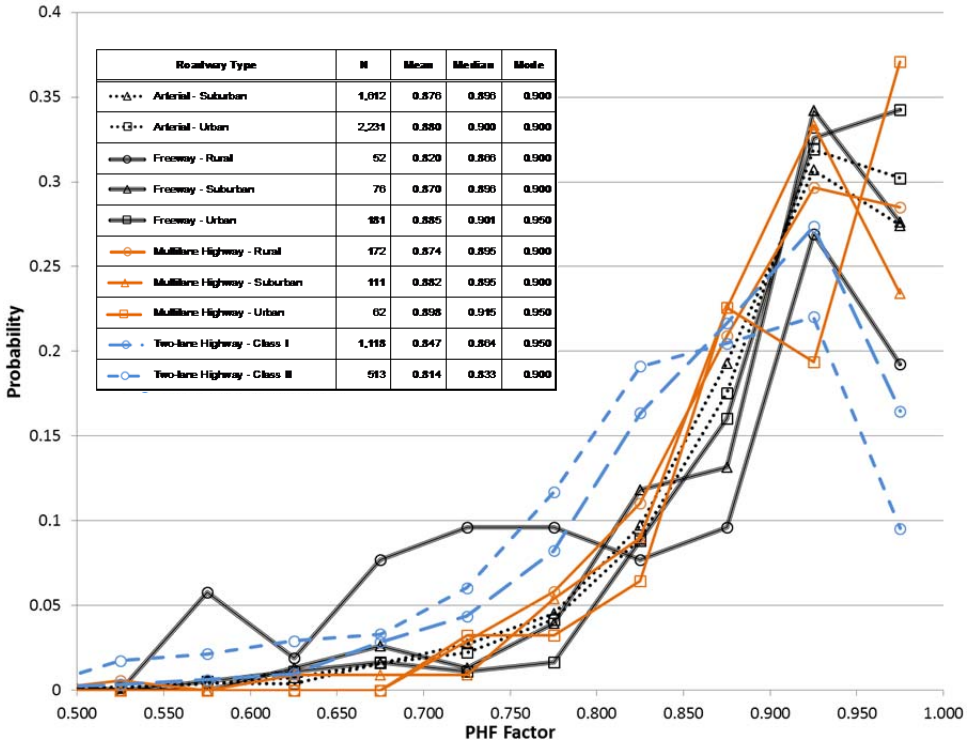

FIGURE 1 PHF factor data.

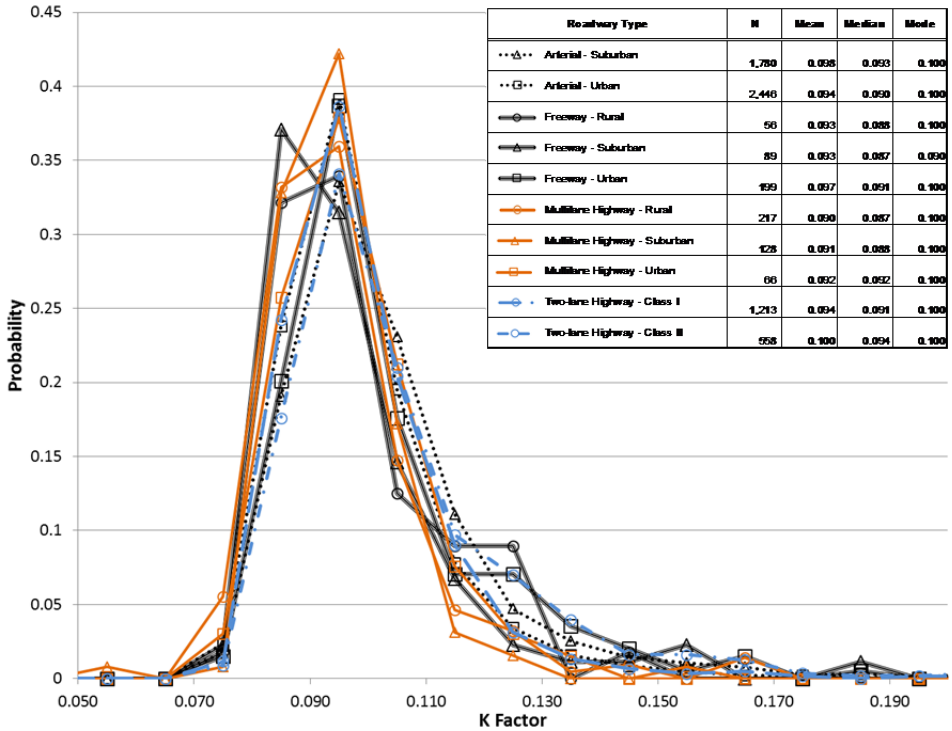

FIGURE 2 *K*-factor data.

Again, the collected data show little difference between facility types and between different area types. Finally, the directional *D*-factor shows the greatest degree of dispersion with a range of frequently observed values from 0.5 to 0.75. The overall mean was 0.61 and the overall median was 0.58, as seen in Figure 3. Similar to the other measures, the distributions across facility types and area types were surprisingly similar.

As a result of these analyses, the team proposed the use of a common *K*-factor for all area and facility types as shown in Table 2, even though national defaults from NCHRP Report 599 suggested greater variability. For PHF, the recommendation was a common default of 0.90, except for slightly lower values for rural freeways and two-lane highways. For the *D*-factor, a common default of 0.60 was proposed, except for a lower value for suburban multilane highways, and a higher value for rural freeways.

In addition to these default values that were supported by field data, various additional defaults had to be developed. In the absence of North Carolina specific data, many of these were based on discussion with North Carolina DOT and traffic engineers, supported by national defaults from the HCM 2010 and NCHRP Report 599 as applicable. Table 3 shows a subset of these defaults for urban arterials and two-lane highways, with the full list available in the research report (*12*). In addition to NCLOS default values, the table presents program limits, which restrict the user's input to the listed boundary conditions, and practical limits, which guide the user to common input for best and worst case practical values.

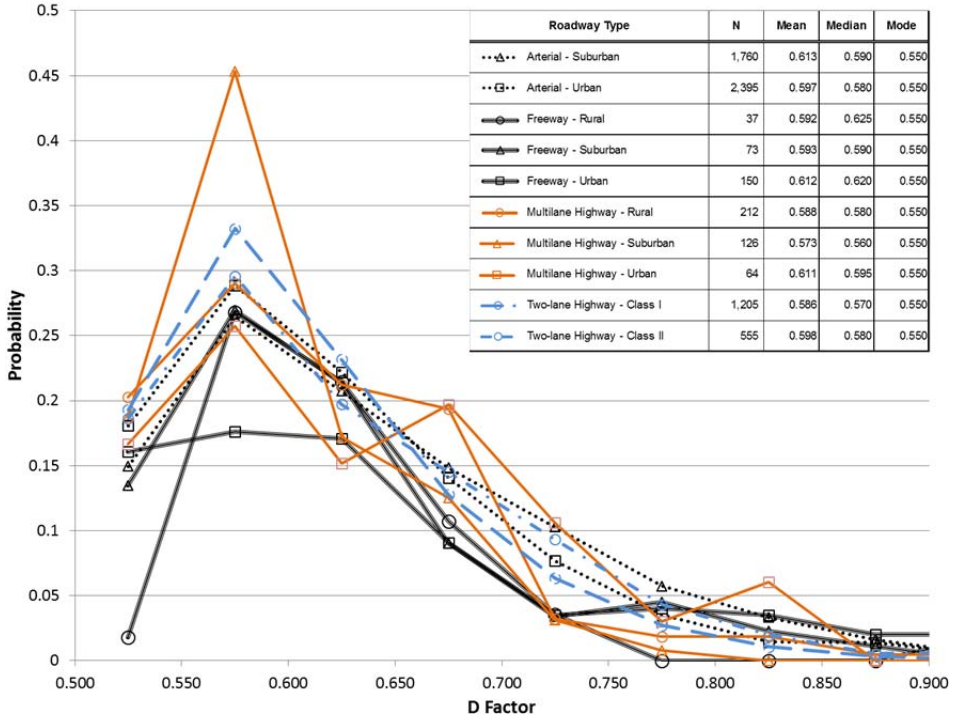

FIGURE 3 *D*-factor data.

TABLE 2 North Carolina Traffic Characteristic Data

Factor	Facility Type	Urban		Suburban		Rural	
		NC	National[a]	NC	National[a]	NC	National[a]
K	Freeway	0.09	0.08–0.10	0.09	NA	0.09	0.09–0.13
	Multilane highway	0.09	0.08–0.12	0.09	NA	0.09	0.09–0.12
	Two-lane highway	NA	0.09–0.14		0.09–0.14	0.09	0.09–0.14
	Arterials	0.09	NA	0.09	NA	NA	NA
D	Freeway	0.60	0.55	0.60	NA	0.65	0.55
	Multilane highway	0.60	0.50–0.65	0.55	NA	0.60	0.50–0.65
	Two-lane highway	NA	0.50–0.65		0.50–0.65	0.60	0.50–0.65
	Arterials	0.60	NA	0.60	NA	NA	NA
PHF	Freeway	0.90	0.94	0.90	NA	0.85	0.94
	Multilane highway	0.90	0.95	0.90	NA	0.90	0.88
	Two-lane highway	NA	0.82	NA	NA	0.85	NA
	Arterials	0.90	0.92	0.90	NA	NA	NA

NOTE: NC = North Carolina; NA = not available.
[a] National data represents recommended defaults from HCM 2010 and NCHRP Report 599.

IMPLEMENTATION

The software implementation of the NCLOS methodology is separated into different modules for each facility type. These modules include freeways, multilane highways, two-lane highways, and arterials. The software was programmed to be consistent with HCM 2010, but there are several nuances that were incorporated. The operational analysis methodologies for basic freeway segments and multilane highways recommend using the nearest 5-mph FFS increment for quantification. As plotting LOS versus AADT is a principal feature of NCLOS, the use of 5-mph increments resulted in step function outputs. To avoid this outcome, where an additional vehicle could significantly change the analysis results, the software utilizes interpolation to determine FFS.

Another significant deviation relates to the HCM 2010 chapter on urban streets. The procedure for operational analysis uses the new signalized intersection methodology in Chapter 18 (*13*); it requires iterative computer calculations and includes a complicated incremental queue accumulation method used to estimate uniform delay at a signal. This method was considered to be too complex for direct implementation in NCLOS. Further, it would have required very detailed signal timing parameters that are not available at the planning-level stage. Consequently, NCLOS uses the Quick Estimation Method for Urban Street Segments found in Chapter 30, Section 4 of HCM 2010 (*10*, *14*). This methodology provides a more appropriate level of calculation for planning applications. The LOS metric for an urban street is based on a measure known as percent FFS, which is calculated by the ratio of average travel speed (ATS) to the FFS on the facility. The method was configured to estimate the ATS and determine LOS for arterials. An example of the output from the arterial facility type in NCLOS is shown in Figure 4.

TABLE 3 NCLOS Default Data for Arterials and Two-Lane Highways

Facility Type		Input	Program Limits: Restrict Input Within Boundary Conditions		Practical Limits: Alert Users of Uncommon Input		NCLOS Default Value			
			Min.	Max.	Worst	Best	Urban	Suburban	Rural	Source
Arterials	Traffic Factors	BFFS (mph)	30	70	30	60	45	45		4
		K	0.04	1.00	0.13	0.08	0.090	0.093		1
		Midsegment volume (vph)	0	10,000	0	5,000	User	User		4
		Other delays (s)	0	100	0	50	10	10		4
		PHF	0.25	1	0.75	1.00	0.9	0.9		1
		Platoon ratio	0	1	0.2	0.8	0.6	0.6		4
		Saturated flow rate (per lane)	1,300	1,900	1,500	1,900	1,800	1,800		4
		Startup time lost (s)	1	4	1	2.5	1.5	1.5		4
		Total delay due to turns (s)	0	100	0	50	10	10		4
		Upstream v/c ratio	0.2	2.5	1.5	0.5	0.9	0.8		4
	Roadway Factors	Access points per mile	0	60	60	0	10	10		4
		Cycle length (s)	60	300	80	200	120	120		4
		G/C ratio	0	1	0.1	0.6	0.35	0.35		4
		Intersection width (ft)	24	120	36	84	60	60		4
		Length (ft)	0	100,000	0	20,000	10,000	10,000		4
		Length with restrictive median (ft)	0	100,000	0	20,000	2,000	2,000		4
		No. of lanes (per direction)	1	8	1	4	2	2		4
		Proportion with curb	0	100	50	100	100	0		4
		Speed limit	15	60	25	60	45	45		4
Two-Lane Highway	Traffic Factors	*D*	0.50	1.00	0.90	0.50			0.6	1
		FFS	30	80	45	65			60	4
		K	0.04	1.00	0.13	0.08			0.09	1
		PHF	0.25	1	0.75	1.00			0.85	1
		Percent RVs	0	100	10	0			0	4
		Percent trucks–buses	0	100	40	0			5.8	1
	Roadway Factors	Access points per mile	0	100	40	0			8	2
		BFFS	30	80	45	65			60	3
		Terrain type	NA	NA	NA	NA			Level	2
		Lane width	8	14	9	12			12	2, 3
		Lateral clearance	0	12	0	6			6	2, 3
		Length of grade (mi)	0	10	5	0			0	4
		Percent grade	–100	100	12	0			0	4
		Percent no-passing zones[a]	0	100	100	0			20	3
		Two-lane class	I	I	I	I			I	4

NOTE: min. = minimum; max. = maximum; no. = number.

[a] 80% no passing zones for mountainous terrain with limited sight distance.

SOURCES: North Carolina Traffic Volume Data; NCHRP Report 599; Previous NCLOS Default Value; and Ideal Case or Professional Judgment.

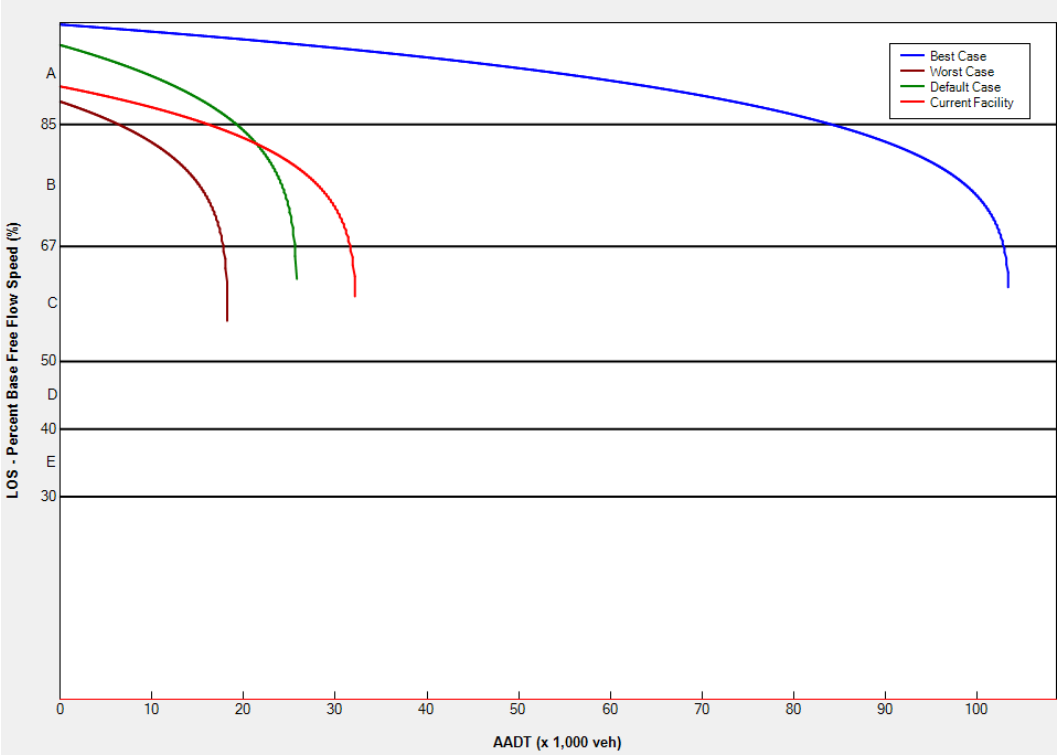

FIGURE 4 Arterial graph from NCLOS.

This graph presents the user with a set of curves for best, worst, and default cases as well as the current facility, or user-defined curve. As the capacity (AADT) increases, the slope increases and the curve drops off, suggesting that the highway facility operates well at low and moderate volume levels but rapidly deteriorates as volume increases. An assessment of the current facility shows that it performs close to the North Carolina average default. In the planning context, there may be additional opportunities for improvement by adjusting traffic and roadway parameters in order to reach the best-case scenario.

Two-lane roads are classified into one of three categories: Class I, Class II, or Class III in accordance to the HCM 2010 criteria. Class I is a facility which has motorists who expect relatively high speeds, Class II has motorists who do not necessarily expect high speeds, and Class III serves moderately developed areas. These typology definitions are subjective and can be challenging to apply in practice, particularly on a statewide level. The calculations for the service level of these roads are dictated by the classification designated by the user. However, the resulting accuracy of the outputs from this process subsequently relies on whether the appropriate classification was chosen. The evaluation of each highway class is informed by various measures of effectiveness including percent of the FFS, ATS, or percent time spent following another vehicle. It should be noted that when using the HCM methodology Class II two-lane highways will yield a higher capacity than that of Class I highways given the same input values. Although counterintuitive at first examination, the methodology attempts to address driver perception in that expectations are less demanding for Class II routes. Accordingly, the analyst must use judgment in selecting input values for the discrepancies in classification. The

NCLOS application allows this comparison between classification type selections by viewing the results for each class.

Figure 5 presents an example two-lane facility in each class with their associated maximum AADT volumes for various LOS levels. The NCLOS implementation is unique in that it takes all three LOS service measures in the two-lane procedure and plots the results on a common y-axis scale. To accomplish this, note that the y-axis scale had to be reversed for some service measures, where ATS and percent of free-flow speed (PFFS) range from low to high when moving upward on the *y*-axis scale, while percent time spent following (PTSF) ranges from high to low. The three graphs have further been scaled to show a consistent representation of these service measures.

The results suggest that the subject facility performs slightly above the average default for the service measures of PTSF and PFFS in Figures 5*b* and 5*c*. For the ATS measure, the facility performs well below average, and falls below the allowable worst case for low AADT ranges. Interestingly, at a common AADT of 10,000 vehicles per day, the ATS, PTSF, and PFFS measures suggest a LOS of D, D, and C, respectively. This points to challenges when applying the two-lane highway method, where the charts and the resulting LOS can offer different results depending on the class selected.

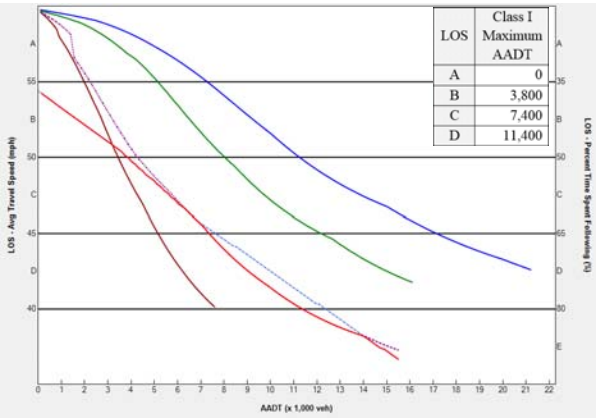

(a)

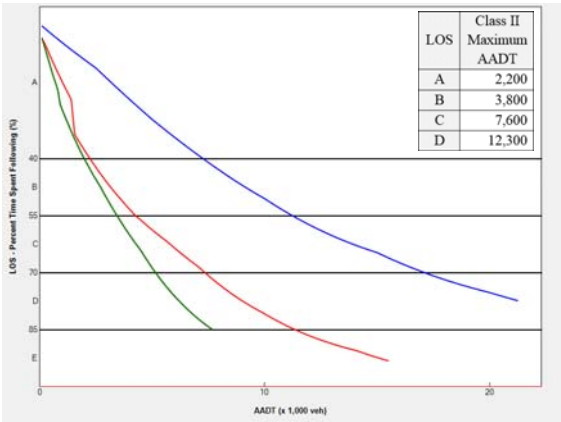

(b)

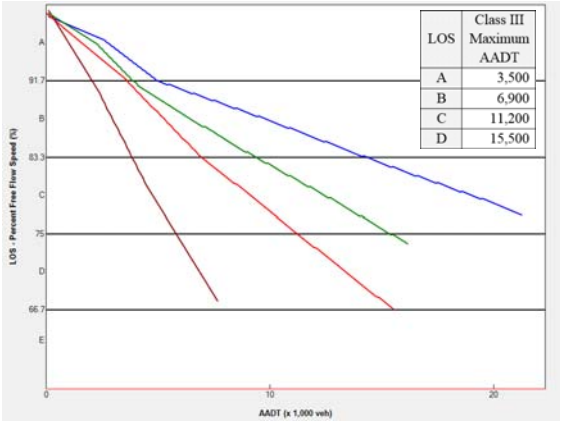

(c)

FIGURE 5 Two-lane NCLOS output for each class: (*a*) Class I; (*b*) Class II; and (*c*) Class III.

A comparison of the output for each of the three cases does not indicate which case is most appropriate for the specific roadway facility, since each case is based on assumptions pertaining to that situation. However, it is possible to obtain more information about the relationship of unrelated measures of effectiveness by examining their correlation at LOS thresholds and then examining when each measure controls the LOS output. The lower LOS value should be identified based on either ATS or PTSF, which can be completed by performing two computations and then selecting the lower LOS value. However, when graphically displaying continuous LOS and AADT curves for both measures of effectiveness, a relationship between the measures must be established. Figure 6 displays the relationship of ATS and PTSF for a two-lane Class I facility, which was created based on values acquired at each LOS threshold. These measures are inversely related and are not linearly correlated. The values have no physical correlation to each other (i.e., 55-mph travel speed ≠ 40% PTSF). This graph does not imply that a driver traveling at 55 mph on a Class I facility would expect to follow another vehicle 40% of the time. Instead, this relationship represents the equivalence of a driver's perception on a Class I facility of traveling at 55 mph or spending 40% of their time following another vehicle.

Employing the correlation between the measures of effectiveness, Figure 7 shows a composite two-lane highway analysis graph with both measures and a red line indicating which of the dashed measures of effectiveness lines are controlling the overall LOS. In this example, the PTSF measure controls the LOS from 7,500 to 14,000 vehicles per day (vpd).

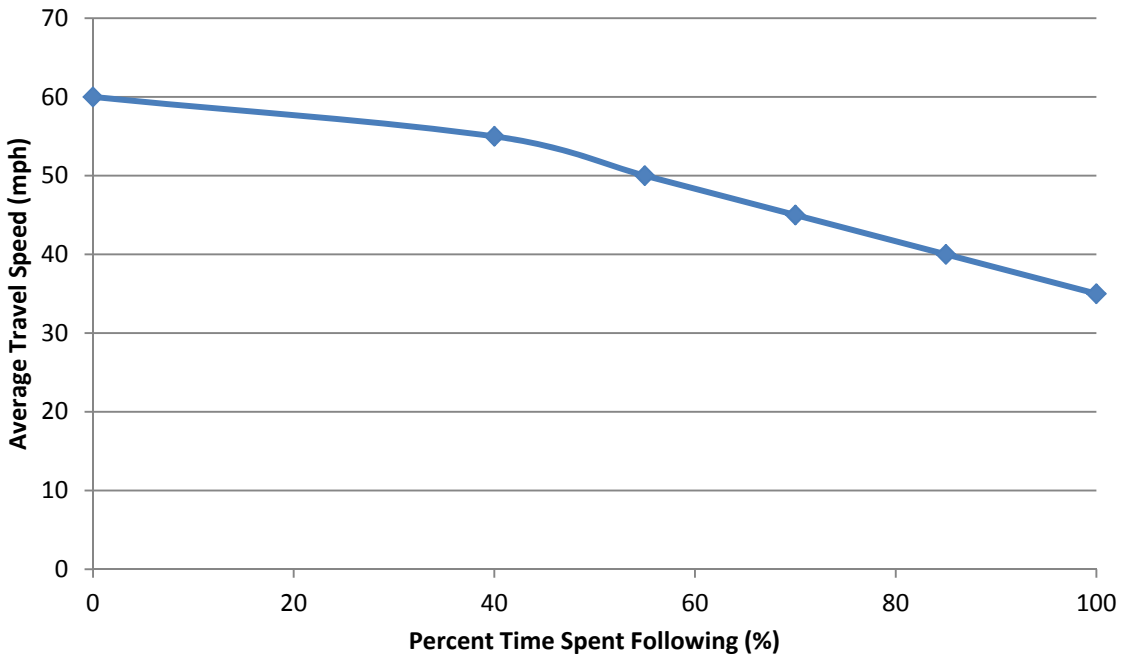

FIGURE 6 Two-lane Class I ATS and PTSF perception equivalence graph.

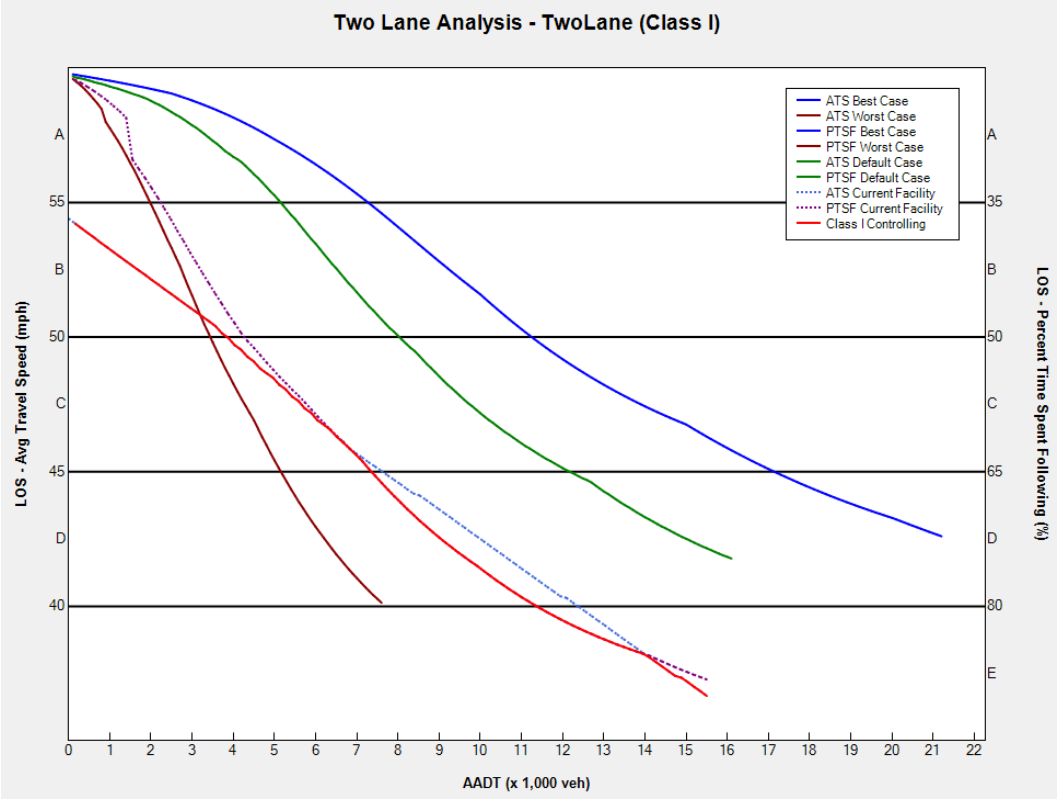

FIGURE 7 Two-lane highway Class I LOS graph

SUMMARY

This section summarizes the maximum capacity outputs calculated from the default values in NCLOS. The output represents the maximum AADT volumes, the threshold between LOS E and LOS F, calculated by NCLOS rounded to the nearest hundred. The summary is organized by highway facility, area type, and total number of lanes in both directions. Table 4 tabulated capacity outputs were derived by the LOS E performance measures for facilities within the limits of the facility characteristics in North Carolina.

CONCLUSIONS AND RECOMMENDATIONS

The NCLOS software is a tool developed to implement HCM 2010 for planning-level assessment of freeway, multilane highway, two-lane highway, and arterial facilities. The program can be utilized to determine capacities and service volume thresholds. The visual aspect of the program output, aided by the display of best and worst case conditions, allows for an intuitive assessment of the facility performance, and a better interpretation of the subject segment performance relative to the range of expected conditions in North Carolina. The user can attempt various scenarios by altering the input values to represent possible design considerations for a particular highway. Additionally, NCLOS enables users to produce a numerical report detailing the results of the analysis as well as the ability to export the calculated capacity to transportation planning software.

TABLE 4 NCLOS Daily Service Volumes for LOS E

Highway Facility	Maximum Capacity for LOS E Under Default Conditions by Highway Facility, Area Type, and Number of Lanes					
	Area Type	Total Number of Lanes				
		2	4	6	8	10
Freeways	Urban	37,600	75,100	112,700	150,300	187,900
	Suburban	41,100	82,200	123,300	164,400	205,500
	Rural	35,900	71,700	107,600	143,400	179,300
Multilane highways	Urban	NA	66,600	100,000	133,300	166,600
	Suburban	NA	74,800	112,200	149,600	187,000
	Rural	NA	75,800	113,600	151,500	189,400
Two-lane highways	Urban	NA	NA	NA	NA	NA
	Suburban	NA	NA	NA	NA	NA
	Rural	15,500	NA	NA	NA	NA
Arterials	Urban	15,800	31,700	47,600	63,500	79,400
	Suburban	15,800	31,700	47,600	63,500	79,300
	Rural	NA	NA	NA	NA	NA

NOTE: NA = the combination of highway facility and area type are not applicable by definition or for North Carolina highways; North Carolina DOT default values for urban and suburban area types do not differ for freeways and superstreets.

By updating input definitions and default values, the procedures have been calibrated to reflect specific observed conditions within the state of North Carolina. However, it is emphasized that default values should always be scrutinized for any new facility, and local adjustments should be made for facilities that fall outside the range of defaults. The analysis of default values generally showed few distinct trends across facility types and geographic region, although various outlier locations were observed in each of the data sets. While the defaults appear to provide a good general representation of expected conditions in North Carolina, user judgment should always be applied to unusual sites.

ACKNOWLEDGMENTS

This paper was derived from a study that was funded by the North Carolina Department of Transportation. North Carolina DOT has not evaluated or adopted the findings of this paper or accepted or rejected any of its conclusions. The authors acknowledge the efforts of those who supported the research and enabled the project to be successfully completed.

REFERENCES

1. *Highway Capacity Manual 2010*. Transportation Research Board of the National Academies, Washington, D.C., 2010.
2. Fain, S. J., C. M. Cunningham, R. S. Foyle, and N. M. Rouphail. NCDOT Level of Service Software Program for Highway Capacity Manual Planning Applications. Report FHWA/NC/2006-06. North Carolina Department of Transportation, August 2006.
3. Zegeer, J. D., M. Vandehey, M. L. Blogg, and K. Nguyen. Default Values for Highway Capacity and Level-of-Service Analyses. In *Transportation Research Record: Journal of the Transportation Research Board: No 2071*, Transportation Research Board of the National Academies, Washington, D.C., 2008, pp. 35–43.
4. Schoen, J. A., A. May, W. Reilly, and T. Urbanik. Speed-Flow Relationships for Basic Freeway Sections. Final Report, NCHRP Project 3-45. JHK & Associates, Tucson, Ariz., May 1995.
5. Roess, R. Re-Calibration of the 75-mi/h Speed-Flow Curve and the FFS Prediction Algorithm for HCM 2010. Research Memorandum, NCHRP Project 3-92. Polytechnic Institute of New York University, Brooklyn, N.Y., January 2009.
6. Hall, F. L. and K. Agyemang-Duah. Freeway Capacity Drop and the Definition of Capacity. In *Transportation Research Record 1320*, TRB, National Research Council, Washington, D.C., 1991, pp. 91–98.
7. Reilly, W., D. Harwood, J. Schoen, and M. Holling. Capacity and LOS 3 Procedures for Rural and Urban Multilane Highways. NCHRP Project 3-33, Final Report. JHK & Associates, Tucson, Ariz., May 1990.
8. Washburn, S. S., D. S. McLeod, and K. G. Courage. Adaptation of the "Highway Capacity Manual" 2000 for Planning-Level Analysis of Two-Lane and Multilane Highways in Florida. In *Transportation Research Record: Journal of the Transportation Research Board, No. 1802,* Transportation Research Board of the National Academies, Washington, D.C., 2002, pp. 62–68.
9. Harwood, D. W., I. B. Potts, K. M. Bauer, J. A. Bonneson, and L. Elefteriadou. Two-Lane Road Analysis Methodology in the *Highway Capacity Manual*. Final Report, NCHRP Project 20-7 (160). Midwest Research Institute, Kansas City, Mo., September 2003.
10. Bonneson, J., M. Pratt, and M. Vandehey. Predicting the Performance of Automobile Traffic on Urban Streets: Final Report. NCHRP Project 3-79. Transportation Research Board of the National Academies, Washington, D.C., January 2008.
11. Chapter 17. *Highway Capacity Manual 2010*. Transportation Research Board of the National Academies, Washington, D.C., 2010.
12. Findley, D. J., J. C. Chang, C. L. Vaughan, B. J. Schroeder, and R. S. Foyle. NCLOS Program 2010 Update. Report FHWA/NC/2012-05. North Carolina Department of Transportation, June 2013.
13. Chapter 18. *Highway Capacity Manual 2010*. Transportation Research Board of the National Academies, Washington, D.C., 2010.
14. Chapter 30. *Highway Capacity Manual 2010*. Transportation Research Board of the National Academies, Washington, D.C., 2010.

EXTENDED ABSTRACT

Influence of Undesignated Pedestrian Crossings on Midblock Capacity of Urban Roads

ASHISH DHAMANIYA
SV National Institute of Technology, India.

SATISH CHANDRA
Indian Institute of Technology Roorkee

The *Highway Capacity Manual 2010* (HCM 2010) is the most referred-to document in the world for calculation of capacity of road infrastructure. The manual describes the detailed procedure for determination of capacity and level of service on urban roads and intersections. For urban and suburban arterials, the manual recognizes that roadside development may be intense and can produce friction which may limit driver's choice of speed. They include but not limited to pedestrians; nonmotorized vehicles; parked and stopped vehicles; bus stops and bus bays; and commercial activities along the road. The pedestrians crossing an urban road at undesignated places are not uncommon in developing countries like India and they force the motor vehicles to provide suitable gaps for their crossing.

The locations where pedestrians cross the road invariably are undesignated with no pedestrian cross marks. It particularly happens on segment where distance between the intersections is quite large (more than 1 mi) and also on urban roads located in commercial areas or residential areas. These crossings at undesignated locations have twofold effects: pedestrian put themselves on risk and traffic speed and capacity are adversely affected. The problem of influence of pedestrian cross-flow on capacity and performance of urban midblock sections is not addressed in the HCM 2010 or in Indian Roads Congress guidelines. The present study was taken up with the objective of evaluating the effect of pedestrians crossing on midblock capacity of six-lane divided urban arterials under mixed traffic condition in India and to compare the results with those reported in the literature.

Data were collected on 12 sections of six-lane urban arterial roads in three different populous cities of India. Six sections were selected without any side friction to estimate the base value of capacity. Remaining six sections were with pedestrian flow across the road at undesignated crossing. Data were collected in field through videography and speed–volume data were extracted in the laboratory. All vehicles in the traffic stream were divided into five different categories: small car, big car, heavy vehicles, three-wheelers, and two-wheelers. As the traffic on Indian urban roads is heterogeneous in nature with wide variation in the static and dynamic characteristics of different types of vehicles, one class of vehicles cannot be considered equal to any other vehicle class as there is considerable difference in their physical and flow characteristics. One way of accounting this nonuniformity in the static and dynamic characteristics of vehicles is to convert all vehicles in to a common unit and the most accepted unit for this purpose is the passenger car unit (PCU).

In the present study, the PCUs were calculated using Equation 1 which is based on the concept that PCU is directly proportional to the ratio of speed, and inversely proportional to the space occupancy ratio with respect to the standard design vehicle which in the present study is small car.

$$PCU_i = \frac{V_c / V_i}{A_c / A_i} \quad (1)$$

Where V_c and V_i are speed of small car and vehicle type i, respectively, and A_c and A_i are their projected rectangular area on the road. The PCU factors were calculated for each type of vehicle in each 5-min count on a section to convert mixed traffic flow into homogenous flow in PCU/h. The data were analyzed to obtain the composition of traffic volume [vehicles per hour (vph)] and speed (km/h) of each type of vehicle on different sections. The speed–flow data were plotted to derive the capacity of the section using fundamental diagram method. The midblock capacity of a six-lane divided urban road without the influence of pedestrian flow was found to vary from 1,500 to 2,100 pcph/lane in three cities and these are termed as base capacity. This variation in base capacity is attributed to the different free-flow speeds in these cities. Effect of pedestrian cross-flow is evaluated on midblock capacity of urban road by comparing the capacity of a section with pedestrian cross-flow with that of the base section. The capacity values and pedestrian cross-flow at each of the sections are given in Table 1.

The effect of pedestrian cross-flow is to reduce both the stream speed and capacity of the section and similar trend is observed in the present study also. Last column in Table 1 indicates percent reduction in capacity due to pedestrian cross-flow with respect to capacity of the base section in three cities. It is interesting to note that the reduction in capacity of section F where pedestrian flow is 200 pedestrians per hour (ped/h), is quite negligible. Therefore, it may be stated that there is no reduction in midblock capacity of an urban road as long as cross pedestrian volume is less than 200 ped/h. However it needs some more attention of researchers as the pedestrian cross flow of 250 ped/h (section D) has resulted in 16.73% loss in capacity, which is quite high when compared with 0.81% loss at pedestrians' cross-flow of 200 ped/h. Figure 1 shows the variation in percent reduction in capacity with pedestrian cross-flow. This curve is drawn considering the data points corresponding to more than 200 ped/h and it can be described by a second degree polynomial as given in Equation 2.

$$\text{Percent reduction in capacity} = 11.09 + 0.025 * Q_{\text{ped}} - 8 \times 10^{-6} * Q^2_{\text{ped}} \quad (2)$$

where Q_{ped} is the pedestrian cross-flow (ped/h).

TABLE 1 Capacity and Pedestrian Cross-Flow at Different Sections

Section with Pedestrain Cross-Flow	Direction Capacity (PCU/h)	Lane Capacity (PCU/h/lane)	Lane Capacity of Base Section (PCU/h)	Pedestrian Cross-Flow (ped/h)	Reduction in Capacity (%)
A	4,739	1,580	2,100	682	24.76
B	4,950	1,733	2,100	508	21.43
C	3,120	1,040	1,500	1,360	30.67
D	4,122	1,374	1,650	250	16.73
E	3,990	1,330	1,650	350	19.39
F	6,249	2,083	2,100	200	0.81

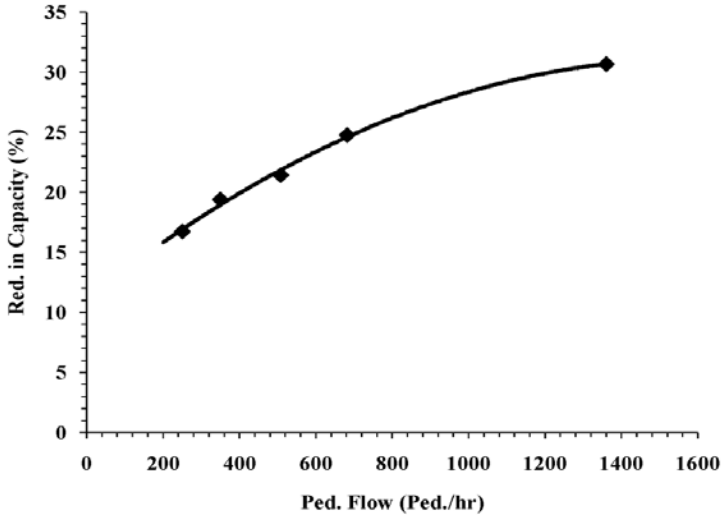

FIGURE 1 Reduction in capacity of six-lane road with pedestrain cross-flow.

Crossing of a road by a pedestrian is essentially a gap-acceptance process where the pedestrian would evaluate the gap available in all the lanes to be crossed before entering the road. Availability of the gap would depend on traffic volume in the lane and acceptance (or rejection) of the gap would depend upon the perception of the pedestrians about the gap. This pedestrian vehicle interaction is a complex phenomenon and has deep safety implications apart from creating loss in capacity of the road. Indian standards suggest that pedestrian crossing facility must be provided whenever PV^2 (where P is the pedestrian volume per hour and V is the traffic volume per hour) is more than 2×10^8 for undivided roads. The value of PV^2 at all sections selected for the present study is more than 2×10^8 as the volume range at all the sections are more than 1,000 vph which indicates the need of a pedestrian facility and at majority of these sections, pedestrian footbridges have been provided. However, pedestrians choose to cross the road at-grade to save time. The effect of pedestrian crossings on capacity of six-lane urban arterial roads may be evaluated from the presented model which may be useful for planners. Safety of pedestrians or motor vehicles due to such behavior of pedestrian may be another important are for further research.

EXTENDED ABSTRACT

Capacity Estimation for Weaving Segments Using a Lane-Changing Model

XU WANG
YING LUO
TONY Z. QIU
University of Alberta, Canada

XINPING YAN
Wuhan University of Technology, China

During peak periods, freeway bottlenecks can be activated by intensive lane changing at weaving segments, where merging and diverging areas are in close proximity. This weaving phenomenon has a major impact on capacity. Much research has been devoted to investigating capacity estimation models for weaving segments. However, due to the model parameters, they are difficult to directly adopt in active traffic management strategies to estimate real-time maximum discharge flow.

Thus, there are four objectives of this paper:

1. Develop a capacity estimation method using a lane changing model and linear optimization, which is potentially applicable for traffic operation;
2. Evaluate the proposed method in two configurations of weaving segments;
3. Investigate sensitivity and correlation between weaving capacity and flow proportions; and
4. Estimate real-time maximum discharge flow rate in peak hours.

With these objectives in mind, this study combined linear optimization using a lane-changing model as a constraint. The highest concentration of flow and rate of lane changing occur in a "critical region." Within the critical region, a function of vehicle flows and lane changing rates can be defined as the weaving capacity. Based on this definition, this study applies a four-step procedure to estimate weaving capacity (Figure 1). First, basic geometry and traffic information are needed to determine configuration characteristics of a segment. With these configuration characteristics, the maximum length of a weaving segment (L_{max}) is computed referring to the *Highway Capacity Manual 2010* (HCM 2010). As defined in HCM 2010, volume ratio (VR) is the ratio of weaving flow rate over total flow rate at a weaving segment and is the number of lanes from which a weaving maneuver may be made with one or no lane changes. Then, only the segment whose length (L_s) is less than L_{max} is regarded as a weaving segment. Second, the region with the highest concentration of lane changes is selected as a critical region within the weaving segment. Meanwhile, the traffic data requires further reduction to determine the weaving and nonweaving flow rate. Next, for each lane that is involved in the weaving maneuvers, its critical density is applied in the MH model. The results obtained from the MH model are the maximum lane changes that weaving vehicles can actually make. With all the information in hand, the capacity estimation problem is established as a linear optimization problem by applying the aforementioned definition of capacity, while weaving capacity is solved with several constraints for traffic movements.

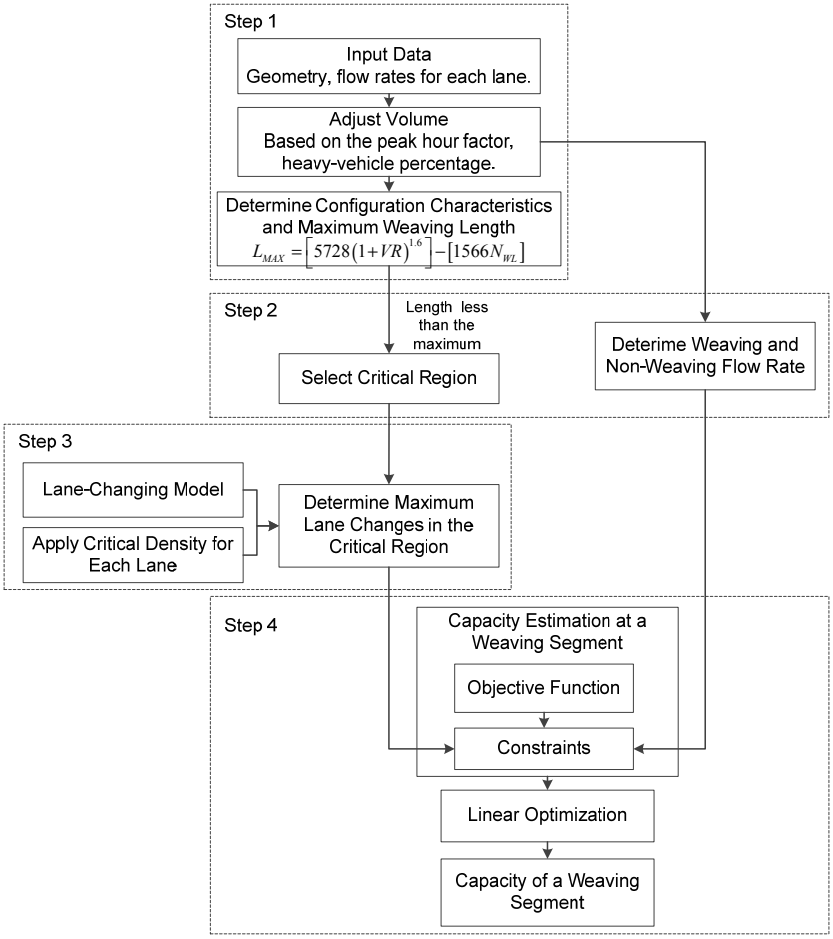

FIGURE 1 Methodology flowchart

The proposed method is evaluated and analyzed for sensitivity with field data from two weaving segments on Whitemud Drive in Edmonton, Alberta, Canada. The capacity estimates from the proposed model were consistent with that from the HCM 2010 model and with field observations. Moreover, it was also observed that the weaving capacity is sensitive to weaving maneuvers (Table 1). Finally, the proposed method was applied to estimate the real-time maximum discharge flow rate; the estimates matched field measurements.

There are four major findings of this research:

1. Most lane changes happen near the merge gore, which can be considered the critical region, and the capacity there can represent the whole weaving segment.
2. The proposed approach provides similar results compared with HCM 2010 results and field observations.
3. When the weaving flow ratio is small, an increased number of weaving vehicles rarely changes weaving capacity, whereas, when weaving ratio is moderate or large, weaving behaviors notably decrease weaving capacity.
4. The proposed approach can capture real-time maximum discharge flow, which is a main input for traffic operation strategies. These findings could lead to implementations in designing optimal traffic control strategies.

TABLE 1 Capacity Estimation Results

Model Inputs									
	Observed Flow (vph)				**Model Parameters**			**Basic Capacity (vphpl)**	
	q_{FF}	q_{FR}	q_{RF}	q_{RR}	W_1	W_2	VR	c_{BF}	c_{BR}
Site 1	3006	1619	79	237	0.80	0.25	0.016	2100	1600
Site 2	4097	1593	441	9	0.72	0.02	0.3313	1400	1300

Estimation Results				
Capacity Estimates / **Site**	**Field Observations**		**HCM 2010 Estimation (vphpl)**	**Proposed Method (vphpl)**
	Max. 15 min (vphpl)	**Max. Queue Discharge (vphpl)**		
Site 1 21-May-2013	1837	1456	1857	1867
Site 2 16-May-2013	1299	1139	1285	1257

NOTE: vph = vehicles per hour; vphpl = vph per lane.

EXTENDED ABSTRACT

Lane Utilization at Two-Lane Arterial Approaches to Double Crossover Diamond Interchanges

CHUNHO YEOM
BASTIAN J. SCHROEDER
CHRISTOPHER CUNNINGHAM
CHRISTOPHER VAUGHAN
NAGUI M. ROUPHAIL
Institute for Transportation Research and Education, NC State University

JOSEPH E. HUMMER
Wayne State University

Double crossover diamond interchanges (DCD), also known as diverging diamond interchange (DDI), are popular and promising alternative interchange designs that are increasingly being implemented nationwide. The most unique feature of a DCD interchange is that through movements on the arterial road have to cross each other twice to complete their movements, while enabling left-turn movements from the arterial to the freeway to proceed without stopping at the downstream intersection. Consequently, interchanges with heavy left-turn movements are good candidates for DCD implementation. This unique feature of a DCD interchange motivates the need to research the lane utilization at the upstream approach intersection of DCD interchanges, as the lane use could be unbalanced. The unbalanced lane utilization could have a significant effect on operations at the first crossover and the interchange. Figure 1 presents a DCD interchange, depicting points of interest from the perspective of lane utilization.

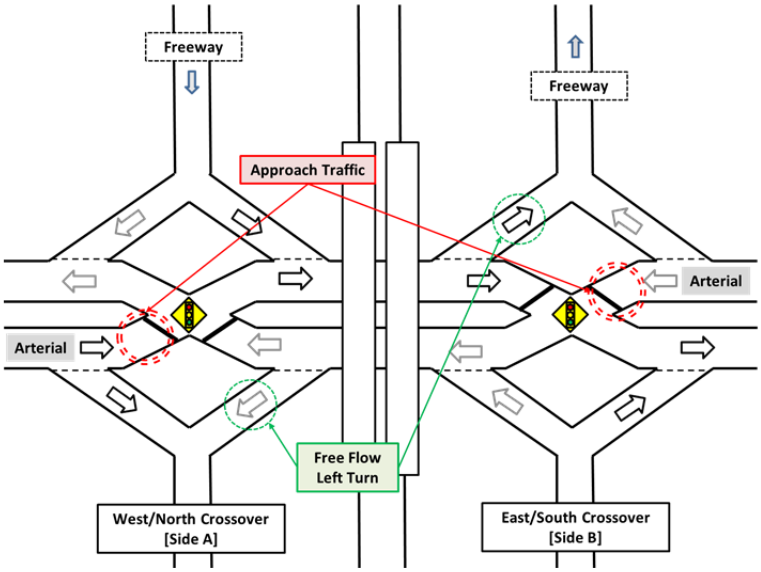

FIGURE 1 DCD interchange diagram highlighting approaches of interest.

This study examined lane utilization factors provided in the *Highway Capacity Manual 2010* (HCM 2010) for conventional diamond interchanges, and found that they are not generally applicable to DCDs. The study proposed a field calibrated lane utilization model with data obtained at three DCD sites. The two-regime model is depicted below:

Regime I. Left-Turn Demand Ratio ≤0.35:

Left-lane utilization (f_{L1}) = 0.2129 × R_{DL} + 0.525 (1)

Regime II. Left-Turn Demand Ratio >0.35:

Left-lane utilization (f_{L1}) = 0.5386 × R_{DL} + 0.411 (2)

where

f_{L1} = Fraction of the left-lane utilization (number of left-lane vehicle/total vehicle) and
R_{DL} = Left-turn demand ratio at the downstream intersection.

In Equations 1 and 2, the left-turn demand ratio is estimated by the number of left-turn vehicles at the downstream intersection divided by the number of total arriving traffic at the upstream intersection. As such, the model predicts left-lane utilization ratio at the upstream intersection of DDIs by the ratio of left-turn movements at the downstream intersection.

The new model fit observed conditions at the DCD sites better than previously developed HCM 2010 factors. The model was then validated using three additional DCD interchanges. These three sites were not used in model development, but offer similar geometric configuration from the model development sites. The validation results confirmed that the new model adequately predicts DCD lane utilization as presented in Figure 2.

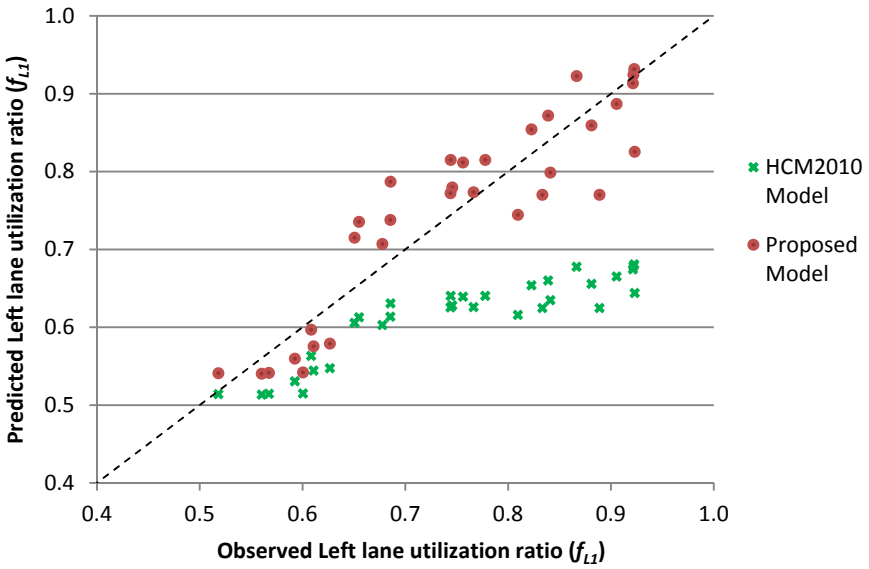

FIGURE 2 Left-lane utilization prediction comparison.

The results indicate that the HCM 2010 models tended to predict left-lane utilization mostly below actual field observations, whereas the proposed model predictions were closer to the field observations consistently. The root mean square error for the left-lane utilization ratio is 0.0518 for the proposed model, which is almost a third of the 0.1574 value for the HCM 2010 model.

It is therefore recommended to use the proposed lane utilization model at two-lane arterial approaches to DCD interchanges as presented in Equations 1 and 2 depending on the predicted left-turn demand ratios at the downstream intersection. Future research needs to include developing a model for two-lane approaches to DCDs based on a larger data set and at more sites with different distances between crossovers. The authors also recommend extending the lane utilization models to include three- and four-lane arterial approaches to DCDs. When studying three- or four-lane approaches, it must be noted whether the leftmost lane is shared with through movement or operates as an exclusive left turn. Other variables such as distance from an adjacent upstream intersection, volume-to-capacity ratios, queue lengths, or heavy vehicles would also be important to analyze for two-, three-, and four-lane models. Last, the use of a simulation program to model and validate a lane utilization behavior to DCDs could be another option to experiment with in future studies.

THE NATIONAL ACADEMIES

Advisers to the Nation on Science, Engineering, and Medicine

The **National Academy of Sciences** is a private, nonprofit, self-perpetuating society of distinguished scholars engaged in scientific and engineering research, dedicated to the furtherance of science and technology and to their use for the general welfare. On the authority of the charter granted to it by the Congress in 1863, the Academy has a mandate that requires it to advise the federal government on scientific and technical matters. Dr. Ralph J. Cicerone is president of the National Academy of Sciences.

The **National Academy of Engineering** was established in 1964, under the charter of the National Academy of Sciences, as a parallel organization of outstanding engineers. It is autonomous in its administration and in the selection of its members, sharing with the National Academy of Sciences the responsibility for advising the federal government. The National Academy of Engineering also sponsors engineering programs aimed at meeting national needs, encourages education and research, and recognizes the superior achievements of engineers. C. D. (Dan) Mote, Jr., is president of the National Academy of Engineering.

The **Institute of Medicine** was established in 1970 by the National Academy of Sciences to secure the services of eminent members of appropriate professions in the examination of policy matters pertaining to the health of the public. The Institute acts under the responsibility given to the National Academy of Sciences by its congressional charter to be an adviser to the federal government and, on its own initiative, to identify issues of medical care, research, and education. Dr. Victor J. Dzau is president of the Institute of Medicine.

The **National Research Council** was organized by the National Academy of Sciences in 1916 to associate the broad community of science and technology with the Academy's purposes of furthering knowledge and advising the federal government. Functioning in accordance with general policies determined by the Academy, the Council has become the principal operating agency of both the National Academy of Sciences and the National Academy of Engineering in providing services to the government, the public, and the scientific and engineering communities. The Council is administered jointly by both Academies and the Institute of Medicine. Dr. Ralph J. Cicerone and C. D. (Dan) Mote, Jr., are chair and vice chair, respectively, of the National Research Council.

The **Transportation Research Board** is one of six major divisions of the National Research Council. The mission of the Transportation Research Board is to provide leadership in transportation innovation and progress through research and information exchange, conducted within a setting that is objective, interdisciplinary, and multimodal. The Board's varied activities annually engage about 7,000 engineers, scientists, and other transportation researchers and practitioners from the public and private sectors and academia, all of whom contribute their expertise in the public interest. The program is supported by state transportation departments, federal agencies including the component administrations of the U.S. Department of Transportation, and other organizations and individuals interested in the development of transportation. **www.TRB.org**

www.national-academies.org

TRB

TRANSPORTATION RESEARCH BOARD
500 Fifth Street, NW
Washington, DC 20001